

INFORMATION TO USERS

This manuscript has been reproduced from the microfilm master. UMI films the text directly from the original or copy submitted. Thus, some thesis and dissertation copies are in typewriter face, while others may be from any type of computer printer.

The quality of this reproduction is dependent upon the quality of the copy submitted. Broken or indistinct print, colored or poor quality illustrations and photographs, print bleedthrough, substandard margins, and improper alignment can adversely affect reproduction.

In the unlikely event that the author did not send UMI a complete manuscript and there are missing pages, these will be noted. Also, if unauthorized copyright material had to be removed, a note will indicate the deletion.

Oversize materials (e.g., maps, drawings, charts) are reproduced by sectioning the original, beginning at the upper left-hand corner and continuing from left to right in equal sections with small overlaps. Each original is also photographed in one exposure and is included in reduced form at the back of the book.

Photographs included in the original manuscript have been reproduced xerographically in this copy. Higher quality 6" x 9" black and white photographic prints are available for any photographs or illustrations appearing in this copy for an additional charge. Contact UMI directly to order.

UMI[®]

Bell & Howell Information and Learning
300 North Zeeb Road, Ann Arbor, MI 48106-1346 USA
800-521-0600



Université d'Ottawa • University of Ottawa



National Library
of Canada

Acquisitions and
Bibliographic Services

395 Wellington Street
Ottawa ON K1A 0N4
Canada

Bibliothèque nationale
du Canada

Acquisitions et
services bibliographiques

395, rue Wellington
Ottawa ON K1A 0N4
Canada

Your file Votre référence

Our file Notre référence

The author has granted a non-exclusive licence allowing the National Library of Canada to reproduce, loan, distribute or sell copies of this thesis in microform, paper or electronic formats.

The author retains ownership of the copyright in this thesis. Neither the thesis nor substantial extracts from it may be printed or otherwise reproduced without the author's permission.

L'auteur a accordé une licence non exclusive permettant à la Bibliothèque nationale du Canada de reproduire, prêter, distribuer ou vendre des copies de cette thèse sous la forme de microfiche/film, de reproduction sur papier ou sur format électronique.

L'auteur conserve la propriété du droit d'auteur qui protège cette thèse. Ni la thèse ni des extraits substantiels de celle-ci ne doivent être imprimés ou autrement reproduits sans son autorisation.

0-612-38771-2

Abstract

This work is concerned with the preparation and examination of guanidinate complexes. One method of synthesis of such ligands, as presented in Chapter 2, is the insertion of carbodiimide into a metal-amido group. The direct reactions of $M(\text{NMe}_2)_5$ with either dicyclohexylcarbodiimide ($\text{CyN}=\text{C}=\text{NCy}$) or diisopropylcarbodiimide (${}^i\text{PrN}=\text{C}=\text{N}{}^i\text{Pr}$) proceeded smoothly at room temperature under nitrogen to yield $[\text{RNC}(\text{NMe}_2)\text{NR}]M(\text{NMe}_2)_4$ ($M = \text{Ta}, \text{Nb}; \text{R} = \text{Cy}, {}^i\text{Pr}$). The spectroscopic characterization of these materials is consistent with a symmetrical chelating bidentate guanidinate anion bonded to a pseudo-octahedral metal center. Confirmation of these details was provided by a single crystal X-ray diffraction study in the case of $[\text{CyNC}(\text{NMe}_2)\text{NCy}]\text{Ta}(\text{NMe}_2)_4$. The reaction of dimethylamido lithium and carbodiimide ($\text{RN}=\text{C}=\text{NR}$) formed lithium guanidinate $[\text{RNC}(\text{NMe}_2)\text{NR}]\text{Li}$ ($\text{R} = \text{Cy}, {}^i\text{Pr}, \text{TMS}$). These species were confirmed by ${}^1\text{H}$ and ${}^{13}\text{C}$ NMR. All of these compounds formed in very good yield and no secondary compound were inspected.

In chapter 3, we prepared $\text{N},\text{N}',\text{N}''$ tricyclohexylguanidine and triisopropylguanidine. With this guanidine ligand, we focus on the elimination of amido ligands from homoleptic $\text{Ta}(\text{V})$ and $\text{Nb}(\text{V})$ dimethylamido complexes. The protonation of the metal-amido groups of $M(\text{NMe}_2)_5$ with trialkylguanidines yielded a series of novel complexes with formulae $[\text{RNC}(\text{NR})\text{NR}]M(\text{NMe}_2)_3$ ($M = \text{Ta}, \text{Nb}; \text{R} = \text{Cy}, {}^i\text{Pr}$). These complexes contained dianionic $\text{N}, \text{N}', \text{N}''$ trialkylguanidinate ligands which were coordinated in a chelating bidentate mode.

Single crystal X-ray study of $[\text{CyNC}(\text{NCy})\text{NCy}]\text{Ta}(\text{NMe}_2)_3$ and $[\text{ⁱPrNC}(\text{NⁱPr})\text{NⁱPr}]\text{Ta}(\text{NMe}_2)_3$ confirmed the connectivity of these species. Attempts to prepare bis(guanidinate) complexes by the reaction with two guanidine ligands were not successful.

The complex $\text{TaCl}(\text{NMe}_2)_3\{[\text{CH}_3)_2\text{CHN}]_2\text{CN}(\text{H})\text{CH}(\text{CH}_3)_2\}$ was also isolated and crystallographically characterized.

In Chapter 4, the direct reaction of Ta and Nb alkyl complexes $\text{M}(\text{Me})_x\text{Cl}_y$ ($\text{M} = \text{Ta}$, $x = 3$, $y = 2$; $\text{M} = \text{Nb}$, $x = 2$, $y = 3$) with N,N',N''-tricyclohexylguanidine and N,N',N''-triisopropylguanidine was investigated. The isolated products were the result of a single proton transfer and incorporation of a monoanionic guanidinate ligand. Two of these compounds $\text{TaMe}_2\text{Cl}_2(\text{CyN})_2\text{C}(\text{NCy})$ and $\text{NbMeCl}_3(\text{CyN})_2\text{C}(\text{NHCy})$ were characterized by single crystal X-ray diffraction analysis and confirmed the bonding features of the guanidinate ligands. The preliminary results of efforts to get a second alkyl elimination are also reported.

For God did not give us a spirit of timidity
But a spirit of power, of love, of self-discipline.

II Timothy 1:7

Dedicated to the loving memories
of
my beloved grand mothers
Daw Thone and *Daw Mya Kyi*

Acknowledgements

Thank you God, for giving me this valuable life.

Many people have made the successful completion of my graduate studies possible and I am grateful to them. First, I would like to acknowledge Dr. Darrin Richeson, my supervisor, who has been an incredible source of inspiration and knowledge for me to learn from. Without his support, understanding and encouragement I would not have been able to achieve this degree. He is the best mentor, the greatest boss, and a precious brother.

I would also like to thank Dr. Susannah Scott who was always there for me with her most beautiful smile. I would especially like to thank Dr. Christian Detellier, Dr. Sandro Gambarotta and Dr. Brian Hollebome who guided me down the right path.

I also thank the support staff, Corinne Bensimon, who taught me XRF and XRD, and especially Glen Facey, Raj Capoor for their support and time for my NMR, Glenn Yap for all my crystal structures, and Vladimir Kuznetsov for his time with my EA work.

I am very grateful to my formal boss Dr. Hans Walli Kling from Henkel KGaA (Dusseldorf) and Dr. Rewat Tantayanon from Henkel Thai who has always kept contact and encouraged me to turn my life towards the academic field again.

I would really like to thank my co-workers from Sandro's Lab and Susannah's lab who have made the lab an enjoyable place to work. Especially to my special lab-mate Stephen Foley, a big thank-you for keeping track of me and making me feel like I was on a roller coaster all my time at the University of Ottawa. Without him, I would not know whether to smile or cry.

Thanks go to my First Baptist Church and my beloved Diane and John Lugsdins who saved my life in this strange big country. Without their support, help and care I would have given up and returned back home from the beginning. I owe both of you and will always try to pay you back, not with money, but with love. You gave me a most enjoyable and heart-warming home for more than two years, free.

Then, my first room-mate Chitchamai Larksarp, who understood my international student condition and financial need. I will not forget your help. Finally, my best friend Mary King who loves me so dearly and always cheered me up whenever I was so depressed. I counted the bright stars with your encouragement.

List of abbreviations

NMR	=	Nuclear Magnetic Resonance
ppm	=	parts per million
IR	=	Infra-red
thf	=	Tetrahydrofuran
ORTEP	=	Oak Ridge Thermal Elipsoid Program
ⁱ Pr	=	isopropyl
Cy	=	Cyclohexyl
Ph	=	Phenyl
Cp	=	Cyclopentadienyl
Cp*	=	Pentamethyl cyclopentadienyl
Cp'	=	Methyl cyclopentadienyl
Me	=	methyl
°A	=	angstroms
cm ⁻¹	=	wave number
Py	=	pyridine
gm	=	grams
MHz	=	frequency in megahertz
mmol	=	millimoles
ml	=	milliliter
R	=	alkyl group
TMEDA	=	N,N,N',N' tetramethylethylenediamine
X	=	halogen

List of Figures

- Figure 2.1 The ORTEP diagram of $\text{Ta}(\text{NMe}_2)_4[\text{CyNC}(\text{NMe}_2)\text{NCy}]$ (2.1) showing one of the two unique molecules in the unit cell. 40
- Figure 2.2 The ORTEP diagram of $\text{Ta}(\text{NMe}_2)_4[\text{CyNC}(\text{NMe}_2)\text{NCy}]$ (2.1) showing one of the two unique molecules in the unit cell. 41
- Figure 3.1 The ORTEP diagram of N, N', N''-Tricyclohexylguanidinium-chloride $\{[\text{CyN}(\text{H})]_2\text{CNHCy}\}\text{Cl}$ (3.1) 56
- Figure 3.2 The ORTEP diagram of N, N', N''-Triisopropylguanidine $\{[\text{PrN}(\text{H})]_2\text{CN}^{\text{Pr}}\}$ (3.2) showing one of the unique molecules in the unit cell. 59
- Figure 3.3 The ORTEP diagram of N, N', N''-Triisopropylguanidine $\{[\text{PrN}(\text{H})]_2\text{CN}^{\text{Pr}}\}$ (3.2) showing one of the unique molecules in the unit cell. 60
- Figure 3.4. The ORTEP diagram of $\text{Ta}(\text{NMe}_2)_3[(\text{CH}_3)_2\text{CHN}]_2\text{CNCH}(\text{CH}_3)_2$ (3.4) 66
- Figure 3.5 The ORTEP diagram of $\text{Ta}(\text{NMe}_2)_3[(\text{CyN})_2\text{C}(\text{NCy})]$ (3.5) 72
- Figure 3.6 The ORTEP diagram of $\text{TaCl}(\text{NMe}_2)_3\{[(\text{CH}_3)_2\text{CHN}]_2\text{CN}(\text{H})\text{CH}(\text{CH}_3)_2\}$ 78
- Figure 4.1. The ORTEP diagram of $\text{NbMeCl}_3(\text{CyN})_2\text{C}(\text{NHCy})$ (4.1) 92
- Figure 4.2 The ORTEP diagram of $\text{TaMe}_2\text{Cl}_2\{[(\text{CH}_3)_2\text{CHN}]_2\text{C}[\text{NHCH}(\text{CH}_3)_2]\}$ (4.4) 97

List of Tables

Table 2.1. Summary of crystal data and structure refinement for Ta(NMe ₂) ₄ [CyNC(NMe ₂)NCy]	36
Table 2.2. Bond lengths [Å] for Ta(NMe ₂) ₄ [CyNC(NMe ₂)NCy] (2.1)	37
Table 2.3. Bond angles [deg] for Ta(NMe ₂) ₄ [CyNC(NMe ₂)NCy] (2.1)	38
Table 3.1. Crystal data and structure refinement for N, N', N''-Tricyclohexylguanidine {[CyN(H)] ₂ CNCy}HCl	54
Table 3.2. Bond lengths [Å] and angles [deg] for 3.1	55
Table 3.3. Crystal data and structure refinement for N, N', N''-Triisopropylguanidine {[ⁱ PrN(H)] ₂ CN ⁱ Pr}	58
Table 3.4. Bond lengths [Å] for 3.2.	61
Table 3.5. Bond angles [deg] for 3.2.	62
Table 3.6. Crystal data and structure refinement for Ta(NMe ₂) ₃ [(CH ₃) ₂ CHN] ₂ CNCH(CH ₃) ₂ 3.3.	67
Table 3.7. Bond lengths [Å] for 3.3.	68
Table 3.8. Bond angles [deg] for 3.3.	69
Table 3.9. Crystal data and structure refinement for Ta(NMe ₂) ₃ [(CyN) ₂ C(NCy)] 3.5	71
Table 3.10. Bond lengths [Å] for 3.5	73
Table 3.11. Bond angles [deg] for 3.5	74
Table 3.12. Summary of crystal data collection and structure refinement for TaCl(NMe ₂) ₃ {[(CH ₃) ₂ CHN] ₂ CN(H)CH(CH ₃) ₂ }	79
Table 3.13. Bond lengths [Å] for TaCl(NMe ₂) ₃ {[(CH ₃) ₂ CHN] ₂ CN(H)CH(CH ₃) ₂ }	80
Table 3.14. Bond angles [deg] for TaCl(NMe ₂) ₃ {[(CH ₃) ₂ CHN] ₂ CN(H)CH(CH ₃) ₂ }	81

Table 4.1 Crystal data and structure refinement for $\text{NbMeCl}_3(\text{CyN})_2\text{C}(\text{NHCy})_4$	93
Table 4.2 Bond lengths [Å] for 4.1	94
Table 4.3 Bond angles [deg] for 4.1	95
Table 4.4. Crystal data and structure refinement for $\text{TaMe}_2\text{Cl}_2\{[(\text{CH}_3)_2\text{CHN}]_2\text{C}[\text{NHCH}(\text{CH}_3)_2]\}$	98
Table 4.5. Bond lengths [Å] for 4.4	99
Table 4.6. Bond angles [deg] for 4.4	100

Table of Contents

Chapter 1.	Introduction and Literature Survey	
	Ligand design	1
	Literature review	7
	Goals, Hypotheses and Approaches	14
	References for Chapter 1	19
Chapter 2.	Insertion Routes to Tetrasubstituted Guanidinate complexes of M(V) (M = Nb, Ta)	
	Introduction	23
	Experimental	28
	Results and Discussion	33
	References for Chapter 2	44
Chapter 3.	Reactions Between Guanidines and M(NMe₂)₅ (M = Ta, Nb) Protonation Pathways to metal Guanidinate Complexes I	
	Introduction	46
	Experimental	48
	Results and Discussion	52
	Preparation of Guanidinate Complexes	63
	Isolation of TaCl(NMe ₂) ₃ { [(CH ₃) ₂ CHN] ₂ CN(H)CH(CH ₃) ₂ }	75
	References for Chapter 3	82
Chapter 4.	Reaction Between Guanidines with Metal Alkyl Groups Protonation Pathways to Metal Guanidinate Complexes II	
	Introduction	83
	Experimental	85
	Results and Discussion	89
	References for Chapter 4	101

Chapter 1.

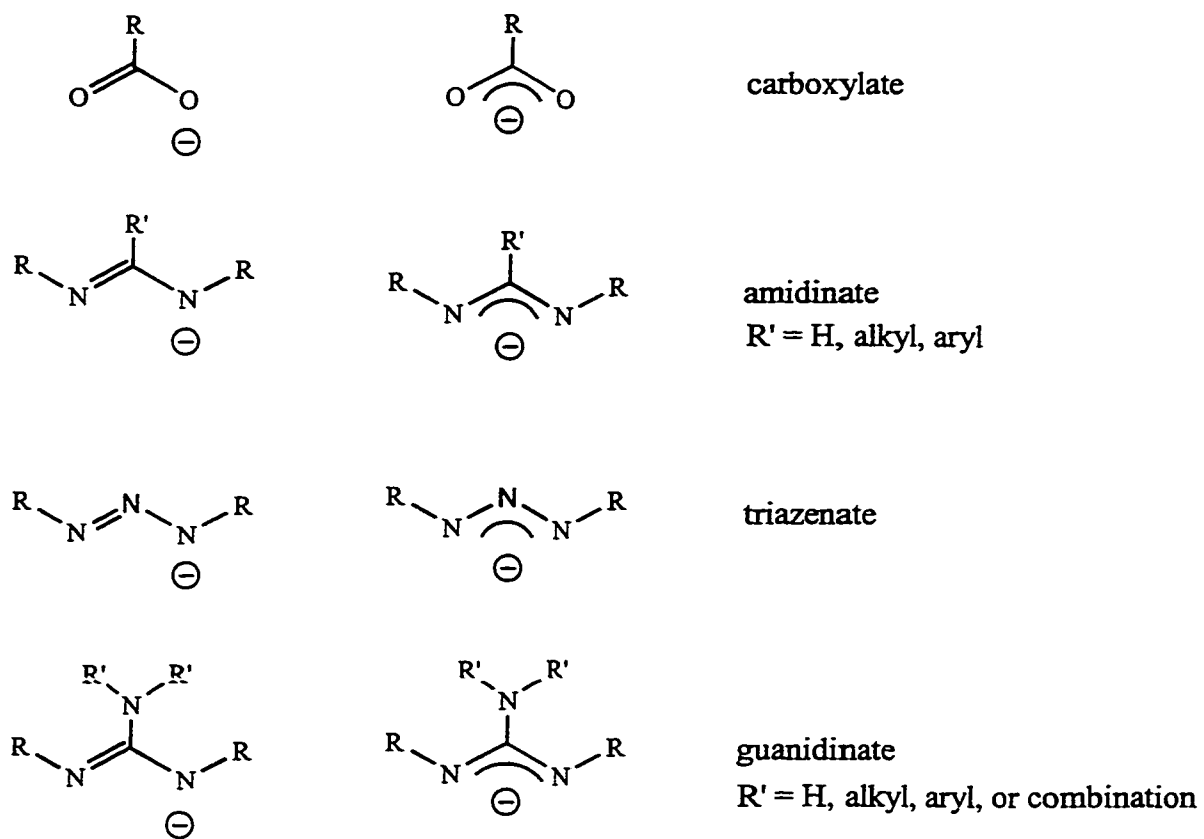
Introduction and Literature Survey

Ligand design

Ligand design is important in organometallic chemistry due to each ligand's unique characteristics such as (i) the difference in electronic and steric effects which are useful to tune the activity of the metal complexes. (ii) ability to stabilize the oxidation state of the metal by their coordination.

Amidates and triazates, the anionic 1,3-nitrogen analogues of carboxylates, are well established as versatile and flexible ligand systems for a variety of transition metal and main group metal centers (Scheme 1.1).¹ Among the important features of these species are the increased donor ability of nitrogen relative to oxygen and the potential to explore both the steric and electronic effects induced by the variation of organic substituents in the ligand framework. This is particularly true and has been heavily exploited in the amidate ligand system, for which a wide variety of organic substituents on both nitrogens and the central carbon atoms have been reported.² Such variations lead to the observation that both of these ligands are frequently encountered in a variety of coordination modes.

Guanidine, the amidine of carbamic acid ($\text{H}_2\text{NC(O)OH}$), also falls into this general class of ligands and, in contrast to the aforementioned species, has received limited attention in inorganic coordination and organometallic chemistry. Guanidines may be stronger donor ligands than amidates and will certainly possess all of the same coordination properties of amidines. The presence of an additional nitrogen atom that can play a role in the coordination of these species is a key difference between these ligands. Furthermore, this third nitrogen center can bear either one or two organic substituents (NR'_2 or $\text{N(H)R}'$) depending on the degree of substitution. This allows investigations based on variation of the R' substituents and/or the role of the NH function in either hydrogen bonding or further reactivity of the ligand.



Scheme 1.1

When considering the substitution of the five guanidine hydrogen atoms, only one isomer is possible for the mono and pentasubstituted compounds. Variable substitution patterns are available for the di, tri, and tetrasubstituted compounds. For the simplest case in which all of the organic substituents are equivalent, each of these offers two possible structural isomers, which are represented in Scheme 1.2. Two methods of enumerating these isomers are used in the literature; both methods are shown for the isomers displayed in Scheme 1.2.

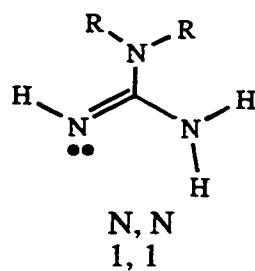
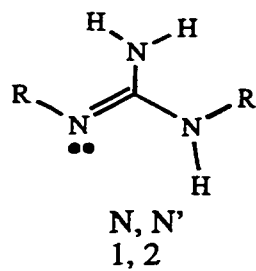
Guanidinate anions possess several important resonance structures, some of which are unique to this system. The discussion here is limited to the anions of the N, N', N''-trisubstituted and the N, N, N', N''-tetrasubstituted compounds with the resonance contributors summarized in Scheme 1.3. The presence of the second active hydrogen (N-H function) for the trisubstituted species begs the consideration of dianions of this compound.

The presence of a lone pair of electrons on the NR'_2 or $\text{N(H)R}'$ functions allows the zwitterionic resonance structure for the monoanionic species (I and II). In order for this particular contribution to be important two requirements should be met. First, the N centers must be planar, sp^2 hybridized with the lone pair of electrons localized in p orbital. Secondly, for there to be substantial overlap of this p orbital with the π system of the anion, there must be a small dihedral angle between the planes defined by the CNR'_2 or $\text{CN(H)R}'$ groups and that defined by the conjugated NCN moiety. Keeping in mind these two requirements, it is interesting to note that although the ability to stabilize the positive charge on nitrogen is likely to be superior for the disubstituted NR'_2 group relative to monosubstituted $\text{N(H)R}'$, the attendant steric congestion caused by the two organic substituents would probably encourage a larger dihedral angle thus discouraging the appropriate orientation for π conjugation.

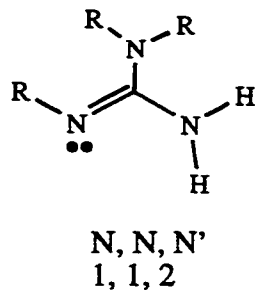
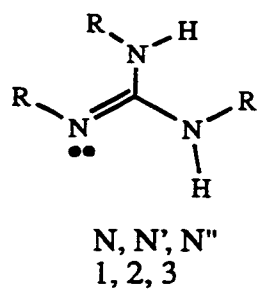
Clearly, the role of substituents from both an electronic and a steric standpoint will be important in analyzing the bonding in guanidinate anions.

The N, N', N''-trisubstituted guanidinate anion can be deprotonated to yield a dianionic species (Scheme 1.3). Such a compound is isoelectronic with carbonate anion and could exhibit similar π delocalization involving the three pairs of p electrons on three sp^2 hybridized nitrogen centers. Again, as with the monoanions, the requirement of a planar CN_3 core is also necessary to achieve the Y-conjugation shown for **III** in Scheme 1.3.

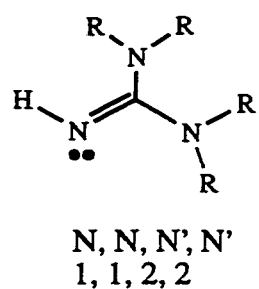
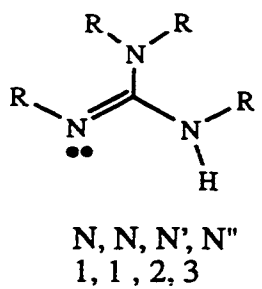
Disubstituted



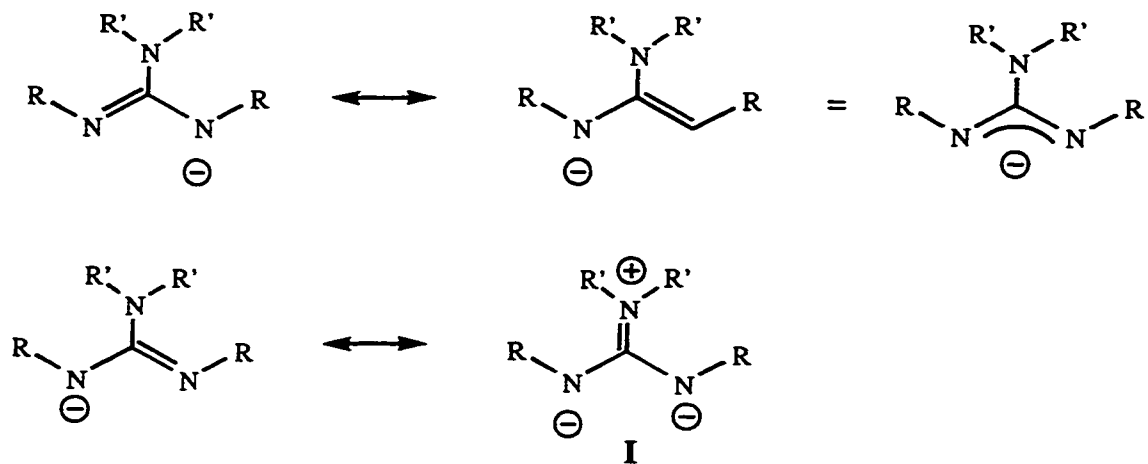
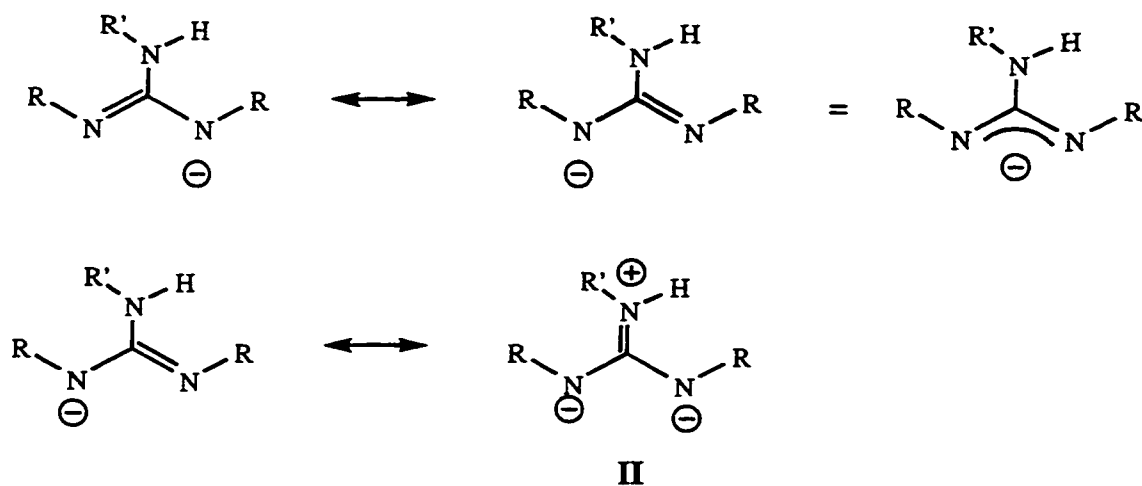
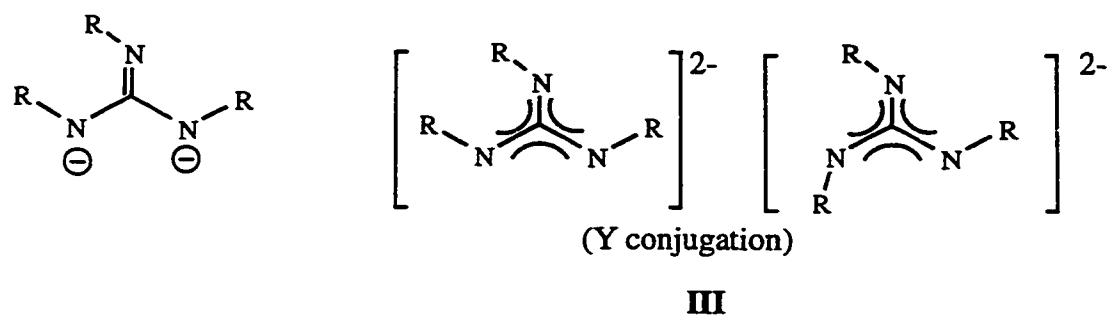
Trisubstituted



Tetrasubstituted



Scheme 1.2

tetrasubstituted monoanionictrisubstituted monoanionictrisubstituted dianionic

Scheme 1.3

Literature review:

These considerations provide a foundation for an examination of the literature and the role of guanidines and particularly guanidinate anions in inorganic chemistry. Mehrotra has organized inorganic compounds containing guanidine moieties into three classes: cationic guanidinium salts, neutral adducts, and substitution products.³ The following discussion is based on this organization.

Exploiting the basicity of the imine lone pair on guanidine and its derivative forms the bulk of the inorganic chemistry of these species. Perhaps the simplest use of guanidines has been as guanidinium salts derived by the ready protonation of these rather strong bases. These compounds are not particularly pertinent to this thesis and will not be considered further.

In addition to their appearance as counter ions for inorganic anions, guanidines have been reported to function as neutral donors, through the imine nitrogen lone pair, to metal centers. Such species constitute the second class of compounds.

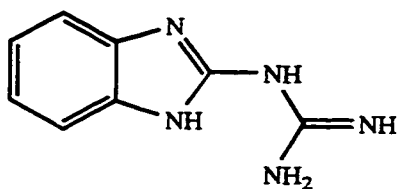
The third class of guanidine containing compounds, substituted products, consists of complexes that possess guanidinate anions and dianions. Several modes of binding can be suggested for these compounds some of which are summarized in Scheme 1.4. Structures **IV**, **V**, and **VI** display monodentate, chelating bidentate, and bimetallic bidentate bonding modes respectively. Similar structures have been observed for both amidinate and triazenate anions. The importance of considering the resonance structure of **V** has been previous mentioned.

The potential to generate a dianion in the case of a trisubstituted guanidine would likely yield a bidentate species. Two modes of binding chelating (**VII**) and bimetallic bidentate (**VIII**) are likely and two other possible binding modes for the dianion, **IX** and **X**, are presented in Scheme 1.4. Neither the tridentate bimetallic (**IX**) nor the π bonded (**X**) ligand have yet been observed. It is interesting to note that structure **X** is a triazo analogue of trimethylenemethane.

These last two ligand-metal interactions seem to be especially enticing given that such motifs are not possible for the related amidinate or triazenate systems.

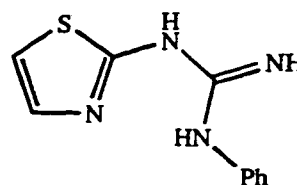
The first neutral donor complexes employing a tetrasubstituted guanidine (1,1,3,3-tetramethylguanidine) were reported long ago. Guanidine coordinates to Lewis acidic boron compounds to form a series of $(\text{NH}_2)_2\text{CN}(\text{H})\text{BR}_3$ species.⁴ In addition, tetramethyl guanidine, $\text{HN}=\text{C}(\text{NMe}_2)_2$, forms a variety of adducts with several transition metals through donation of the imine electron pair.⁵ These species have been proposed to be simple adducts with monodentate ligands. This has been confirmed by single crystal X-ray structures in some cases.

Other substituted guanidines that have been used for adduct formation include N-phenyl-N'-(2-thiazolyl)guanidine (**XI**) and 2-guanidinobenzimidazole (**XII**) and N,N'-diphenylguanidine.⁶



2-guanidinobenzimidazole

XI

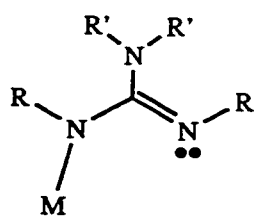


N-phenyl-N'-(2-thiazolyl)guanidine

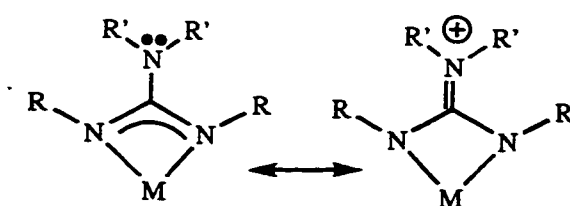
XII

Tetramethyl guanidine forms adducts with AlR_3 ($\text{R} = \text{Me}, \text{Et}$) and AlCl_3 .⁷ Heating the organoaluminum species caused elimination of RH and formation of the substituted compounds $(\text{Me}_2\text{N})_2\text{C}=\text{NAlR}_2$. A similar reaction with the $[(\text{Me}_2\text{N})_2\text{C}=\text{N}(\text{H})]\text{AlCl}_3$ did not proceed but $(\text{Me}_2\text{N})_2\text{C}=\text{NAlCl}_2$ could be synthesized by reaction of $(\text{Me}_2\text{N})_2\text{C}=\text{NLi}$ with AlCl_3 . These last two compounds represent early examples of the appearance of guanidinate anions.

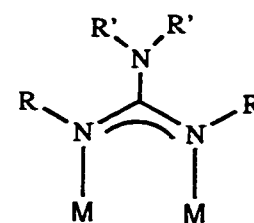
tetrasubstituted monoanionic and monoanionic trisubstituted



IV



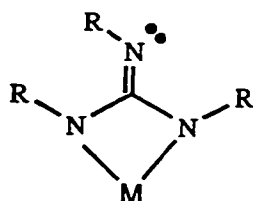
V



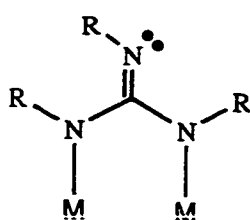
VI

R' = alkyl or H

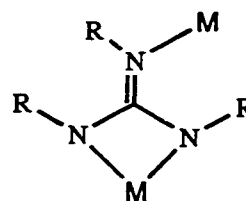
dianionic trisubstituted



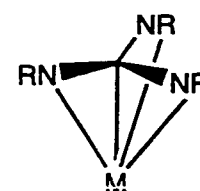
VII



VIII



IX



X

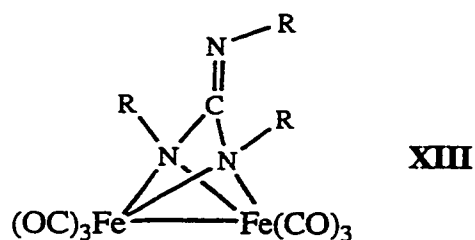
Scheme 1.4

Another early example of a guanidinate anion compound is $(\text{Me}_2\text{N})_2\text{C}=\text{NLi}$ which has been structurally characterized and shown to be hexameric.⁸

A series of tetrasubstituted guanidinate complexes with general formula of bis(dimethylamido)bis(guanidinate)M (M = Ti, Zr, Hf) represent early examples of guanidinate anions coordinated to transition metals.⁹ These complexes were prepared in what appears to be a general reaction of $\text{M}(\text{NMe}_2)_4$ with di(p-tolyl)carbodiimide and dicyclohexylcarbodiimide to yield the coordinated tetrasubstituted guanidates, N-p-tolyl-N',N'-dimethyl-N''-p-tolylguanidinate or N-cyclohexyl-N',N'-dimethyl-N''-cyclohexylguanidinate respectively.

Similar reactions were observed with some main group metals amido functions.^{9,10}

Before 1995, there is a single report of a dianionic guanidinate anion employed as a ligand.¹¹ The syntheses of N, N', N''-tricyclohexylguanidine and N, N', N''-triisopropylguanidine dianion coordinated to a dinuclear iron hexacarbonyl framework (**XIII**) were reported. These compounds were isolated as the unanticipated product of the reaction of $\text{Fe}(\text{CO})_5$ and carbodiimide. The crystal structure of the cyclohexyl complex was determined.



Recent years have seen a renewed interest in all aspects of guanidinate coordination chemistry. For example, guanidines have been used as neutral monodentate ligands for a variety of transition metals.

Treatment of CoCl_2 with 1,2,3-triphenylguanidine produced tetrahedral $\text{Co}[\text{PhN}=\text{C}(\text{NHPH})_2]\text{Cl}_2$. A structural study revealed that the guanidine was coordinated only

through the imine nitrogen atom. Similar treatment of $\text{Ag}(\text{O}_3\text{SCF}_3)$ with 1,2,3-triphenylguanidine gave the linear cationic species $\text{Ag}[\text{PhN}=\text{C}(\text{NHPH})_2]_2^+$ with an uncoordinated triflate anion. Single crystal X-ray analysis of this salt indicated that although the triflate anion was uncoordinated to the Ag(I) center, it was hydrogen bonded to the guanidine N-H function.¹²

Other recent examples of structurally characterized neutral adducts of guanidine ligands include 1,1,2,2-tetramethyl guanidine as a monodentate ligand in

$\text{Tc}(\text{N})(\text{SC}_6\text{H}_4)_2(\text{NHC}(\text{NMe}_2)_2)_2$ ¹³ and the compounds $\text{PtI}_2(\text{NHR}_2)[\text{HN}=\text{C}(\text{NR}'_2)_2]$ ¹⁴

($\text{R}' = \text{Et}, -(\text{CH}_2)_5-, -(\text{CH}_2\text{CH}_2\text{OCH}_2\text{CH}_2)-$).

N,N'-diphenyl and N, N', N''-triphenylguanidine are reported to react with $\text{MnBr}(\text{CO})_5$ to yield the neutral coordinated guanidine complexes *cis*- $\text{Mn}(\text{Br})\{\text{PhN}=\text{C}(\text{NHPH})(\text{NHR})\}(\text{CO})_4$ and *fac*- $\text{Mn}(\text{Br})\{\text{PhN}=\text{C}(\text{NHPH})(\text{NHR})\}_2(\text{CO})_3$ ($\text{R} = \text{H}, \text{Ph}$).¹⁵ Heating and addition of excess ligand produced $\text{Mn}\{(\text{PhN})_2\text{C}(\text{NHR})(\text{CO})_4$ ($\text{R} = \text{H}, \text{Ph}$) which was proposed to contain a bidentate anionic guanidine. In a similar reaction $\text{CpMo}(\text{CO})_3\text{Cl}$ reacted with elimination of HCl to lead to formation of $\text{CpMo}(\text{CO})_2(\text{PhNC}(\text{NHR})\text{NPh})$ ($\text{R} = \text{H}, \text{Ph}$). Crystal structures of these molybdenum compounds confirmed the bidentate binding of the guanidinate ligand.

The first example of a bridging guanidine monoanion (structure VI in Scheme 1.4) between two Pt(II) centers $\{\text{Pt}_2(2,2':6',2''\text{-terpyridine})_2[(\text{NH})_2\text{CNH}_2]\}^{3+}$ was reported in 1992.¹⁶

Several other late transition metal complexes of guanidinate anions have also been reported recently. The reaction of $(\text{Cp}^*\text{RhCl}_2)_2$ or $[(\eta^5\text{-MeC}_6\text{H}_4^i\text{Pr})\text{RuCl}_2]_2$ with 4 equivalents of 1,2,3-triphenylguanidine gave monomeric complexes with chelating guanidinate monoanions and concomitant precipitation of guanidinium hydrochloride salt in both cases.¹⁷ These complexes represented the first structurally characterized examples of chelating guanidinate anions (structure V in Scheme 1.4). Proton and carbon NMR spectra indicated a 2:1 ratio for the

phenyl groups of the triphenylguanidinate ligand consistent with unrestricted rotation about the C-N(H)Ph bond. Single crystal X-ray studies indicated that the ligand possessed a planar CN₃ core and the authors speculated that the uncoordinate N atom was sp² hybridized. However, there was no information provided on the angle of the C-N(H)R plane relative to the N-C-N-M plane. In addition, the C-N(H)Ph bond distance and the unrestricted rotation observed in the NMR spectra indicate that there is little π conjugation in these systems.

N,N'-diphenylguanidine has been reported to react with Ru(II), Os(II) and Ir(III) hydrides, through protonation of the M-H function and elimination of H₂, to yield chelating guanidinate complexes.¹⁸ MH₂(CO)(PPh₃)₃ (M = Ru, Os) give complexes with a bidentate diphenylguanidinate ligand, MH(PhNC(NH₂)NPh)(CO)(PPh₃)₂. Similar reaction with the triflate complexes, M(O₃SCF₃)₂(CO)(PPh₃)₃, gave bis(guanidinate) compounds with one bidentate and one monodentate ligand. Reaction of Ir(H)₃(PPh₃)₃ with diphenylguanidine produced Ir(H)₂(PPh₃)₂(PhNC(NH₂)NPh) in which the guanidinate ligand was bidentate.

Flexibility in the donor properties of guanidinate ligands was further demonstrated by the report of a quadruply bonded Mo-Mo complex, Mo₂{ μ - η^2 -[(PhN)₂CN(H)Ph]₄}, with four bridging triphenylguanidinate monoanions.¹⁹ This complex was prepared by the reaction of the Mo(CO)₆ with 1,2,3-triphenylguanidine through a combination substitution and redox reaction to generate Mo(II) and H₂. This complex could be reversibly oxidized by both one and two electrons. An X-ray crystal structure of the parent and cationic complexes showed a planar CN₃ core and indicated a planar sp² N(H)Ph group. However, the measured angles between these two planes defined by these groups ranged from 55.3(8)° to 31(1)° and this, combined with the C-N(H)Ph bond distances, indicated little π conjugation between these moieties.

There are also several interesting recent examples of main group complexes with coordinated guanidinate anions and dianions.

The dilithiation of triphenylguanidine with n-butyllithium in hexane has been reported.²⁰ Single crystal X-ray structural analysis revealed the dianion to be planar. The authors noted that this novel triazatrimethylenemethane system $(\text{C}(\text{NPh})_3)^{2-}$ was isoelectronic with trimethylenemethane $(\text{C}(\text{CH}_2))^{2-}$ and carbonate (CO_3^{2-}) anions. The possibility of π delocalization or Y-conjugation (structure **III** in Scheme 1.3) was addressed by the authors. However, one important piece of information, the relative orientation of the C-NPh planes, was not provided. The ^{13}C NMR of the dianion exhibited equivalent phenyl substituents at 293K indicating that this species may be fluxional in solution. Unfortunately, there is only a single brief report for the 'reaction' of this dilithiotriphenylguanidine with $\text{Cd}(\text{NTMS}_2)_2$.²¹ In fact a single crystal X-ray analysis of the product of this reaction revealed it to be a 'co-complex' of the two starting materials.

The reaction of N,N',N''-triisopropylguanidine with $\text{Sb}(\text{NMe}_2)_3$ gave a very low yield (10%) of a highly air sensitive complex which exhibited one monoanionic and one dianionic ligand, $\text{Sb}[(^i\text{PrN})_2\text{CNH}^i\text{Pr}][(^i\text{PrN})_3\text{C}]$.²² The ^1H NMR of this compound, which exhibited five isopropyl groups in 1:1:1:1:2 ratio, was interpreted as the result of free rotation about the C-NHR bonds but hindered rotation around the C=NR bonds. A single crystal X-ray analysis of this material showed it to be an interesting material that consisted of a helical array of highly distorted trigonal bipyramidally coordinated Sb centers. Although the ligands span the axial/equatorial sites the observed angles were less than 90° due to the limited bite of the N-C-N function. The helices are held together through hydrogen bonded N...H-N functions which results in indistinguishable monoanionic and dianionic ligands.

One final comment regarding nomenclature should be made before concluding the overview of the pertinent literature. Several different naming schemes for complexes containing guanidine moieties have appeared that may appear to be conflicting and could lead to confusion. The term "guanidinium" has been applied to both the coordinated and the protonated species. While this is certainly appropriate for the later species, one is cautioned not to be misled by the use of this name in the case of neutral guanidine molecules coordinated to a metal center through the imine lone pair of electrons. The terms "guanidino" and "guanidinate" have both been used for anionic or substituted guanidine-based ligands. In keeping with the common use of amidinate and triazenate for the analogous ligands, this thesis will consistently use guanidinate when discussing deprotonated ligands.

Goals, Hypotheses and Approaches:

The investigations reported in this thesis began with an interest in extending the expertise of our group with alkyl substituted amidinate ligands to include guanidinate ligands. More specifically this thesis focuses on guanidates with the high degree of substitution, i.e. the N, N', N''-trialkyl substituted or N, N, N', N''-tetra (alkyl) substituted species. In addition, all the alkyl substituents were restricted to being equivalent in order to eliminate the possibility of different isomers being formed in the product complexes. Other reasons for restricting the scope of these investigations to this realm are detailed in the remainder of this chapter and in the following chapters.

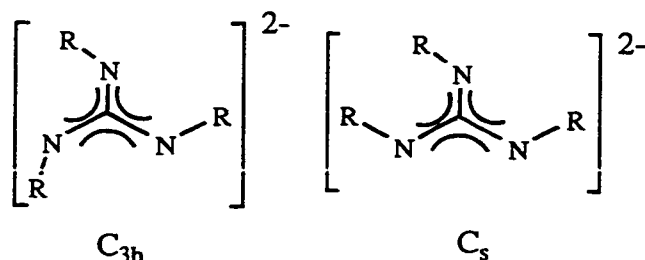
As previously described, a key feature of ligands with the general formula $RNXNR^-$ ($X = CNR'_2, CR',$ or N) is the ability to modify the organic substituents which may in turn allow rational variations to the steric and electronic parameters of the system. Guanidinate anions offer

several unique characteristics that formed the basis of the work in this thesis. These features are all coupled to the presence of a third nitrogen site within the ligand and, although they are intimately interconnected, they can be broken into three broad themes: efforts to manipulate the sterics, electronics and ultimately the bonding properties of these ligands.

Perhaps the most obvious of these features is the ability to change the size/sterics of substituents on the third nitrogen center. Alkyl groups offer the most direct means of implementing such changes. While phenyl substituted guanidates have received considerable attention in the recent literature,^{15,17,19,20,21} the ability to vary the steric parameters of aryl groups is more limited and not as straightforward. The steric impact of variations of the organic groups on the third nitrogen atom clearly depends on the orientation of the NR'_2 or $\text{N(H)R}'$ moieties within the ligand.

The electronic features that arise from the additional resonance are a second unique aspect of guanidate ligands. These have been summarized in Scheme 1.3. In particular, structures I and II, which do not have counterparts in amidinate ligands, are noteworthy. The π delocalization of the NR'_2 or $\text{N(H)R}'$ lone pair increases the charge on the nitrogen atoms bonded to the metal. This should lead to an increase the metal-ligand bond energy in the complex especially in the case of high oxidation states or electron deficient metals. Furthermore, restriction of the R groups to alkyls removes the possibility of unanticipated resonance contributions and, through inductive effects, will likely increase the donor ability of the ligand. The steric interactions of the R and R' groups will also exert an effect on the relative orientation of the NR'_2 or $\text{N(H)R}'$ groups to the N-C-N plane.

Finally, the presence of the third nitrogen center in guanidates affords binding modes that are not available in case of amidinate ligands (Scheme 1.4). In particular, the ability to generate dianionic ligands from a trisubstituted guanidine may offer some novel coordination modes (structures IX and X). Again, the interplay of steric interactions of the R' and R groups as well as the degree of π electronic delocalization will have a direct impact here. For example, the interactions of the bulky alkyl groups might promote a C_{3h} orientation for the dianion as opposed to the C_s orientation observed in case of $Li_2(C(NPh)_3)^{20}$. Efforts to get the dianionic form of the ligand should be favored by electron deficient metals in high oxidation states. As



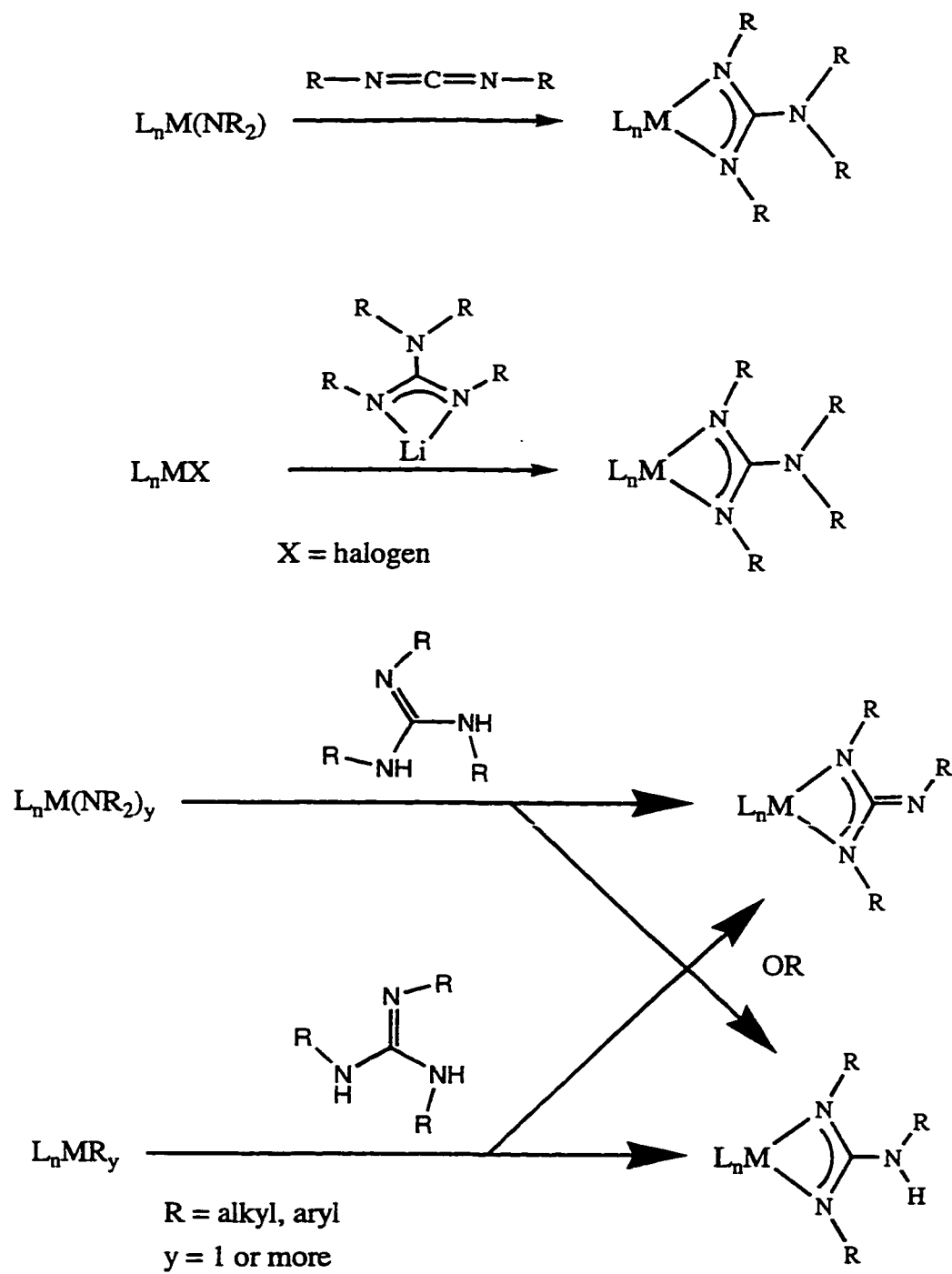
noted above, the dianionic species is isoelectronic with trimethylene methane dianion that is known to coordinate a wide range of metal in the η^4 mode (structure X).^{23,24}

As this thesis work began, the central objective was the synthesis of complexes with guanidinate ligands with the goal of exploring the issues of metal-ligand bonding outlined above. This requires the development of fundamental ideas regarding the introduction of guanidinate anions and dianions in coordination chemistry, the features that favor different binding modes of the ligand, and the general reactivity characteristics of these complexes. The literature provides some ideas on methods for introduction of guanidates into the coordination sphere of a metal but very few principles for predicting bonding modes and essentially nothing regarding the reactivity of such complexes.

When considering the methodology for the introduction of the ligands, several routes were considered. The ones chosen for investigation in this thesis are summarized in Scheme 1.5.

Insertion reactions of carbodiimides into transition metal-N(amido) bonds offer a known but surprisingly unused route to transition metal complexes of guanidates.⁹ This avenue is limited by the availability of a transition metal amido species. Efforts to extend this reaction to high oxidation state Ta and Nb amido complexes are presented in Chapter 2. A two step variation involving first the insertion of carbodiimide into a main group metal-N(amido) bond followed by a metathesis reaction with a transition metal halide may also be a viable method to generate guanidate anions or dianions. In Chapter 2, the reaction of lithium amido compounds with carbodiimides to generate the guanidate anion followed by reaction with metal halides is discussed as a potential synthetic route.

Chapters 3 and 4 present efforts to employ direct reaction of trisubstituted guanidines with metal-amido or metal-alkyl functions respectively. Such reactions would proceed by protonation of the functional group, release of amine or alkyl and generation/introduction of the guanidate anion. Although restricted by the ability to prepare the appropriate metal complexes, this route was found to offer a simple method to produce complexes with monoanionic and dianionic guanidate ligands.



Scheme 1.5

References for Chapter 1.

- ¹ (a) Barker, J; Kilner M. *Coordination Chemistry Reviews*, **1994**, *133*, 219. (b) Moore, D. S.; Robinson, S. D. *Adv. Inorg. Chem. Radiochem.* **1986**, *30*, 1.
- ² Coles, M.P.; Jordan, R.F. *J. Am. Chem. Soc.* **1997**, *119*, 8125. Coles, M.P.; Swenson, D. C.; Jordan, R.F.; Young, V.G. *Organometallics* **1997**, *16*, 5183. Zhou, Y.; Richeson, D. S. *Inorg. Chem.* **1996**, *35*, 1423. Berno, P.; Hao, S.; Minhas, R.; Gambarotta, S. *J. Am. Chem. Soc.* **1994**, *116*, 7417 and references therein.
- ³ Mehrotra in *Comprehensive Coordination Chemistry*, Abel, E. W.; Stone, F. G. S.; Wilkinson, G. Eds.; Pergamon Press: Oxford, U.K., 1995 Vol. 4, Chapter 2, and references therein.
- ⁴ (a) Yuzhakova, G. A.; Lapkin, I. I.; Drovneva, R. P.; Mazilkina, M. V. *Russ. J. Inorg. Chem* **1981**, *51*, 880 (b) Yuzhakova, G. A.; Drovneva, R. P.; Vakhnin, M. I.; Lapkin, I. I. *Russ. J. Inorg. Chem.* **1977**, *48*, 740
- ⁵ Longhi, R.; Drago, R. S. *Inorg. Chem.* **1965**, *4*, 11.
- ⁶ Canty, A. J.; Fyfe, M.; Gatehouse, B. M. *Inorg. Chem.* **1978**, *6*, 1467. Ghosh, S. P., Bhattacharjee, P.; Dubey, L.; Mishra, L. K. *J. Indian. Chem. Soc.* **1977**, *54*, 230. Banerjee, A. K.; Ghosh, S. P. *J. Indian. Chem. Soc.* **1974**, *51*, 720. Malik, W. U.; Srivastava, P. K.; Mehra, S. C. *J. Indian. Chem. Soc.* **1973**, *50*, 739.

- ⁷ Snaith, R.; Wade, K.; Wyatt, B. K. *J. Chem. Soc. (A)* **1970**, 380.
- ⁸ Clegg, W.; Snaith, R.; Shearer, H. M. M.; Wade, K.; Whitehead, G. *J. Chem. Soc., Dalton Trans.* **1983**, 1309. Pattison, L.; Wade, K.; Wyatt, B. K. *J. Chem. Soc. (A)* **1968**, 837.
- ⁹ Chandra, G.; Jenkins, A. D.; Lappert, M. F.; Srivastava, R. C. *J. Chem. Soc. (A)* **1970**, 2250.
- ¹⁰ For examples with M = B see: Jefferson, R.; Lappert, M. F.; Prokai, B.; Tilley, B. P. *J. Chem. Soc.* **1966**, 1584. For examples with M = Si, Ge, Sn see: (a) Matsuda, I.; Itoh, K.; Ishii, Y. *Journal of Organometallic Chemistry* **1974**, *69*, 353. (b) George, T.A; Jones, K.; Lappert, M. F. *J. Chem. Soc.* **1965**, 2157.
Example with Mg: Srinivas, B.; Chang, C.-C.; Chen, C.-H.; Chiang, M. Y.; Chen, I.-T.; Wang, Y.; Lee, G.-H. *J. Chem. Soc., Dalton Trans.* **1997**, 957.
- ¹¹ Bremer, N. J.; Cutcliffe, A.B.; Farona, M. F.; Kofron, W. G. *J. Chem. Soc. A.* **1971**, 3264.
Bremer, N. J.; Cutcliffe, A.B.; Farona, M. F. *J. Chem. Soc., Chem. Commun.* **1970**, 932.
- ¹² Bailey, P. J.; Grant, K. J.; Pace, S.; Parsons, S.; Stewart, L. J. *J. Chem. Soc., Dalton Trans.* **1997**, 4263.
- ¹³ deVries, N.; Costello, C. E.; Jones, A. G.; Davison, A. *Inorg. Chem.* **1990**, *29*, 1348.
- ¹⁴ Fehlhammer, W. P.; Metzner, R.; Sperber, W. *Chem. Ber.* **1994**, *127*, 829.

- ¹⁵ da S. Maia, J. R.; Gazard, P. A.; Kilner, M. Batsanova, A. S.; Howard, J. A. K. *J. Chem. Soc., Dalton Trans.* **1997**, 4625.
- ¹⁶ Yip, H.-K.; Che, C.-M.; Zhou, Z.-Y.; Mak, T. C. W. *J. Chem. Soc., Chem. Commun.* **1992**, 1369.
- ¹⁷ Bailey, P. J.; Mitchell, L. A.; Parsons, S. *J. Chem. Soc., Dalton Trans.* **1996**, 2839.
- ¹⁸ Robinson, S. D.; Sahajpal, A. *J. Chem. Soc., Dalton Trans.* **1997**, 3349.
- ¹⁹ Bailey, P. J.; Bone, S. F.; Mitchell, L. A.; Parsons, S.; Taylor, K. J.; Yellowless, L. J. *Inorg. Chem.* **1997**, *36*, 867.
- ²⁰ Bailey, P. J.; Blake, A. J.; Kryszczuk, M.; Parsons, S.; Reed, D. *J. Chem. Soc., Chem. Commun.* **1995**, 1647.
- ²¹ Bailey, P. J.; Mitchell, L. A.; Raithby, P. R.; Rennie, M.-A.; Verhorevoort, K.; Wright, D. S. *Chem. Commun.* **1996**, 1351.
- ²² Bailey, P. J.; Gould, R. O.; Harmer, C. N.; Pace, S.; Steiner, A.; Wright, D. S. *Chem. Commun.* **1997**, 1161.
- ²³ Jones, M. D.; Kemmit, R. D. W. *Adv. Organomet. Chem.* **1987**, *27*, 279 and references therein.

²⁴ For examples of heterotrimethylene methane ligands see: Seyferth, D.; Wang, T.; Davis, W. *M. Organometallics* **1994**, *13*, 4134. Hartwig, J. F.; Andersen, R. A.; Bergman, R. G. *J. Am. Chem. Soc.* **1990**, *112*, 5670. Ando, W.; Choi, N.; Kabe, Y. *J. Am. Chem. Soc.* **1990**, *112*, 4574. Ando, W.; Yamamoto, T.; Saso, H.; Kabe, Y. *J. Am. Chem. Soc.* **1991**, *113*, 2791. Kabe, Y.; Yamamoto, T.; Ando, W. *Organometallics* **1994**, *13*, 4606. Jarvis, J. A. J.; Job, B. E.; Kilbourn, B. T.; Mais, R. H. B.; Owston, P. G.; Todd, P. F. *J. Chem. Soc., Chem. Commun.* **1967**, 1149. Armstrong, D. R.; Mulvey, R. E.; Barr, D.; Snaith, R.; Wright, D. S.; Clegg, W.; Hodgson, M. *J. Organomet. Chem.* **1989**, *362*, C1. Ohe, K.; Ishihara, T.; Chatani, N.; Murai, S. *J. Am. Chem. Soc.* **1990**, *112*, 9646.

Chapter 2. Insertion Routes to Tetrasubstituted Guanidinate complexes of M(V) (M = Nb, Ta).

Introduction

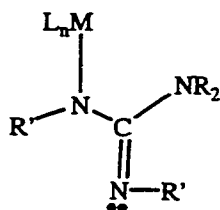
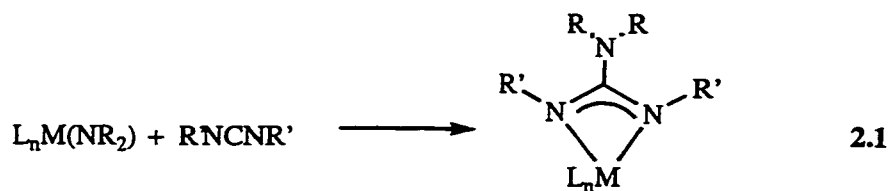
Insertion reactions are one of the most general and significant reactions in organometallic and coordination chemistry.¹ Among the features that make insertion reactions important are the following:

1. Their use provides elegant and simple syntheses for a wide variety of new compounds, especially those having functional groups.
2. In identifying their role, many important processes, particularly catalytic processes, are better understood.

Insertion reactions of metal complexes of type L_nM-X may be classified according to the nature of the M-X bond and the identity of the inserting species.

As outlined in Chapter 1, this thesis is concerned with the preparation and examination of guanidinate complexes. One method of synthesis of such ligands, also presented in Chapter 1, is the insertion of carbodiimide into a metal-amido group. In the case of a disubstituted amido ligand this reaction would yield a tetrasubstituted guanidinate ligand. In the case of a monosubstituted amido ligand, the insertion yields a trisubstituted guanidinate. The general form of this reaction is given as equation (2.1). After 1,2 insertion of the C=N bond, A, the coordination of the imine lone pair would yield the bidentate guanidinate anion. An alternative but equivalent view of this reaction

is as the nucleophilic addition of an negatively charged amido ligand to the central, positively polarized C atom of the carbodiimide.

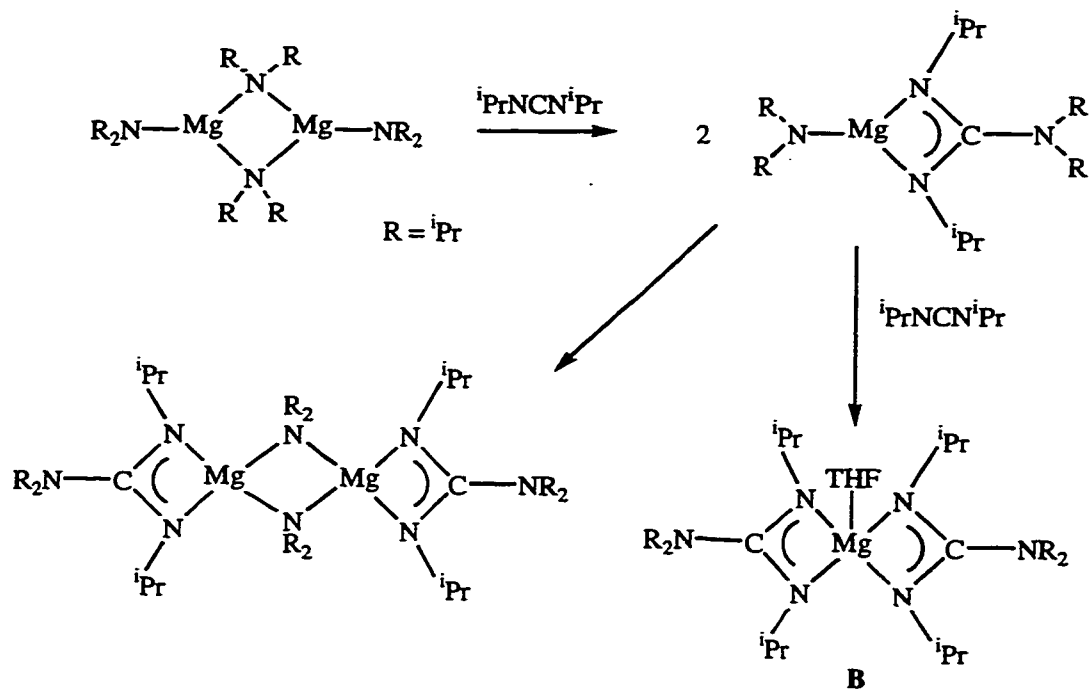


A

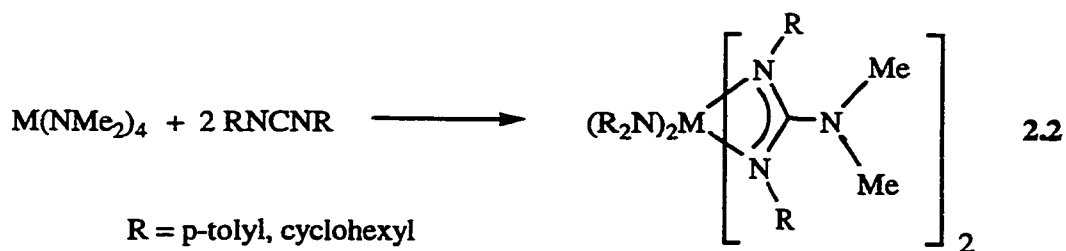
While the insertion reactions of carbodiimides is rather well-known for a variety of $M-H^2$ and $M-R^{3,4}$ species where M is either a main group or transition metal, the analogous reactions with $M-Cl^5$ and $M-N^{6,7,8,9}$ are less well developed especially for the transition metals. The insertion reactions of metal complexes with related isoelectronic species such as isocyanates and isothiocyanates are outside the scope of this thesis. In general, the reported results for the insertion of carbodiimides indicate that the reactions proceed in excellent yields and it is rare for mixtures of products to be obtained.

Two reports are of particular pertinence to this thesis. The first is the report of a series of carbodiimide insertion reactions into magnesium amides, which are summarized in Scheme 2.1.⁶ Complex B was characterized by X-ray crystallography.

Scheme 2.1



The second represents the only reported example of insertion of carbodiimides into transition metal amido functions. In what appears to be a general reaction (eq. 2.2), $M(\text{NMe}_2)_4$ ($M = \text{Ti}, \text{Zr}, \text{Hf}$) reacted in a clean fashion with di(*p*-tolyl)carbodiimide or dicyclohexylcarbodiimide to yield a series of bis(dimethylamido)bis(guanidinato) M complexes where the tetrasubstituted guanidinate, *N*-*p*-tolyl-*N'*,*N'*-dimethyl-*N''*-*p*-tolylguanidinate or *N*-cyclohexyl-*NN'*-dimethyl-*N''*-cyclohexylguanidinate respectively,

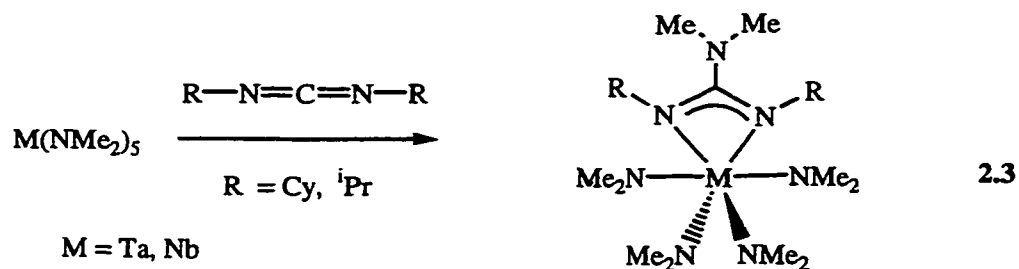


was derived by an insertion reaction.⁹ These complexes have formulae and structures postulated on the basis of C, H, N microanalysis, mass spectrometry, IR spectra and degradation studies. No attempts were made to prepare the monoinsertion product and these researchers report that further reactions with carbodiimide did not proceed.

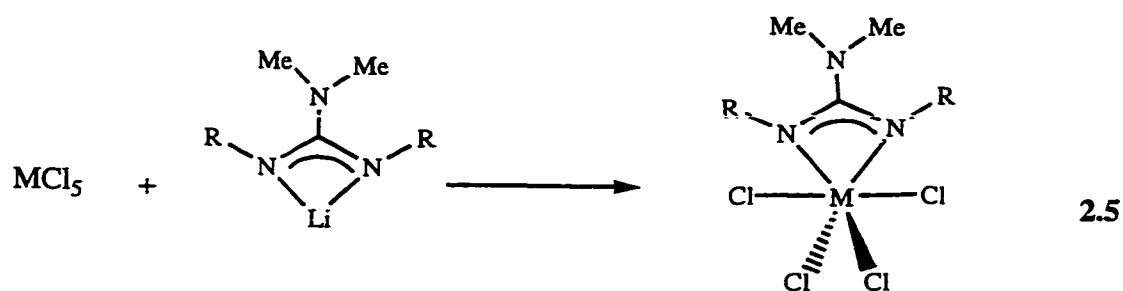
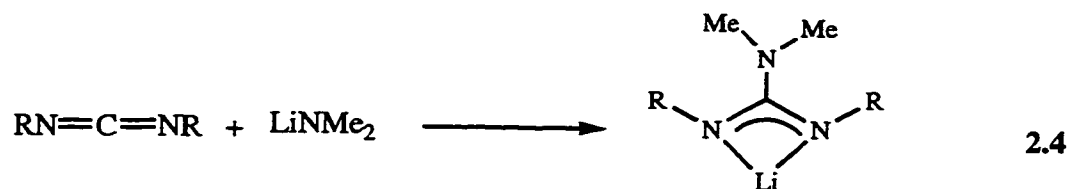
In the case of zirconium, this reaction has been generalized to include insertion of carbodiimides into Zr-P and Zr-As bonds.¹⁰ The complexes $\text{Cp}'_2\text{ZrCl}[\text{P}(\text{SiMe}_3)_2]$ and $\text{Cp}'_2\text{ZrCl}[\text{As}(\text{SiMe}_3)_2]$ are reported to undergo insertion of $\text{RN}=\text{C}=\text{NR}$ ($\text{R} = \text{iPr}, \text{Ph}$) into the Zr-P bond or Zr-As bond with the formation of $\text{Cp}'_2\text{Zr}\{\text{RNC}[\text{P}(\text{SiMe}_3)_2]\text{NR}\}\text{Cl}$ and $\text{Cp}'_2\text{Zr}\{\text{RNC}[\text{As}(\text{SiMe}_3)_2]\text{NR}\}\text{Cl}$ respectively. Crystal structures for two of these compounds show that the central ZrN_2CE fragment ($\text{E} = \text{As}, \text{P}$) exhibits similar bond lengths and angles.

This chapter explored two different routes, both based on the reaction of metal amides with carbodiimides, for introduction of tetrasubstituted guanidinate ligands into complexes of Ta and Nb:

1. Direct reaction of Ta and Nb dimethylamido complexes with carbodiimides to yield complexes with bidentate guanidinate complexes (eq. 2.3). Obviously, this methodology is limited to the use of available metal amido complexes.



2. Formation of the tetrasubstituted guanidinate anion by the insertion of carbodiimide into the lithium (dimethyl)amido bond followed by a metathesis reaction of these species with metal chlorides (eq. 2.4 and 2.5). This method has the potential to be more general than the first.



Experimental

General Considerations: All manipulations were carried out in either a nitrogen filled drybox or under nitrogen using standard Schlenk-line techniques. Solvents were distilled under nitrogen from Na/K alloy. Deuterated benzene and deuterated pyridine were dried by vacuum transfer from potassium. Diisopropylcarbodiimide and dicyclohexylcarbodiimide and bis(trimethylsilyl)carbodiimide were purchased from Aldrich and used without further purification. Preparation of Ta(NMe₂)₅ and Nb(NMe₂)₅ was carried out according to literature procedures.¹¹ ¹H NMR spectra were run on either a Gemini 200 MHz or Bruker 500 MHz spectrometer, as specified, with deuterated benzene or pyridine as a solvent and internal standard. All elemental analyses were run on a Perkin Elmer PE CHN 4000 elemental analysis system.

Ta(NMe₂)₄[CyNC(NMe₂)NCy] (2.1)

A Schlenk flask was charged with CyNCNCy (0.10g, 0.48mmol) in 20 ml of hexane. TaN(Me₂)₅ (0.20g, 0.48mmol) was added slowly to this solution. The reaction mixture was stirred for 24 hrs at room temperature followed by removal of solvent under oil pump vacuum. The product was subsequently recrystallized from toluene at -30 °C to yield 0.245 g (80%) of **1**, slightly yellowish crystals.

¹H NMR (C₆D₆, ppm) 3.52, (s, 12H, NMe₂), 3.39 (s, 12H, NMe₂), 2.50 (s, 6H, NMe₂), 3.10(br, 2H, C₆H₁₁), 2.48 (s, 6H, NMe₂), 1.1-1.9(m, 20H, C₆H₁₁).

¹³C NMR (C₆D₆, ppm) 167.7 (NC(NMe₂)N), 56.9 (NCH), 48.7 (TaNCH₃), 48.2 (TaNCH₃), 40.84 (CNCH₃), 35.4, 27.2, 26.4 (3s, C₆H₁₁).

Anal. Calcd for $C_{23}H_{52}N_7Ta$: C 45.46; H 8.63; N 16.14. Found: C 45.77; H 9.05; N 16.64.

$Nb(NMe_2)_4[CyNC(NMe_2)NCy]$ (2.2)

A Schlenk flask was charged with $CyNCNCy$ (0.264g, 1.28mmol) in 20 mL of hexane. To this solution, 0.400g of $Nb(NMe_2)_5$ (1.28mmol) was added to produce a blood red solution mixture which was stirred overnight at room temperature. The solvent was removed under oil pump vacuum, and the 0.458 g of residue was extracted with diethyl ether, concentrated to 30mL and cooled to $-30^\circ C$ to give 0.240g of **2** (70% yield) light orange color crystals.

1H NMR (C_6D_6 , ppm) 3.20 (br, 2H, C_6H_{11}), 1.15-1.90 (m, 20H, C_6H_{11}), 3.38 (s, 12H, $NbNMe_2$), 3.22 (s, 12H, $NbNMe_2$), 2.53 (s, 6H, $CNMe_2$)

^{13}C NMR (C_6D_6 , ppm) 167.23 ($NC(NMe_2)N$), 57.18 (NCH), 49.57 ($NbNCH_3$), 50.13 ($NbNCH_3$), 40.95 ($CNCH_3$), 35.67, 27.19, 26.50 (3s, C_6H_{11}).

Anal. Calcd for $C_{23}H_{52}N_7Nb$: C 53.16; H 10.09; N 18.87. Found: C 53.51; H 10.46; N 18.44.

$Ta(NMe_2)_4[(CH_3)_2CHNC(NMe_2)NCH(CH_3)_2]$ (2.3)

Following a procedure similar to the synthesis of **1** using 0.20g $Ta(NMe_2)_5$ (0.49mmol) and 0.062g $(CH_3)_2CHNCNCH(CH_3)_2$ (0.49 mmol) in hexane followed recrystallization from toluene at $-30^\circ C$. Complex **3** was isolated in 94% yield (0.25g) light yellow compound.

1H NMR (C_6D_6 , ppm) 3.75 (br, 2H, $CHMe_2$), 1.19 (d, 12H, $CH(CH_3)_2$), 3.52(s, 12H, $TaNMe_2$), 3.39(s, 12H, $TaNMe_2$), 2.47(s, 6H, NMe_2).

^{13}C NMR (C_6D_6 , ppm) 163.80 (NC(NMe₂)N), 47.54 (NCHMe₂), 48.51 (TaN(CH₃)₂),
48.10 (TaN(CH₃)₂), 40.65 (CN(CH₃)₂), 25.00 (CH(CH₃)₂).

Anal. Calcd for C₁₇H₄₄N₇Ta: C 38.71; H 8.41; N 18.59. Found: C 39.02; H 8.91; N
18.09.

Nb(NMe₂)₄[(CH₃)₂CHNC(NMe₂)NCH(CH₃)₂] (2.4)

Following a procedure similar to the synthesis of **2** using 0.40g Nb(NMe₂)₅ (1.28 mmol) and 0.162 g (CH₃)₂CHNCNCH(CH₃)₂ (1.28 mmol) in hexane produced a blood red solution. After stirring for 24 hours at room temperature followed by work-up and recrystallization from toluene at -30 °C, light orange complex **4** was isolated in 71% yield (0.40g).

^1H NMR (C_6D_6 , ppm) 3.75 (br, 2H, CHMe₂), 1.19 (d, 12H, CH(CH₃)₂), 3.24 (s, 12H, NbNMe₂), 3.40 (s, 12H, NbNMe₂), 2.52 (s, 6H, NMe₂)

^{13}C NMR (C_6D_6 , ppm) 167.10 (NC(NMe₂)N), 47.80 (NCHMe₂), 49.41 (NbN(CH₃)₂),
49.90 (NbN(CH₃)₂), 40.81 (CN(CH₃)₂), 25.31 (CH(CH₃)₂).

Anal. Calcd for C₂₃H₅₂N₇Nb: C 46.46; H 10.09; N 22.31. Found: C 47.01; H 10.61; N
22.04.

Li(NMe₂)C(NTMS)₂ (2.5)

In the dry box, N, N'-bis(trimethylsilyl)carbodiimide 0.500 g (2.68 mmol) was dissolved in 20mL of hexane in a round bottom flask. To this solution, 0.13 g (2.68 mmol) of LiNMe₂ was slowly added while stirring. The originally clear solution first became milky white and then clear and colorless over 15 minutes. Attempts to isolate the salt by simple removal of the reaction solvent under vacuum gave a colorless sticky material, which was

very soluble in hydrocarbon solvent. This feature made accurate weighing of the material difficult and as a result accurate microanalysis was not possible. However, it was possible to obtain NMR spectra of this material for comparison with starting materials.

In general, the original reaction mixture was used in subsequent reactions.

^1H NMR(C_6D_6 ,25C,200MHz) 2.83 (s, 6H, NMe_2), 0.26(s, 18H, NSiMe_3)

^{13}C NMR (C_6D_6 ,25C,200MHz) 169.50(CN_3), 38.99(NMe_2), 2.57 (TMS- CH_3)

$\text{Li}(\text{NMe}_2)\text{C}(\text{NCH}(\text{CH}_3)_2)_2$ (2.6)

Following a procedure similar to the preparation of **1**, 0.5 g (2.42 mmol) N, N'-diisopropylcarbodiimide was reacted with 0.12 g (2.42 mmol) of LiNMe_2 in 20mL of hexane. At first, the solution became a milky color that became clear in 15 minutes. Again, removal of the solvent resulted in a very viscous, sticky oil which was soluble in hydrocarbon solvents. Accurate weighing of the sample was not possible. This feature made accurate weighing of the material difficult and as a result accurate microanalysis was not possible. In general, the original reaction mixture was used in subsequent reactions.

^1H NMR(C_6D_6 ,25C,200MHz) 3.75 (mult.2H, CH) 2.68 (s, 6H, NMe_2), 1.28(d,

$J_{\text{CH}}=6.6\text{Hz}$, 12H, CH_3)

^{13}C NMR (C_6D_6 ,25C,200MHz) 165.80 (CN_3), 45.23(NMe_2) 43.60 (CH), 25.90 (CH_3)

Li(NMe₂)C(NC₆H₁₁)₂ (2.7)

Following the procedure described for the preparation of **1**, 0.5 g (2.42 mmol) of N, N'-dicyclohexylcarbodiimide reacted with LiNMe₂ (0.12 g, 2.42 mmol) in 20 mL of hexane 20 mL. Similar observations were made during reaction as in the case of **1**. The material isolated by removal of the reaction solvent was a very viscous oil, which was soluble in hydrocarbon solvents. This feature made accurate weighing of the material difficult and as a result accurate microanalysis was not possible.

¹H NMR(C₆D₆,25C,200MHz) 3.39 (sept, 2H, CH), 2.74(s, 6H, NMe₂), 2.21-1.2(br, 20H, C₆H₁₁)

¹³C NMR (C₆D₆,25C,200MHz) 164.00(CN₃), 43.79(NMe₂) 54.53(CH), 37.01, 26.96, 26.21 (C₆H₁₁)

Results and Discussion

The direct reactions of pentakis(dimethylamido)M (M = Ta, Nb) complexes with both dicyclohexylcarbodiimide and diisopropylcarbodiimide proceeded smoothly at room temperature under nitrogen to provide good yields of complexes **2.1-2.4** (equation 2.3). Only in the case of the Nb reactions was a dramatic color change noted during reaction. The origin of this phenomenon is not clear but, given the fact that all of the products are pale in color, this red material is likely a minor product or impurity. These new guanidinate-containing complexes were characterized by spectroscopic methods and in the case of **2.1** by a single crystal X-ray diffraction study.

Both the ^1H and ^{13}C NMR spectra are consistent with the single insertion product. The most obvious changes from the starting materials were a shift in signals for the alkyl groups originating on the carbodiimides and the division of the dimethylamino protons signal (singlets at 3.25 and 3.12 ppm for the Ta and Nb starting materials respectively) into three singlets. The integrated ratios of the signals assigned to the NMe_2 groups (1:2:2) as well as their chemical shifts provided the first direct evidence for the number of guanidinate and amido ligands within the compounds. The observation of a single resonance for the cyclohexyl and isopropyl protons on the α carbon indicated a structure with either a symmetric arrangement of the ligands or one that was fluxional. ^{13}C NMR was consistent with the proton spectrum in all cases and revealed the central, sp^2 C of the guanidine ligands which had undergone a substantial shift from the starting carbodiimides (142.1 and 140.2 ppm for Cy and ^iPr respectively).

Despite attempts to provoke the incorporation of a second equivalent of carbodiimide through prolonged reaction time and increased temperature, only the

monoinsertion products were observed. Multiple insertion products have been observed in the analogous reactions of $\text{Me}_x\text{MCl}_{5-x}$ ($\text{M} = \text{Ta}, \text{Nb}; x = 1, 2, 3$) with carbodiimides RNCNR ($\text{R} = \text{isopropyl, cyclohexyl, p-tolyl}$) to give acetamidinate complexes $\text{MCl}_4[\text{RN-C(Me)=NR}]$, $\text{MeMCl}_3[\text{RN-C(Me)=NR}]$, and $\text{MCl}_3[\text{RN-C(Me)=NR}]_2$.^{3(b), 12} Furthermore, a double insertion product is reported for the reaction of $\text{M}(\text{NMe}_2)_5$ ($\text{M} = \text{Ti, Zr, Hf}$) with carbodiimides to yield bis(guanidinate) complexes $[(\text{p-tolylN})_2\text{CNMe}_2]_2\text{M}(\text{NMe}_2)_2$ and $[(\text{CyN})_2\text{CNMe}_2]_2\text{M}(\text{NMe}_2)_2$.⁹

These observations can be attributed to two possible factors. The first is the increased steric congestion of complexes **2.1-2.4** compared to the monoinsertion products $\text{MCl}_4[\text{RN-C(Me)=NR}]$ and $[(\text{RN})_2\text{CNMe}_2]\text{M}(\text{NMe}_2)_3$ compounds. The second possibility for the decreased reactivity of **2.1-2.4** towards further insertion may arise from the increased π donating ability of amido versus chloro and the consequent reduction in the acidity of the Ta or Nb center. Further support for the idea that steric constraints may play a role in these reactions is provided by the fact that attempts to get a similar insertion reaction with bis(trimethylsilyl)carbodiimide have been completely unsuccessful.

In order to confirm the structural details of complexes **2.1-2.4** a single crystal X-ray analysis of one of these compounds was undertaken. Complex **2.1** crystallized in the triclinic space group P-1 with two independent molecules in the asymmetric unit. Selected bond distances and angles are provided in Tables 2.1, 2.2, and 2.3 for both molecules. As shown in Figures 2.1 and 2.2, both of these molecules display Ta(V) centers in a distorted octahedral-based coordination geometry with very similar bonding features. The coordination environment of Ta contains a tetrasubstituted, bidentate guanidinate ligand derived from the insertion of a dicyclohexylcarbodiimide into one of

the Ta-NMe₂ ligands of the starting material along with four remaining NMe₂ ligands.

Completing the equatorial plane defined by the coordinated N-C-N function are two dimethylamido ligands (N(4), N(5) or N(12), N(13)). Two axial dimethylamido functions (N(6), N(7) or N(14), N(15)) complete the Ta coordination sphere (average N-Ta-N angle of 177.1°). The guanidinate ligand binds to Ta through two nitrogen atoms to yield a planar four-membered ring of sp² hybridized N and C centers with an average bite angle of 58.6°. The delocalized π interaction within the NCN moieties (N(1)-C(13)-N(2) and N(8)-C(36)-N(9)) leads to partial double bonded C-N distances which average 1.33 Å. The distances and angles within this cyclic arrangement are reminiscent of those in the structurally characterized seven coordinate bis(diisopropylacetamidinato) and bis(dicyclohexylacetamidinato) complexes Cl₃Ta(RNC(CH₃)NR)₂ (R = ⁱPr, Cy).¹²

The third guanidinate nitrogen (N(3) and N(10)) was derived from a dimethylamido function and lies just slightly out of the ligand plane. For example the N(3)-C(13)-Ta(1) angle is 174.1(3)°. Although this exocyclic nitrogen appears to be distorted toward planar, sp² hybridization (deviation from planarity of 0.19 and 0.17 Å). The angles of the mean planes defined by the C-NMe₂ and the bidentate NCN fragments average 80.7°. This feature militates against conjugation of the N-C-N π system and the lone pair on these NMe₂ groups. In accord with this are the N(3)-C(13) and N(10)-C(36) distances (average = 1.42 Å) which are consistent with N-C single bond.

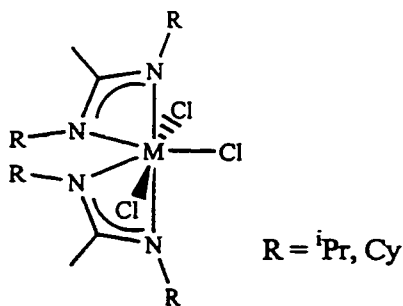


Table 2.1. Summary of crystal data and structure refinement for



Empirical formula	$\text{C}_{23}\text{H}_{57}\text{N}_7\text{Ta}$	
Formula weight	607.67	
Temperature	153(2) K	
Wavelength	0.71073 Å	
Crystal system	Triclinic	
Space group	P-1	
Unit cell dimensions	$a = 10.3664(6)$	$\alpha = 81.304(1)$ deg.
	$b = 14.6400(9)$ Å	$\beta = 88.894(1)$ deg.
	$c = 18.549(1)$ Å	$\gamma = 89.103(1)$ deg.
Volume, Z	$2782.0(3)$ Å ³ , 2	
Density (calculated)	1.451 Mg/m ³	
Absorption coefficient	3.973 mm ⁻¹	
F(000)	1248	
Crystal size	0.10 x 0.10 x 0.10 mm	
Theta range for data collection	1.11 to 28.68 deg.	
Limiting indices	$-13 \leq h \leq 7$, $-19 \leq k \leq 19$, $-24 \leq l \leq 24$	
Reflections collected	17104	
Independent reflections	12070 [R(int) = 0.0260]	
Absorption correction	None	
Refinement method	Full-matrix least-squares on F ²	
Data / restraints / parameters	12066 / 0 / 559	
Goodness-of-fit on F ²	1.050	
Final R indices [I > 2σ(I)]	R1 = 0.0357, wR2 = 0.0747	
R indices (all data)	R1 = 0.0502, wR2 = 0.0865	
Largest diff. peak and hole	1.288 and -1.124 e Å ⁻³	

Table 2.2. Bond lengths [Å] for Ta(NMe₂)₄[CyNC(NMe₂)NCy] (2.1)

Ta(1)-N(5)	2.011(4)	N(10)-C(38)	1.459(8)
Ta(1)-N(4)	2.013(4)	N(11)-C(40)	1.460(7)
Ta(1)-N(6)	2.025(4)	N(11)-C(39)	1.458(7)
Ta(1)-N(7)	2.038(4)	N(12)-C(42)	1.454(6)
Ta(1)-N(1)	2.246(4)	N(12)-C(41)	1.459(7)
Ta(1)-N(2)	2.280(4)	N(13)-C(46)	1.449(6)
Ta(1)-C(13)	2.695(5)	N(13)-C(45)	1.462(6)
Ta(2)-N(12)	2.015(4)	N(14)-C(44)	1.455(7)
Ta(2)-N(11)	2.019(4)	N(14)-C(43)	1.451(7)
Ta(2)-N(14)	2.041(4)	C(1)-C(6)	1.523(7)
Ta(2)-N(13)	2.045(4)	C(1)-C(2)	1.533(7)
Ta(2)-N(9)	2.258(4)	C(2)-C(3)	1.530(8)
Ta(2)-N(8)	2.263(4)	C(3)-C(4)	1.508(8)
N(1)-C(13)	1.331(6)	C(4)-C(5)	1.518(7)
N(1)-C(6)	1.469(6)	C(5)-C(6)	1.527(7)
N(2)-C(13)	1.318(6)	C(7)-C(12)	1.531(6)
N(2)-C(12)	1.466(5)	C(7)-C(8)	1.541(6)
N(3)-C(13)	1.427(6)	C(8)-C(9)	1.515(8)
N(3)-C(14)	1.442(6)	C(9)-C(10)	1.519(8)
N(3)-C(15)	1.442(7)	C(10)-C(11)	1.540(7)
N(4)-C(16)	1.460(7)	C(11)-C(12)	1.528(6)
N(4)-C(17)	1.461(7)	C(24)-C(29)	1.514(7)
N(5)-C(18)	1.454(7)	C(24)-C(25)	1.529(7)
N(5)-C(19)	1.464(6)	C(25)-C(26)	1.520(7)
N(6)-C(21)	1.455(7)	C(26)-C(27)	1.523(7)
N(6)-C(20)	1.465(7)	C(27)-C(28)	1.523(7)
N(7)-C(23)	1.455(6)	C(28)-C(29)	1.534(7)
N(7)-C(22)	1.465(6)	C(30)-C(35)	1.517(7)
N(8)-C(36)	1.328(6)	C(30)-C(31)	1.528(7)
N(8)-C(29)	1.479(6)	C(31)-C(32)	1.517(9)
N(9)-C(36)	1.334(6)	C(32)-C(33)	1.515(9)
N(9)-C(35)	1.465(6)	C(33)-C(34)	1.537(7)
N(10)-C(36)	1.415(6)	C(34)-C(35)	1.530(7)
N(10)-C(37)	1.426(8)		

Table 2.3. Bond angles [deg] for Ta(NMe₂)₄[CyNC(NMe₂)NCy] (2.1)

N(5)-Ta(1)-N(4)	105.3(2)	C(36)-N(9)-Ta(2)	94.4(3)
N(5)-Ta(1)-N(6)	91.6(2)	C(35)-N(9)-Ta(2)	144.1(3)
N(4)-Ta(1)-N(6)	89.7(2)	C(36)-N(10)-C(37)	116.6(5)
N(5)-Ta(1)-N(7)	91.0(2)	C(36)-N(10)-C(38)	119.5(5)
N(4)-Ta(1)-N(7)	90.4(2)	C(37)-N(10)-C(38)	116.4(5)
N(6)-Ta(1)-N(7)	177.3(2)	C(40)-N(11)-C(39)	108.6(4)
N(5)-Ta(1)-N(1)	98.4(2)	C(40)-N(11)-Ta(2)	125.5(4)
N(4)-Ta(1)-N(1)	156.2(2)	C(39)-N(11)-Ta(2)	125.8(3)
N(6)-Ta(1)-N(1)	87.9(2)	C(42)-N(12)-C(41)	109.0(4)
N(7)-Ta(1)-N(1)	90.9(2)	C(42)-N(12)-Ta(2)	126.2(3)
N(5)-Ta(1)-N(2)	157.0(2)	C(41)-N(12)-Ta(2)	124.5(3)
N(4)-Ta(1)-N(2)	97.7(2)	C(46)-N(13)-C(45)	108.4(4)
N(6)-Ta(1)-N(2)	89.9(2)	C(46)-N(13)-Ta(2)	131.2(3)
N(7)-Ta(1)-N(2)	87.5(2)	C(45)-N(13)-Ta(2)	120.4(3)
N(1)-Ta(1)-N(2)	58.66(14)	C(44)-N(14)-C(43)	108.7(4)
N(5)-Ta(1)-C(13)	127.9(2)	C(44)-N(14)-Ta(2)	124.6(3)
N(4)-Ta(1)-C(13)	126.7(2)	C(43)-N(14)-Ta(2)	125.7(3)
N(6)-Ta(1)-C(13)	87.2(2)	C(6)-C(1)-C(2)	111.1(4)
N(7)-Ta(1)-C(13)	90.6(2)	C(1)-C(2)-C(3)	111.0(4)
N(1)-Ta(1)-C(13)	29.50(13)	C(4)-C(3)-C(2)	111.3(5)
N(2)-Ta(1)-C(13)	29.24(13)	C(3)-C(4)-C(5)	111.0(5)
N(12)-Ta(2)-N(11)	104.7(2)	C(6)-C(5)-C(4)	112.4(4)
N(12)-Ta(2)-N(14)	89.9(2)	N(1)-C(6)-C(5)	110.7(4)
N(11)-Ta(2)-N(14)	91.4(2)	N(1)-C(6)-C(1)	112.7(4)
N(12)-Ta(2)-N(13)	89.8(2)	C(5)-C(6)-C(1)	110.6(4)
N(11)-Ta(2)-N(13)	91.7(2)	C(12)-C(7)-C(8)	110.5(4)
N(14)-Ta(2)-N(13)	176.9(2)	C(9)-C(8)-C(7)	111.6(4)
N(12)-Ta(2)-N(9)	158.4(2)	C(8)-C(9)-C(10)	110.8(4)
N(11)-Ta(2)-N(9)	96.9(2)	C(9)-C(10)-C(11)	110.3(5)
N(14)-Ta(2)-N(9)	90.3(2)	C(12)-C(11)-C(10)	111.5(4)
N(13)-Ta(2)-N(9)	88.9(2)	N(2)-C(12)-C(11)	111.2(4)
N(12)-Ta(2)-N(8)	99.8(2)	N(2)-C(12)-C(7)	112.0(4)
N(11)-Ta(2)-N(8)	155.5(2)	C(11)-C(12)-C(7)	110.6(4)
N(14)-Ta(2)-N(8)	87.6(2)	N(2)-C(13)-N(1)	113.6(4)
N(13)-Ta(2)-N(8)	89.4(2)	N(2)-C(13)-N(3)	125.9(4)
N(9)-Ta(2)-N(8)	58.61(14)	N(1)-C(13)-N(3)	120.5(4)
C(13)-N(1)-C(6)	119.3(4)	N(2)-C(13)-Ta(1)	57.6(2)
C(13)-N(1)-Ta(1)	94.3(3)	N(1)-C(13)-Ta(1)	56.2(2)
C(6)-N(1)-Ta(1)	145.4(3)	N(3)-C(13)-Ta(1)	174.1(3)
C(13)-N(2)-C(12)	121.6(4)	C(29)-C(24)-C(25)	110.8(4)
C(13)-N(2)-Ta(1)	93.1(3)	C(26)-C(25)-C(24)	112.7(4)

C(12)-N(2)-Ta(1)	144.7(3)	C(27)-C(26)-C(25)	110.3(4)
C(13)-N(3)-C(14)	120.2(4)	C(26)-C(27)-C(28)	111.3(4)
C(13)-N(3)-C(15)	114.1(4)	C(27)-C(28)-C(29)	111.8(4)
C(14)-N(3)-C(15)	116.7(4)	N(8)-C(29)-C(24)	112.6(4)
C(16)-N(4)-C(17)	108.0(5)	N(8)-C(29)-C(28)	109.8(4)
C(16)-N(4)-Ta(1)	126.2(4)	C(24)-C(29)-C(28)	110.3(4)
C(17)-N(4)-Ta(1)	125.7(4)	C(35)-C(30)-C(31)	112.4(4)
C(18)-N(5)-C(19)	108.2(4)	C(32)-C(31)-C(30)	112.3(5)
C(18)-N(5)-Ta(1)	125.3(4)	C(31)-C(32)-C(33)	110.0(5)
C(19)-N(5)-Ta(1)	126.3(3)	C(32)-C(33)-C(34)	110.5(5)
C(21)-N(6)-C(20)	107.1(4)	C(35)-C(34)-C(33)	111.3(4)
C(21)-N(6)-Ta(1)	129.2(4)	N(9)-C(35)-C(30)	111.5(4)
C(20)-N(6)-Ta(1)	122.5(4)	N(9)-C(35)-C(34)	110.4(4)
C(23)-N(7)-C(22)	108.8(4)	C(30)-C(35)-C(34)	110.3(4)
C(23)-N(7)-Ta(1)	130.6(3)	N(8)-C(36)-N(9)	112.5(4)
C(22)-N(7)-Ta(1)	120.5(3)	N(8)-C(36)-N(10)	121.6(4)
C(36)-N(8)-C(29)	119.4(4)	N(9)-C(36)-N(10)	125.8(4)
C(36)-N(8)-Ta(2)	94.3(3)		
C(29)-N(8)-Ta(2)	146.2(3)		
C(36)-N(9)-C(35)	121.6(4)		

The four amido groups in each molecule are planar, a feature consistent with π donation of the nitrogen lone pair into a metal d orbital. Furthermore the values for the Ta-NMe₂ distances average 2.03Å which are consistent with a π interaction.¹³

In order to invoke π bonding, planarity and M-N distance is not sufficient, symmetry requirements must be considered. On the basis of a distorted octahedral geometry described above, there would be three d orbitals (d_{xy} , d_{xz} , d_{yz}) available for d-p bonding. Keeping this in mind, the relative orientation of the amido functions suggests maximum π donation. The angle between the mean planes of the axial amides nearly orthogonal (84.4° and 88.4°), an orientation appropriate for the two amides to interact with two orthogonal tantalum d orbitals (d_{xz} , and d_{yz}). The two equatorial amido ligands also exhibit a preferred orientation with the mean Me-N-Me planes at an average of 64° with respect to the plane defined by the Ta and NCN of the guanidine anion. It would appear that the maximum π overlap with the remaining tantalum d orbital (d_{xy}) would be achieved for these ligands if this angle were 90°. Counterbalancing the π overlap are steric interactions between the axial and equatorial amido ligands, which would be maximized for this orientation and the fact that the two amidos are competing for donation to a single orbital.

The second route to preparing tetrasubstituted guanidinate complexes relies on the generation of a lithium guanidinate followed by reaction with a metal halide (eq. 2.4, 2.5). The reaction of LiNMe₂ with RNCNR (R = Cy, ⁱPr, SiMe₃) proceeds in a clean fashion in all three cases. The resultant materials, which could only be isolated as very viscous oils, exhibited ¹H and ¹³C NMR spectra corresponding to the guanidinate anion. Probably the clearest indication that these products are indeed guanidinate anions is the

observation of the central, sp^2 carbon atoms at 164.0, 165.80 and 169.5 ppm, exactly in the range observed for complexes **2.1-2.4**. Note that the ability to prepare $\text{Li}[\text{Me}_3\text{SiNC}(\text{NMe}_2)\text{NSiMe}_3]$ is also consistent with the proposal that steric interactions were the reason for the inability of getting an insertion reaction of $\text{Me}_3\text{SiNCNSiMe}_3$ with $\text{M}(\text{NMe}_2)_5$.

At this stage only preliminary reactivity studies of the lithium guanidates and Ta and Nb pentachlorides have been pursued. These reactions seem to proceed smoothly at room temperature with formation of LiCl. The crude products give NMR spectra that show the presence of the ligands with changes consistent with coordination. Future studies will be carried out to clarify these products.

In this chapter we have noted that complexes **2.1-2.4** can be formed in very good yield. The reaction of LiNMe_2 with RNCNR where $\text{R} = \text{Cy}, ^i\text{Pr}, \text{SiMe}_3$, (complexes **2.5-2.7**) are very stable under inert atmosphere at room temperature.

References for Chapter 2

- ¹ Principles and Application of Organotransition Metal Chemistry, J. Collman, Louis Hegedus, Jack Norton, Richard Finke, 1987 University Science Books
- ² For some examples see: (a) Dionne, M.; Hao, S.; Gambarotta, S. *Can. J. Chem.* **1995**, *73*, 1126 and references therein. (b) Gambarotta, S.; Strologo, S.; Floriani, C.; Chiesi-Villa, A.; Guastitin, C. *J. Am. Chem. Soc.* **1985**, *107*, 6278 and references therein. (c) Harris, A. D.; Robinson, S. D.; Sahajpal, A.; Hursthouse M. B. *J. Chem. Soc. Dalton Trans.* **1981**, 1327 and references therein.
- ³ (a) Gambarotta, S.; Strologo, S.; Floriani, C.; Chiesi-Villa, A.; Guastitin, C. *Inorg. Chem.* **1985**, *24*, 654. (b) Wilkins, J. D. *J. Organomet. Chem.* **1974**, *80*, 349.
- ⁴ For examples of the insertion reaction in to main group metal-carbon bonds see: (a) Srinivas, B.; Chang, C.-C.; Chen, C.-H.; Chiang, M. Y.; Chen, I.-T.; Wang, Y.; Lee, G.-H. *J. Chem. Soc., Dalton Trans.* **1997**, 957. (b) Li, M.-D.; Chang, C.-C.; Wang, Y.; Lee, G.-H. *Organometallics*, **1996**, *15*, 2571. (c) Lechler, R.; Hausen, H.-D.; Weidlein, J. *J. Organomet. Chem.* **1989**, *359*, 1. (d) Kottmair-Maieron, D.; Lechler, R.; Weidlein, J. *Z. Anorg. Allg. Chem.* **1991**, *593*, 111.
- ⁵ (a) Kennepohl, D. K.; Santarsiero, B. D.; Cavell, R. G. *Inorg. Chem.* **1990**, *29*, 5081 and references therein. (b) Schwarz, W.; Rajca, G.; Weidlein, J.; Dehnicke, K. *Z. Anorg. Allg. Chem.* **1985**, *525*, 143.

⁶For examples with M = Mg see: Srinivas, B.; Chang, C.-C.; Chen, C.-H.; Chiang, M. Y.; Chen, L.-T.; Wang, Y.; Lee, G.-H. *J. Chem. Soc., Dalton Trans.* **1997**, 957.

⁷For examples with M = B see: Jefferson, R.; Lappert, M. F.; Prokai, B.; Tilley, B. P. *J. Chem. Soc.* **1966**, 1584.

⁸For examples with M = Si, Ge, Sn see: (a) Matsuda, I.; Itoh, K.; Ishii, Y. *Journal of Organometallic Chemistry* **1974**, *69*, 353. (b) Chandra, G.; Jenkins, A. D.; Lappert, M. F.; Srivastava, R. C. *J. Chem. Soc. (A)* **1970**, 2250. (c) George, T.A.; Jones, K.; Lappert, M. F. *J. Chem. Soc.* **1965**, 2157.

⁹For examples with M = Ti, Zr, Hf see: reference 8(b)

¹⁰(a) Lindenberg, F.; Sieler, J.; Hey-Hawkins, E. *Polyhedron* **1996**, *15*, 1459. (b) Hey-Hawkins, E.; Lindenberg, F. *Z. Naturforsch.* **1993**, *48b*, 951

¹¹Bradley, D. C.; Thomas, I. M. *Can. J. Chem.*, **1962**, *40*, 1355. Bradley, D. C.; Thomas, I. M. *Can. J. Chem.*, **1962**, *40*, 449.

¹²Drew, M. G. B.; Wilkins, J. D. *J. Chem. Soc., Dalton Trans.* **1974**, 1579. Drew, M. G. B.; Wilkins, J. D. *J. Chem. Soc., Dalton Trans.* **1975**, 2611.

¹³Chisholm, M. H.; Tan, L.-S.; Huffman, J. C. *J. Am. Chem. Soc.* **1982**, *104*, 4879.

Chapter 3.

Reactions Between Guanidines and $M(NMe_2)_5$ ($M=Ta,Nb$)

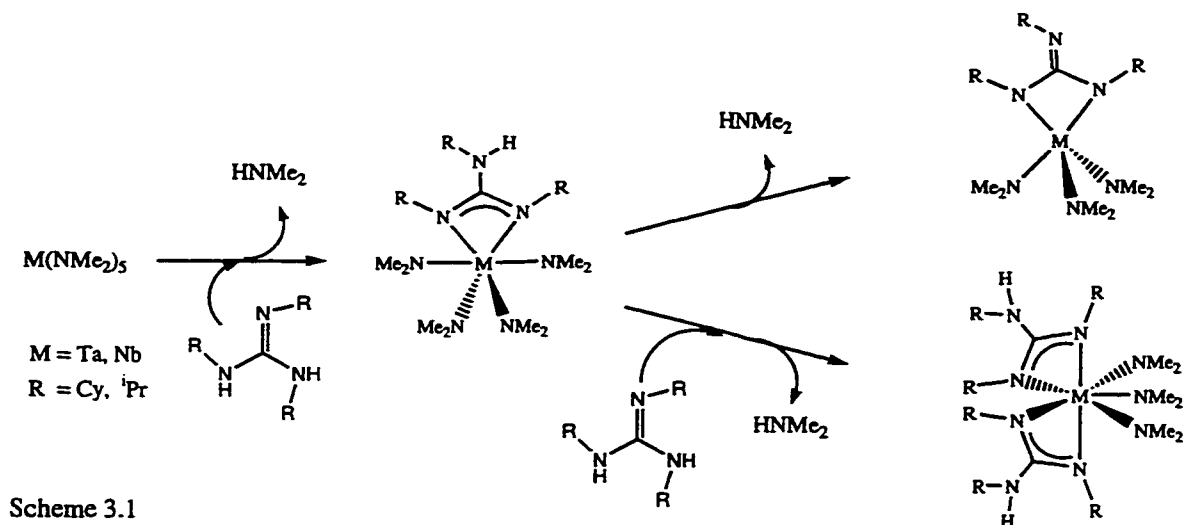
Protonation Pathways to metal Guanidinate Complexes I

Introduction:

Other than the insertion reaction pathways investigated in Chapter 2, several routes have been reported for the introduction of guanidinate ligands. One of the most common and one that has been explored for this thesis is the reaction of the active protons of a tetrasubstituted or trisubstituted guanidine with a metal ligand bond. Literature examples for this type of reaction include the elimination of HX ($X = Cl, Br$) from halo metal complexes,¹ elimination of H_2 from metal hydrides,² elimination of an alkane from a metal alkyl,³ and elimination of amine from a metal amido complex.⁴ In many cases, these reactions also involve the loss of an additional neutral ligand (e.g. CO) in order to open a coordination site for the guanidinate ligand. In only one case has this methodology been used to prepare a complex with a dianionic ligand.⁴ One of our goals is to expand and broaden the procedures of introducing guanidinate ligands and to find general methods for the generation of dianionic guanidinate ligands.

A major limitation of the protonation/elimination reactions is the need to have a reactive ligand within the metal coordination sphere. In addition, for purification purposes, the eliminated group should be easily separated from the product complex. The elimination of an amido group as an amine offers not only a ligand that may be rather easily protonated but there are a variety of known metal amido complexes.

In this chapter the focus is on elimination of amido ligands from homoleptic Ta(V) and Nb(V) dimethylamido complexes (Scheme 3.1).



Scheme 3.1

These materials are well known and easily synthesized in large quantities. The presence of more than one amido ligand may provide the option to either introduce a second guanidinate ligand or to remove a second proton from a coordinated guanidinate anion. An added benefit of these starting materials is the fact that $HNMe_2$ is a volatile side product a feature that should ease purification.

The results for this chapter begin with the reports for the synthesis and characterization of the guanidines that were used in the reactions shown in Scheme 3.1. The reactivity of these ligand precursors with pentakis(dimethylamido)M lead to the preparation of a series of analogous complexes with the formulae, $M(NMe_2)_3[(RN)_2CNR]$. These complexes contained the dianionic N, N', N'' trialkylguanidinate ligand and their properties were probed by spectroscopic means and in two cases by crystallographic characterization. Also reported is the isolation of a related species with containing a monoanionic ligand, $TaCl(NMe_2)_3[(RN)_2CNR]$ (R = cyclohexyl).

Experimental

General Considerations: All manipulations were carried out in either a nitrogen filled drybox or under nitrogen using standard Schlenk-line techniques. Solvents were distilled under nitrogen from Na/K alloy. Deuterated benzene and toluene were dried by vacuum transfer from potassium. Diisopropylcarbodiimide, dicyclohexylcarbodiimide, cyclohexylamine and isopropylamine were purchased from Aldrich and used without further purification. Preparation of Ta(NMe₂)₅ and Nb(NMe₂)₅ was carried out according to literature procedures.⁵ ¹H NMR spectra were run on either a Gemini 200 MHz or Bruker 500 MHz spectrometer, as specified, with deuterated benzene or toluene as a solvent and internal standard. All elemental analyses were run on a Perkin Elmer PE CHN 4000 elemental analysis system.

N, N', N''-Tricyclohexylguanidine {[CyN(H)]₂CNCy} (3.1)

N, N' dicyclohexylcarbodiimide (5.00 g, 24.2mmol), freshly distilled cyclohexylamine (2.88g, 29.0mmol) and hexane (30 mL) were combined in a vessel sealed with a Teflon stopcock under nitrogen. The reaction was heated at 80°C for 48 hrs. Solvent and excess cyclohexylamine were removed under vacuum with gentle heating. The resultant solid was washed three times with distilled hexane and dried under vacuum for 3 hours to produce a white powder of **3.1** (yield 100%).

¹H NMR (C₆D₆, 25°C, ppm) 2.8-3.8 (br m, 5H) 0.9-2.1 (br, 30H)

¹³C NMR (C₆D₆, 25°C, ppm) 148.45(s, CN₃), 51.94, 34.85, 26.62, 25.48 (4 s, C₆H₁₁)

Anal. Calcd for C₁₉H₃₅N₃: C 74.70; H 11.55; N 13.75. Found: C 74.52 ; H 11.31;

N 13.57.

N, N', N''-Triisopropylguanidine {[ⁱPrN(H)]₂CNⁱPr} (3.2)

N, N'-diisopropylcarbodiimide (5.00 g, 39.6mmol), freshly distilled isopropylamine (2.80g, 47.3mmol) and hexane (10 mL) were combined in a vessel sealed with a Teflon stopcock under nitrogen. The reaction was heated at 70°C for 48 hrs. Solvent and excess isopropylamine were removed under vacuum with gentle heating. The resultant solid was washed twice with distilled diethyl ether and dried under vacuum for 3 hours to produce a fine crystalline white powder of **3.2** (yield 100%).

¹H NMR(C₆D₆, 25°C, ppm) 3.0-3.8 (br m, 5H) 0.9-1.2 (br, 18H)

¹³C NMR (C₆D₆, 25°C, ppm) 148.42(CN₃), 44.34(CH), 24.24 (CH₃).

Anal. Calcd for C₁₀H₂₃N₃: C 64.81; H 12.51; N 22.67. Found: C 64.76; H 11.98; N 22.51.

Ta(NMe₂)₃[(CH₃)₂CHN]₂CNCH(CH₃)₂] (3.3)

A Schlenk flask was charged with Ta(NMe₂)₅ (1.00g, 2.49mmol), a stir bar and 30mL of hexane. Compound **3.2** (0.46 g, 2.49 mmol) was added slowly to this solution and the reaction mixture was stirred for 24 hrs at room temperature. Solvent was removed from the bright yellowish solution under vacuum to yield crude **3.3** as a light brown solid. Crystallization from toluene gave 0.75g (60%) of light yellow crystals of **3.3**.

¹H NMR (d₈-toluene, ppm) 4.92 (br m, 1H, NCH), 4.51 (br m, 1H, NCH), 4.33 (sept, 1H, NCH), 3.16(s, 18H, NCH₃), 1.41(d, 6H, CH₃), 1.32(br d, 6H, CH₃), 1.14(br d, 6H, CH₃).

^{13}C NMR (d_8 -toluene, ppm) 152.03 (CN3), 49.62 (br, NCHMe₂), 48.72 (br, NCHMe₂), 45.65 (NCHMe₂), 45.10 (TaNCH₃), 27.51(NCH(CH₃)₂), 25.99 (br, NCH(CH₃)₂), 24.89 (br, NCH(CH₃)₂).

Anal. Calcd for C₁₆H₄₁N₆Ta: C 38.55; H 8.29; N 16.86. Found: C 38.50; H 7.91; N 16.40

Nb(NMe₂)₃[(CH₃)₂CHN]₂CNCH(CH₃)₂] (3.4)

A Schlenk flask was charged with Nb(NMe₂)₅ (1.00g, 3.19mmol), a stir bar and 30mL of hexane. Compound 3.2 (0.592 g, 3.19 mmol) was added slowly to this solution to give a bright orange solution. The reaction mixture was stirred overnight at room temperature. The solvent was removed under vacuum and the residue was crystallized at -30°C from bis(trimethylsilyl)ether to give 0.35 g of microcrystalline 3.4 (26% yield).

^1H NMR (C₆D₆, ppm) 4.78 (br m, 1H, CH), 4.35 (br m, 1H, CH), 3.01 (s, 18H, NCH₃), 1.49 (d, 6H, CH₃), 1.39 (br d, 6H, CH₃), 1.15 (br d, 6H, CH₃).

^{13}C NMR (C₆D₆ ppm) 155.2 (CN3), 50.98 (br, NCHMe₂), 49.96 (br, NCHMe₂), 46.37 (TaNCH₃), 45.77 (NCHMe₂), 27.34(NCH(CH₃)₂), 25.74 (br, NCH(CH₃)₂), 24.68 (br, NCH(CH₃)₂).

Anal. Calcd for C₁₆H₄₁N₆Ta: C 46.82; H 10.07; N 20.48.

Ta(NMe₂)₃[(CyN)₂C(NCy)] (3.5)

A Schlenk flask was charged with Ta(NMe₂)₅ (1.00g, 2.49mmol), a stir bar and 30mL of hexane. Compound 3.1 (0.76 g, 2.49 mmol) was added slowly to this solution and the reaction mixture was stirred for 24 hrs at room temperature. Solvent was removed from

the yellowish solution under vacuum to yield crude **3.5**. Crystallization from bis(trimethylsilyl)ether gave 1.01 g (65%) of slightly yellow crystals of **3.5**.

^1H NMR (C_6D_6 , ppm) 4.52 (br m, 1H, CH), 4.10 (br m, 1H, CH), 3.95 (br m, 1H, CH), 3.14 (s, 18H, NCH_3), 1.2-2.2 (br m, 30H, C_6H_{11})

^{13}C NMR (C_6D_6 , ppm) 152.01(s, CN_3), 57.9, 54.28 (s, 2:1, NCH), 45.14 (NCH_3), 37.91, 35.36, 26.98, 26.61, 25.76 (5 s, C_6H_{11})

Anal. Calcd for $\text{C}_{25}\text{H}_{51}\text{N}_6\text{Ta}$: C 48.69; H 8.34; N 13.63. Found: C 49.04; H 8.74; N 13.01.

$\text{Nb}(\text{NMe}_2)_3[\text{CyN})_2\text{C}(\text{NCy})]$ (3.6**)**

A Schlenk flask was charged with $\text{Nb}(\text{NMe}_2)_5$ (1.00g, 3.19mmol), a stir bar and 30mL of hexane. Compound **3.1** (0.977 g, 3.20 mmol) was added slowly to this solution to give a blood red solution. The reaction mixture was stirred for 36 hrs at room temperature. The solvent was removed under vacuum to yield crude **3.6** (0.61g) which was extracted with diethyl ether. Crystallization at -30°C in bis(trimethylsilyl)ether gave microcrystalline **3.6** in 25% yield.

^1H NMR (C_6D_6 , ppm) 4.5- 3.9 (br m, 3H, CH), 3.07 (s, NCH_3 , 18H) 2.2-1.12 (br, 30H, C_6H_{11})

^{13}C NMR (C_6D_6 , ppm) 158.23 (CN_3), 65.86, 56.10 (s, 2:1, NCH), 46.93 (NCH_3), 38.60, 37.80, 35.91, 26.65, 26.53, 23.02 (6s, C_6H_{11})

Anal. Calcd for $\text{C}_{25}\text{H}_{51}\text{N}_6\text{Nb}$: C 56.80; H 9.72; N 15.90. Found: C 56.52 ; H 9.80 ; N 15.71.

Results and Discussion

Preparation and Characterization of Guanidines

The strategy employed in this chapter is based on the reaction of trisubstituted guanidine with homoleptic metal amido complexes. This approach requires the preparation of the appropriate guanidine. The simple addition reaction of carbodiimide and primary amine offered a satisfactory route to these materials. Based on the availability of the necessary carbodiimides and amines and keeping in mind the objectives that were set forth in Chapter 1, *N,N',N''*-tricyclohexylguanidine (**3.1**) and *N,N',N''*-triisopropylguanidine (**3.2**) were prepared. Spectroscopic and analytical data gave preliminary confirmation of the identity of these species and crystallographic characterization and subsequent reactivity results confirmed these facts.

In both compounds the ^1H NMR spectra gave very broad and rather undiagnostic features especially for the α protons. However, the integrated ratio for the three types of protons in these materials was correct. A useful feature in the ^{13}C NMR of **3.1** and **3.2** was the central sp^2 carbon atoms, which appeared at 148.5 ppm (**3.1**) and 148.4 ppm (**3.2**). Given the facts that the structural features of these starting materials were important for future studies and that their spectroscopic features were not completely definitive, crystallographic confirmation of the identities of **3.1** and **3.2** was sought.

A single crystal of the hydrogen chloride adduct of **3.1** was fortuitously grown from a sample of this compound dissolved in chloroform. The results of a single crystal structural analysis (Table 3.1) of this salt are shown in Figure 3.1 with pertinent distances and angles provided in Tables 3.2.

The compound $[(\text{CyNH})_3\text{C}]^+\text{Cl}^-$ crystallized in the space group $P2_13$ (cubic) with $Z = 4$. The molecule lies on a three-fold axis perpendicular to the guanidinium cation molecular plane passing through the central C(7). This results in a symmetrical central C with three equivalent N(H)Cy groups. The overall positive charge of the cation is balanced with a chloride counterion, which was presumably derived from the crystallization solvent.

The trigonal planar arrangement of the sp^2 hybridized C and three nitrogen atoms allows for a delocalized π system for the cation. The C(7)-N bond distance of $1.333(3)\text{\AA}$ is consistent with partial double character and shorter than the singly bonded N-C(6) distance of $1.460(4)\text{\AA}$.

A single crystal of N, N', N''-triisopropylguanidine (**3.2**) was obtained from hexane and subjected to X-ray analysis (Table 3.3). Compound **3.2** crystallized in space group $P-1$ with two independent molecules in the unit cell, which are shown in Figures 3.2 and 3.3 with corresponding interatomic distances and angles given in Tables 3.4 and 3.5.

The central C atoms in both cases (C(10), C(20)) are, as expected, planar sp^2 hybridized atoms bonded to three different nitrogen atoms. The C-N distances of this central core can be broken into two groups; one short interaction with an average distance of 1.29\AA and the others with an average distance of 1.38\AA . The average N-C(isopropyl) for both molecules is 1.46\AA and represents a single C-N bond distance. These data are consistent with a rather localized CN double bond (N(1)-C(10) and N(4)-C(20)) with indication of some partial π delocalization between this bond and the other amine functions on these species.

Table 3.1. Crystal data and structure refinement for N, N', N''-Tricyclohexylguanidine
 $\{[C_6H_{11}N(H)]_2CNC_6H_{11}\}HCl$ (3.1)

Empirical formula	$C_{19}H_{36}N_3Cl$
Formula weight	341.96
Temperature	293(2) K
Wavelength	0.71073 Å
Crystal system	Cubic
Space group	$P2_13$
Unit cell dimensions	$a = 12.6323(6)$ Å $\alpha = 90$ deg. $b = 12.6323(6)$ Å $\beta = 90$ deg. $c = 12.6323(6)$ Å $\gamma = 90$ deg.
Volume, Z	$2015.8(2)$ Å ³ , 4
Density (calculated)	1.127 Mg/m ³
Absorption coefficient	0.194 mm ⁻¹
F(000)	752
Crystal size	0.10 x 0.10 x 0.10 mm
Θ range for data collection	2.28 to 20.98 deg.
Limiting indices	$-16 \leq h \leq 16$, $-15 \leq k \leq 16$, $-16 \leq l \leq 13$
Reflections collected	7225
Independent reflections	735 [R(int) = 0.0748]
Absorption correction	None
Refinement method	Full-matrix least-squares on F^2
Data / restraints / parameters	731 / 0 / 70
Goodness-of-fit on F^2	1.133
Final R indices [$I > 2\sigma(I)$]	R1 = 0.0389, wR2 = 0.0925
R indices (all data)	R1 = 0.0463, wR2 = 0.0993
Absolute structure parameter	0.0(2)
Largest diff. peak and hole	0.093 and -0.089 e Å ⁻³

Table 3.2 Bond lengths [Å] and angles [deg] for 3.1.

N(1)-C(7)	1.333(3)
N(1)-C(6)	1.460(4)
C(1)-C(6)	1.503(5)
C(1)-C(2)	1.532(6)
C(2)-C(3)	1.504(7)
C(3)-C(4)	1.481(6)
C(4)-C(5)	1.526(5)
C(5)-C(6)	1.503(5)
C(7)-N(1)#1	1.333(3)
C(7)-N(1)#2	1.333(3)
C(7)-N(1)-C(6)	125.4(3)
C(6)-C(1)-C(2)	111.1(4)
C(3)-C(2)-C(1)	111.1(4)
C(4)-C(3)-C(2)	110.5(4)
C(3)-C(4)-C(5)	111.6(3)
C(6)-C(5)-C(4)	109.3(3)
N(1)-C(6)-C(5)	110.5(3)
N(1)-C(6)-C(1)	111.0(3)
C(5)-C(6)-C(1)	110.5(3)
N(1)#1-C(7)-N(1)	119.999(5)
N(1)#1-C(7)-N(1)#2	119.996(4)
N(1)-C(7)-N(1)#2	119.998(5)

Symmetry transformations used to generate equivalent atoms:
 #1 $y-1/2, -z+1/2, -x$ #2 $-z, x+1/2, -y+1/2$

Figure 3.1

The ORTEP diagram of N, N', N''-Tricyclohexylguanidinium-chloride
{[CyN(H)]₂CNHCy} Cl (**3.1**)

It is expected that for such an interaction to be significant the N(H)(ⁱPr) moieties should be sp² rather than sp³ hybridized. Unfortunately, the precise positions of the hydrogen atoms cannot be specified with certainty and therefore, the hybridization of the amine nitrogen atoms can only be inferred from the C(isopropyl)-N-C(sp²) angles (average 121.9°). These compare favorably with the C(isopropyl)-N(imine)-C(sp²) angles which have an average angle of 118.2°.

In addition, π conjugation would be favored by having the nitrogen lone pair of electrons (localized in a p orbital) aligned with the π bond of the imine function. In other words, the mean plane defined by C(isopropyl)-N(amine)-C(sp²) should be coplanar with that defined by C(sp²)-N(imine)-C(isopropyl). Calculation of the angles between the appropriate mean planes gave values of 17.9°, 56.1°, 16.0°, and 46.9°.

All of these features taken together – the bond distances, the indications of sp² hybridization and, the orientation of the amine functions relative to the imine – indicate that there is some conjugation.

Table 3.3. Crystal data and structure refinement for N, N', N''-Triisopropylguanidine

$$\{[\text{PrN}(\text{H})]_2\text{CN}^{\text{Pr}}\} \cdot 3.2$$

Identification code	dr009	
Empirical formula	$\text{C}_{10}\text{H}_{23}\text{N}_3$	
Formula weight	185.31	
Temperature	213(2) K	
Wavelength	0.71073 Å	
Crystal system	Triclinic	
Space group	P-1	
Unit cell dimensions	$a = 9.0775(5)$ Å	$\alpha = 79.229(1)$ deg.
	$b = 9.2390(5)$ Å	$\beta = 82.618(1)$ deg.
	$c = 15.1933(9)$ Å	$\gamma = 78.129(1)$ deg.
Volume, Z	$1219.6(1)$ Å ³ , 4	
Density (calculated)	1.009 Mg/m ³	
Absorption coefficient	0.062 mm ⁻¹	
F(000)	416	
Crystal size	0.20 x 0.20 x 0.20 mm	
Theta range for data collection	1.37 to 28.58 deg.	
Limiting indices	$-11 \leq h \leq 10$, $-8 \leq k \leq 12$, $-20 \leq l \leq 19$	
Reflections collected	7537	
Independent reflections	5285 [R(int) = 0.0176]	
Absorption correction	None	
Refinement method	Full-matrix least-squares on F ²	
Data / restraints / parameters	5284 / 0 / 235	
Goodness-of-fit on F ²	1.008	
Final R indices [I > 2σ(I)]	R1 = 0.0562, wR2 = 0.1542	
R indices (all data)	R1 = 0.0627, wR2 = 0.1652	
Largest diff. peak and hole	0.556 and -0.541 e Å ⁻³	

Figure 3.2.

The ORTEP diagram of *N, N', N''*-Triisopropylguanidine $\{[{}^i\text{PrN}(\text{H})_2\text{CN}{}^i\text{Pr}]\}$ (3.2) Showing one of the unique molecules in the unit cell.

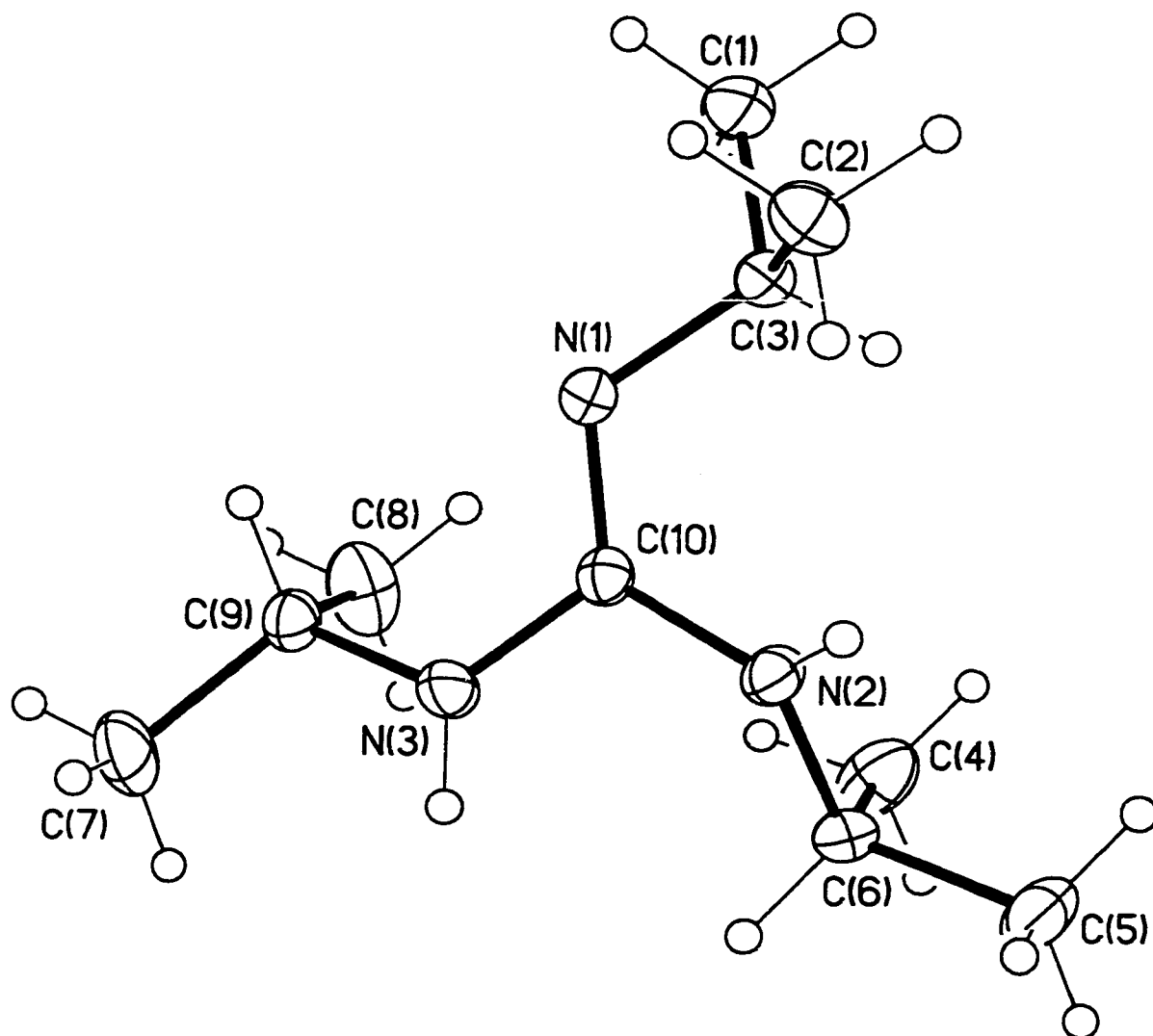


Figure 3.3.

The ORTEP diagram of N, N', N''-Triisopropylguanidine $\{[{}^i\text{PrN}(\text{H})]_2\text{CN}{}^i\text{Pr}\}$ (3.2) Showing one of the unique molecules in the unit cell.

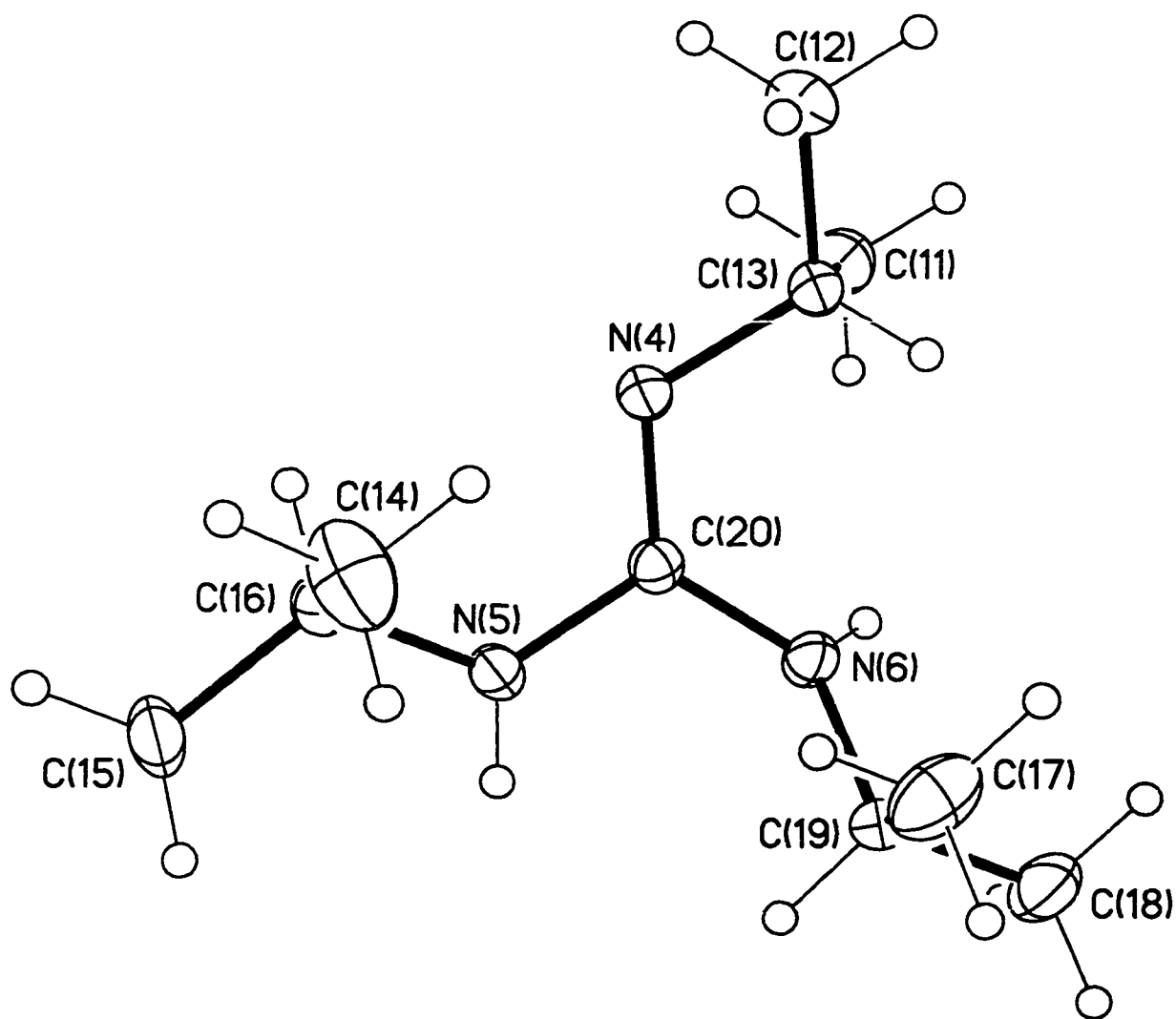


Table 3.4 Bond lengths [Å] for 3.2.

N(1)-C(10)	1.291(2)
N(1)-C(3)	1.465(2)
N(2)-C(10)	1.389(2)
N(2)-C(6)	1.473(2)
N(3)-C(10)	1.370(2)
N(3)-C(9)	1.456(2)
N(4)-C(20)	1.292(2)
N(4)-C(13)	1.462(2)
N(5)-C(20)	1.373(2)
N(5)-C(16)	1.453(2)
N(6)-C(20)	1.391(2)
N(6)-C(19)	1.470(2)
C(1)-C(3)	1.520(2)
C(2)-C(3)	1.524(2)
C(4)-C(6)	1.511(2)
C(5)-C(6)	1.517(2)
C(7)-C(9)	1.516(2)
C(8)-C(9)	1.509(2)
C(11)-C(13)	1.524(2)
C(12)-C(13)	1.522(2)
C(14)-C(16)	1.507(2)
C(15)-C(16)	1.515(2)
C(17)-C(19)	1.509(2)
C(18)-C(19)	1.515(2)

Table 3.5. Bond angles [deg] for 3.2.

C(10)-N(1)-C(3)	118.20(11)
C(10)-N(2)-C(6)	121.84(11)
C(10)-N(3)-C(9)	121.88(12)
C(20)-N(4)-C(13)	118.22(12)
C(20)-N(5)-C(16)	121.99(12)
C(20)-N(6)-C(19)	121.78(11)
N(1)-C(3)-C(1)	108.16(13)
N(1)-C(3)-C(2)	111.44(12)
C(1)-C(3)-C(2)	110.72(13)
N(2)-C(6)-C(4)	112.02(12)
N(2)-C(6)-C(5)	107.36(12)
C(4)-C(6)-C(5)	111.60(14)
N(3)-C(9)-C(8)	111.47(13)
N(3)-C(9)-C(7)	109.49(13)
C(8)-C(9)-C(7)	111.09(14)
N(1)-C(10)-N(3)	119.92(12)
N(1)-C(10)-N(2)	125.95(12)
N(3)-C(10)-N(2)	114.08(11)
N(4)-C(13)-C(11)	111.47(13)
N(4)-C(13)-C(12)	108.31(13)
C(11)-C(13)-C(12)	110.61(14)
N(5)-C(16)-C(14)	111.41(14)
N(5)-C(16)-C(15)	109.61(12)
C(14)-C(16)-C(15)	111.04(14)
N(6)-C(19)-C(17)	111.90(12)
N(6)-C(19)-C(18)	107.87(12)
C(17)-C(19)-C(18)	111.69(14)
N(4)-C(20)-N(5)	120.04(12)
N(4)-C(20)-N(6)	125.90(12)
N(5)-C(20)-N(6)	114.01(11)

Preparation of Guanidinate Complexes

Introduction of the guanidinate ligand proceeded smoothly from the direct reactions of pentakis(dimethylamido)M (M = Ta, Nb) complexes with both **3.1** and **3.2** at room temperature under nitrogen to provide good yields of complexes **3.3-3.6** (Scheme 3.1). These new guanidinate complexes have been characterized by spectroscopic methods, elemental analysis and in the case of **3.3** and **3.5** by a single crystal X-ray diffraction study.

In all cases, the ^1H and ^{13}C NMR spectra of the products were quite similar. The alkyl proton signals shift and divide into several different resonances. This is most clear in the case of isopropyl groups where three clear doublets of equal intensity are evident. The singlet for the amido groups is shifted from that of the starting materials (3.25 ppm for $\text{Ta}(\text{NMe}_2)_5$ and 3.18 ppm for $\text{Nb}(\text{NMe}_2)_5$). The integrated ratio of guanidinate alkyls to amido groups is consistent with a product having a 3:1 ratio of amido to guanidinate ligands. One of the most obvious changes within the guanidinate ligands are the shifts in ^{13}C NMR signals for the central, sp^2 carbon (CN_3) to the 152-158 ppm range (from 148.5 and 148.4 for Cy and ^iPr respectively). All of the spectroscopic evidence indicated that these reactions had proceeded directly to dianionic guanidinate-containing complexes.

Despite attempts to introduce a second equivalent of guanidine through prolonged reaction time and increased temperature, only the monosubstituted products were observed.

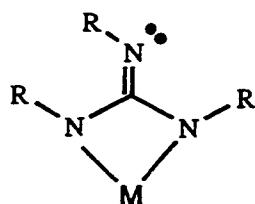
Final confirmation of the spectroscopic features was provided by X-ray diffraction studies. Single crystals of **3.3** were obtained from toluene and subjected to X-ray

analysis. The results of this analysis are provided in Figure 3.4 and Tables 3.6-3.8. The data is consistent with the spectroscopic characterization and gives definitive confirmation of the connectivity for **3.3**.

The coordination environment of the Ta(V) center is constituted of three dimethylamido functions and an N, N', N''-triisopropylguanidinate dianion. The overall coordination number of the Ta atom is five but examination of the interatomic angles indicates that the coordination geometry is better described as based on a distorted tetrahedral ligand array with the bisector of the bidentate guanidinate ligand, the Ta-C(10) vector, defining one of the vertices. The angles formed between the Ta-C(10) vector and the three Ta-N(amido) are 107.9(2)°, 112.60(2)°, and 130.6(3)°. The angles between the three Ta-N(amido) vectors are 92.8(3)°, 93.8(3)°, and 118.9(3)°.

The doubly deprotonated guanidine ligand binds to Ta through only two nitrogen atoms (N(1), N(2)) forming a planar four-membered metallacycle (sum of internal angles = 360°).

The third guanidinate nitrogen atom, N(3), lies outside of the metal coordination sphere and based on the short C(10)-N(3) distance of 1.276(10)Å and the C(10)-N(3)-C(9) angle of 124.6(7)° is best viewed as an sp² hybridized, imine function. These features are consistent with structure VII in which the negative charges are localized on



VII

the two nitrogens bonded to Ta. In fact, the Ta-N(guanidine) distances (average 2.05Å) are actually very close to those observed in the structure of **2.1** and reported for Ta-N amido.⁶ This interpretation is in agreement with the observation of three different ¹Pr groups in the ¹H and ¹³C NMR spectra of **3.3** due to the hindered rotation of the exocyclic C=N.

The CN₃ core (N(1), N(2), N(3) and C(10)) is planar and C(9) deviates only slightly (0.19(3)Å) from this plane. The four p orbitals for the four sp² centers that describe the CN₃ core are in alignment for π conjugation of the N₃C core of the guanidinate (Y conjugation).

The three dimethylamido groups are planar, a feature consistent with π donation of the nitrogen lone pairs into tantalum d orbitals. Furthermore, the values for the Ta-NMe₂ distances average 1.97Å which are slightly shorter than literature values which have invoked a ππ-dπ interaction.⁶ The electron deficiency of the Ta center would allow all three amido ligands to donate their electron pairs to the metal.

The cyclohexylguanidinate analogue of this compound could also be isolated as high quality crystals. Single crystals of **3.5** were obtained from bis(trimethylsilyl)ether and subjected to X-ray analysis (Table 3.9). As can be seen in Figure 3.5, complex **3.5** exhibited very similar coordination geometry to the ¹Pr analogue, **3.3**. A summary of the interatomic distances and angles for **3.5** is provided in Tables 3.10 and 3.11. As with **3.3**, the environment of the Ta(V) center contains three coordinated dimethylamido functions and a N, N', N''-tricyclohexylguanidinate dianion bonded through only two nitrogen atoms (N(1), N(3)) forming a planar four-membered metallocycle.

Figure 3.4. The ORTEP diagram of $\text{Ta}(\text{NMe}_2)_3[(\text{CH}_3)_2\text{CHN}]_2\text{CNCH}(\text{CH}_3)_2$ (3.4),

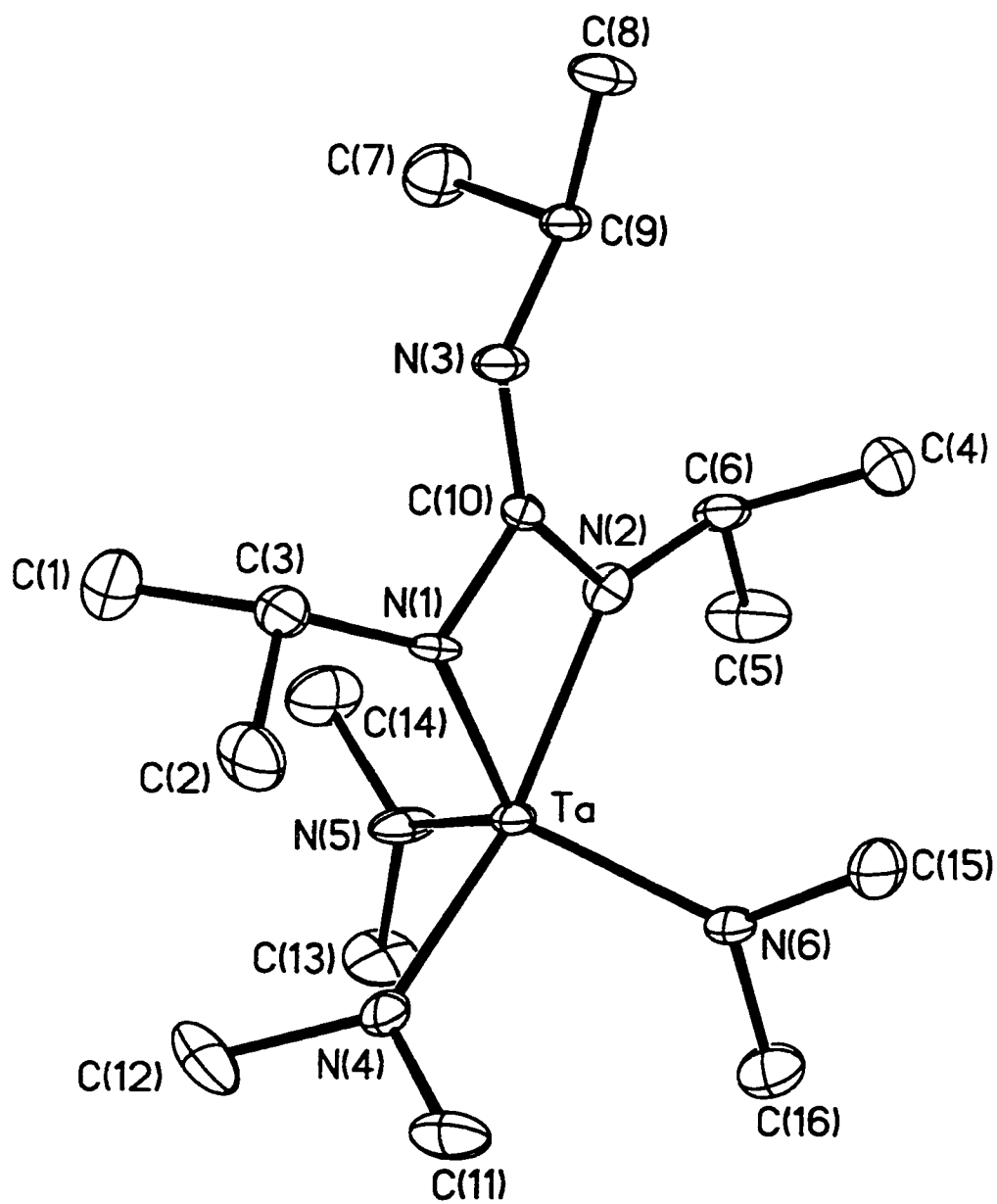


Table 3.6. Crystal data and structure refinement for Ta(NMe₂)₃[(CH₃)₂CHN]₂CNCH(CH₃)₂ 3.3.

Identification code	dr022	
Empirical formula	C ₁₆ H ₃₉ N ₆ Ta	
Formula weight	496.48	
Temperature	203(2) K	
Wavelength	0.71073 Å	
Crystal system	Triclinic	
Space group	P-1	
Unit cell dimensions	a = 10.1317(6) Å	α = 78.068(1) deg.
	b = 10.3748(6) Å	β = 65.405(1) deg.
	c = 12.0067(7) Å	γ = 88.503(1) deg.
Volume, Z	1120.2(1) Å ³ , 2	
Density (calculated)	1.472 Mg/m ³	
Absorption coefficient	4.914 mm ⁻¹	
F(000)	500	
Crystal size	0.2 x 0.4 x 0.4 mm	
Theta range for data collection	1.91 to 22.50 deg.	
Limiting indices	-13 ≤ h ≤ 13, -13 ≤ k ≤ 13, -15 ≤ l ≤ 10	
Reflections collected	4653	
Independent reflections	2886 [R(int) = 0.0600]	
Absorption correction	SADABS empirical	
Max. and min. transmission	0.801504 and 0.345789	
Refinement method	Full-matrix least-squares on F ²	
Data / restraints / parameters	2886 / 0 / 209	
Goodness-of-fit on F ²	1.038	
Final R indices [I > 2σ(I)]	R1 = 0.0478, wR2 = 0.1131	
R indices (all data)	R1 = 0.0514, wR2 = 0.1146	
Extinction coefficient	0.0112(13)	
Largest diff. peak and hole	2.314 and -2.516 e Å ⁻³	

Table 3.7. Bond lengths [Å] for 3.3.

Ta-N(5)	1.956(7)
Ta-N(6)	1.961(6)
Ta-N(4)	1.987(8)
Ta-N(1)	2.004(6)
Ta-N(2)	2.096(7)
Ta-C(10)	2.632(7)
N(1)-C(10)	1.421(10)
N(1)-C(3)	1.489(10)
N(2)-C(10)	1.372(10)
N(2)-C(6)	1.468(11)
N(3)-C(10)	1.276(10)
N(3)-C(9)	1.453(10)
N(4)-C(12)	1.477(11)
N(4)-C(11)	1.502(12)
N(5)-C(14)	1.469(12)
N(5)-C(13)	1.475(11)
N(6)-C(16)	1.460(12)
N(6)-C(15)	1.471(11)
C(1)-C(3)	1.526(12)
C(2)-C(3)	1.513(13)
C(4)-C(6)	1.530(12)
C(5)-C(6)	1.518(13)
C(7)-C(9)	1.522(12)
C(8)-C(9)	1.527(13)

Table 3.8. Bond angles [deg] for 3.3.

N(5)-Ta-N(6)	118.9(3)	C(11)-N(4)-Ta	124.7(6)
N(5)-Ta-N(4)	93.8(3)	C(14)-N(5)-C(13)	110.9(8)
N(6)-Ta-N(4)	92.8(3)	C(14)-N(5)-Ta	122.4(6)
N(5)-Ta-N(1)	117.7(3)	C(13)-N(5)-Ta	126.5(6)
N(6)-Ta-N(1)	121.1(3)	C(16)-N(6)-C(15)	111.7(7)
N(4)-Ta-N(1)	98.4(3)	C(16)-N(6)-Ta	124.7(6)
N(5)-Ta-N(2)	95.8(3)	C(15)-N(6)-Ta	123.6(5)
N(6)-Ta-N(2)	96.2(3)	N(1)-C(3)-C(2)	111.9(6)
N(4)-Ta-N(2)	161.7(3)	N(1)-C(3)-C(1)	110.8(7)
N(1)-Ta-N(2)	63.4(2)	C(2)-C(3)-C(1)	111.4(8)
N(5)-Ta-C(10)	107.9(2)	N(2)-C(6)-C(5)	108.4(7)
N(6)-Ta-C(10)	112.6(2)	N(2)-C(6)-C(4)	113.0(7)
N(4)-Ta-C(10)	130.6(3)	C(5)-C(6)-C(4)	110.5(8)
N(1)-Ta-C(10)	32.2(2)	N(3)-C(9)-C(7)	109.8(7)
N(2)-Ta-C(10)	31.2(2)	N(3)-C(9)-C(8)	108.1(7)
C(10)-N(1)-C(3)	117.7(6)	C(7)-C(9)-C(8)	110.0(8)
C(10)-N(1)-Ta	99.0(4)	N(3)-C(10)-N(2)	138.0(7)
C(3)-N(1)-Ta	139.4(5)	N(3)-C(10)-N(1)	121.1(7)
C(10)-N(2)-C(6)	124.0(7)	N(2)-C(10)-N(1)	100.9(6)
C(10)-N(2)-Ta	96.5(5)	N(3)-C(10)-Ta	169.1(6)
C(6)-N(2)-Ta	139.4(5)	N(2)-C(10)-Ta	52.3(4)
C(10)-N(3)-C(9)	124.6(7)	N(1)-C(10)-Ta	48.8(3)
C(12)-N(4)-C(11)	107.3(8)		
C(12)-N(4)-Ta	127.5(6)		

Again, the coordination geometry is best described as based on a distorted tetrahedral ligand array with the bisector of the bidentate guanidinate ligand, the Ta-C(19) vector, defining one of the vertices. The angles and distances within the Ta(N₂)C cycle are comparable to **3.3**.

Similar considerations apply as with **3.3** to the third guanidinate nitrogen atom, N(2), which lies outside of the metal coordination sphere and exhibits a short C(19)-N(2) distance of 1.28(2)Å and the C(19)-N(2)-C(12) angle of 125.1(12)°. Features that are consistent with structure **VII**. Furthermore, the three different Cy groups exhibited in the ¹H and ¹³C NMR spectra can be attributed to hindered rotation of the C=N.

The alignment of the four p orbitals on N(1), N(2), N(3), and C(19) (the CN₃ core) is slightly better than in **3.3** with C(12) being coplanar with these atoms within the error of measurement (three times the estimated standard deviation).

Like **3.3**, the three dimethylamido groups are planar, a feature consistent with π donation of the nitrogen lone pair into tantalum d orbitals. Furthermore, the values for the Ta-NMe₂ distances average 1.97Å which are slightly shorter than literature values which have invoked a $p\pi$ - $d\pi$ interaction.⁶

Table 3.9. Crystal data and structure refinement for Ta(NMe₂)₃[(CyN)₂C(NCy)] 3.5

Identification code	dr015	
Empirical formula	C ₂₅ H ₅₁ N ₆ Ta	
Formula weight	616.67	
Temperature	203(2) K	
Wavelength	0.71073 Å	
Crystal system	Triclinic	
Space group	P-1	
Unit cell dimensions	a = 9.4155(2) Å	α = 117.075(1) deg.
	b = 13.3188(2) Å	β = 101.744(1) deg.
	c = 13.5215(2) Å	γ = 98.507(1) deg.
Volume, Z	1420.81(4) Å ³ , 2	
Density (calculated)	1.441 Mg/m ³	
Absorption coefficient	3.890 mm ⁻¹	
F(000)	632	
Crystal size	0.10 x 0.10 x 0.06 mm	
Theta range for data collection	1.78 to 23.50 deg.	
Limiting indices	-12 ≤ h ≤ 12, -15 ≤ k ≤ 17, -18 ≤ l ≤ 17	
Reflections collected	9879	
Independent reflections	4190 [R(int) = 0.1153]	
Absorption correction	SADABS empirical	
Max. and min. transmission	0.694497 and 0.322575	
Refinement method	Full-matrix least-squares on F ²	
Data / restraints / parameters	4187 / 0 / 289	
Goodness-of-fit on F ²	1.006	
Final R indices [I > 2σ(I)]	R1 = 0.0737, wR2 = 0.1684	
R indices (all data)	R1 = 0.1039, wR2 = 0.1834	
Largest diff. peak and hole	3.264 and -4.201 e Å ⁻³	

Figure 3.5 The ORTEP diagram of $\text{Ta}(\text{NMe}_2)_3[(\text{CyN})_2\text{C}(\text{NCy})]$ (3.5)

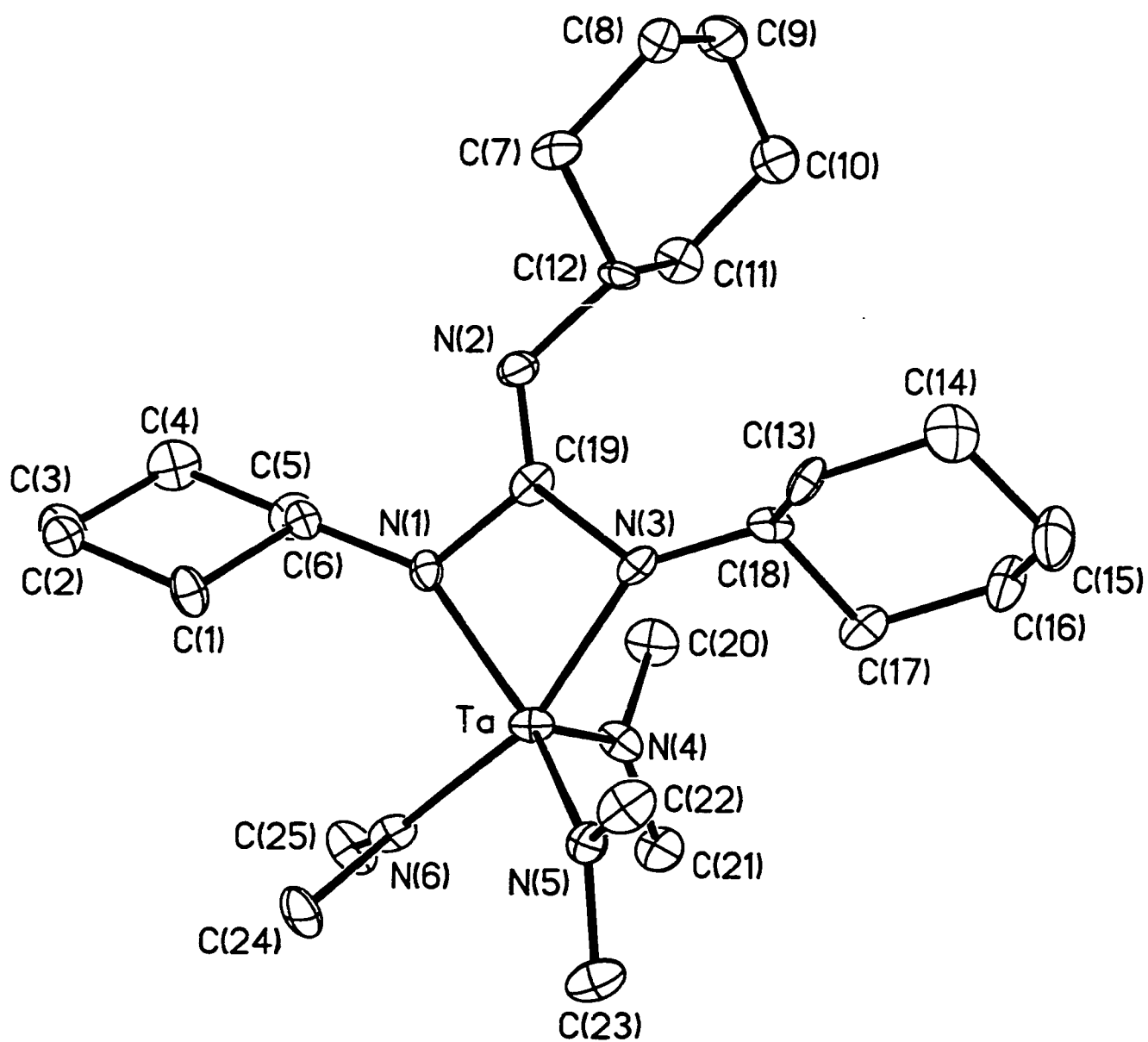


Table 3.10 Bond lengths [Å] for 3.5

Ta-N(4)	1.963(11)
Ta-N(6)	1.967(13)
Ta-N(5)	1.976(11)
Ta-N(1)	2.023(11)
Ta-N(3)	2.120(12)
Ta-C(19)	2.65(2)
N(1)-C(19)	1.44(2)
N(1)-C(6)	1.46(2)
N(2)-C(19)	1.28(2)
N(2)-C(12)	1.46(2)
N(3)-C(19)	1.40(2)
N(3)-C(18)	1.46(2)
N(4)-C(21)	1.45(2)
N(4)-C(20)	1.48(2)
N(5)-C(23)	1.44(2)
N(5)-C(22)	1.50(2)
N(6)-C(24)	1.49(2)
N(6)-C(25)	1.49(2)
C(1)-C(6)	1.51(2)
C(1)-C(2)	1.51(2)
C(2)-C(3)	1.52(2)
C(3)-C(4)	1.53(2)
C(4)-C(5)	1.52(2)
C(5)-C(6)	1.53(2)
C(7)-C(12)	1.54(2)
C(7)-C(8)	1.54(2)
C(8)-C(9)	1.56(2)
C(9)-C(10)	1.51(2)
C(10)-C(11)	1.53(2)
C(11)-C(12)	1.52(2)
C(13)-C(14)	1.48(2)
C(13)-C(18)	1.53(2)
C(14)-C(15)	1.54(2)
C(15)-C(16)	1.54(2)
C(16)-C(17)	1.52(2)
C(17)-C(18)	1.53(2)

Table 3.11 Bond angles [deg] for **3.5**

N(4)-Ta-N(6)	93.4(5)	C(6)-C(1)-C(2)	111.4(12)
N(4)-Ta-N(5)	116.1(5)	C(1)-C(2)-C(3)	112.1(13)
N(6)-Ta-N(5)	92.3(5)	C(4)-C(3)-C(2)	111.1(13)
N(4)-Ta-N(1)	117.6(5)	C(5)-C(4)-C(3)	110.8(13)
N(6)-Ta-N(1)	97.7(4)	C(4)-C(5)-C(6)	112.2(12)
N(5)-Ta-N(1)	124.4(5)	N(1)-C(6)-C(1)	111.5(11)
N(4)-Ta-N(3)	96.2(4)	N(1)-C(6)-C(5)	112.3(11)
N(6)-Ta-N(3)	161.6(4)	C(1)-C(6)-C(5)	109.9(11)
N(5)-Ta-N(3)	97.5(4)	C(12)-C(7)-C(8)	111.8(12)
N(1)-Ta-N(3)	63.8(4)	C(7)-C(8)-C(9)	110.1(13)
N(4)-Ta-C(19)	105.3(4)	C(10)-C(9)-C(8)	111.1(13)
N(6)-Ta-C(19)	130.0(4)	C(9)-C(10)-C(11)	111.9(13)
N(5)-Ta-C(19)	118.0(4)	C(12)-C(11)-C(10)	111.5(12)
N(1)-Ta-C(19)	32.6(4)	N(2)-C(12)-C(11)	113.2(12)
N(3)-Ta-C(19)	31.8(4)	N(2)-C(12)-C(7)	107.1(11)
C(19)-N(1)-C(6)	117.1(11)	C(11)-C(12)-C(7)	110.1(11)
C(19)-N(1)-Ta	98.4(8)	C(14)-C(13)-C(18)	111.8(12)
C(6)-N(1)-Ta	141.5(9)	C(13)-C(14)-C(15)	112.6(14)
C(19)-N(2)-C(12)	125.1(12)	C(16)-C(15)-C(14)	108.3(13)
C(19)-N(3)-C(18)	123.8(12)	C(17)-C(16)-C(15)	112.7(13)
C(19)-N(3)-Ta	95.5(8)	C(16)-C(17)-C(18)	111.0(12)
C(18)-N(3)-Ta	139.6(8)	N(3)-C(18)-C(17)	111.0(11)
C(21)-N(4)-C(20)	112.0(12)	N(3)-C(18)-C(13)	113.4(11)
C(21)-N(4)-Ta	125.8(10)	C(17)-C(18)-C(13)	108.7(11)
C(20)-N(4)-Ta	122.2(10)	N(2)-C(19)-N(3)	137.7(14)
C(23)-N(5)-C(22)	108.9(12)	N(2)-C(19)-N(1)	121.5(12)
C(23)-N(5)-Ta	125.7(10)	N(3)-C(19)-N(1)	100.6(11)
C(22)-N(5)-Ta	125.4(9)	N(2)-C(19)-Ta	164.6(11)
C(24)-N(6)-C(25)	106.1(12)	N(3)-C(19)-Ta	52.7(7)
C(24)-N(6)-Ta	127.0(10)	N(1)-C(19)-Ta	49.0(6)
C(25)-N(6)-Ta	126.8(9)		

Isolation of $\text{TaCl}(\text{NMe}_2)_3\{[(\text{CH}_3)_2\text{CHN}]_2\text{CN}(\text{H})\text{CH}(\text{CH}_3)_2\}$

During the purification of complex 3.3, $\text{Ta}(\text{NMe}_2)_3[(^i\text{PrN})_2\text{C}=\text{N}^i\text{Pr}]$, from the reaction of $\text{Ta}(\text{NMe}_2)_5$ and triisopropylguanidine a crystal was isolated and subjected to X-ray analysis. This complex crystallized in the monoclinic space group $\text{P}2_1/\text{n}$ with four molecules in the unit cell (Table 3.12). The final results of the X-ray analysis provided the structure shown in Figure 3.6 with selected bond distances and angles are provided in Tables 3.13 and 3.14.

The formula for this material, $\text{TaCl}(\text{NMe}_2)_3\{[(\text{CH}_3)_2\text{CHN}]_2\text{CN}(\text{H})\text{CH}(\text{CH}_3)_2\}$ though not consistent with the starting materials can be quite easily rationalized. It appears that the pentakis(amido) starting material contained an impurity of the known complex $\text{Ta}(\text{NMe}_2)_4\text{Cl}^6$ and it was simply the reaction of this species with N, N', N''-triisopropylguanidine that lead to the isolated complex.

Examination of the geometry of the Ta(V) center in this complex reveals that it is based on a distorted octahedral coordination geometry. The coordination environment of Ta is composed of a trisubstituted, bidentate, monoanionic guanidinate ligand, three NMe_2 ligands and a single chloride ligand. The pseudo-equatorial plane can be defined by the planar coordinated N(1)-C(10)-N(2) function, the Ta atom and two dimethylamido nitrogen atoms N(5) and N(6). The sum of the angles of these ligands around Ta is 359° indicating that these groups are indeed planar. The Cl-Ta-N(4) angle of $174.65(11)^\circ$ defines this as the pseudo-axial vector of this compound.

The guanidinate anion is bonded to Ta through only two nitrogens to yield a planar four-membered ring of sp^2 hybridized N and C centers. The delocalized π interaction within the NCN moiety (N(1)-C(10)-N(2)) leads to partial double bonded C-N distances

which average of 1.34Å. The distances and angles within this cyclic arrangement are reminiscent of those in the structurally characterized seven coordinate bis(diisopropylacetamidinato) and bis(dicyclohexylacetamidinato) complexes $\text{Cl}_3\text{Ta}(\text{RNC}(\text{CH}_3)\text{NR})_2$ ($\text{R} = \text{}^i\text{Pr}, \text{Cy}$)⁷ and in compound **2.1** in chapter 2. The third guanidinate nitrogen, N(3), lies just slightly out of the ligand plane ($\text{Ta-C}(10)\text{-N}(3) = 176.5^\circ$).

The only angle that can be used in the evaluation of N(3) hybridization is the C(10)-N(3)-C(9) angle of $121.9(3)^\circ$, which while consistent with sp^2 hybridization is by no means definitive. The question regarding the conjugation of the p orbital of an sp^2 N(3) with the π system of the N(1)-C(10)-N(2) group arises. For significant π interaction to occur between N(3) and C(10), the plane defined by C(9)-N(3)-C(10) should be coincident with the plane defined by N(1)-C(10)-N(2). Calculation of the angle between these mean planes gave an angle of 44.9° . This value tends to discount a major degree of π bonding between N(3) and C(10). However, the rather short N(3)-C(10) distance of $1.379(5)\text{Å}$ compared with the average value for the single bond distances for N-C(H)Me₂ of 1.47Å are consistent with some degree of double bonding between these atoms.

The three amido groups in $\text{TaCl}(\text{NMe}_2)_3\{[(\text{CH}_3)_2\text{CHN}]_2\text{CN}(\text{H})\text{CH}(\text{CH}_3)_2\}$ are planar, a feature consistent with π donation of the nitrogen lone pair into a metal d orbital. Furthermore the values for the Ta-NMe₂ distances average 1.99Å which compare favorably with literature values where $d\pi\text{-}p\pi$ interactions have been invoked.⁶ The orientation of the amido functions is appropriate for π donation. With the pseudo-axial ligands aligned along the z axis, each amido is oriented so that it is aligned to donate to one of the three orthogonal d orbitals available for π bonding (e.g. dxz, dyz, dxy).

The resultant net electron count on the Ta including the π donation from the amido ligands is therefore 18 electrons.

This chapter showed that the elimination of amine from a metal amido complex to form metal guanidinate complexes are successful and give high yields.

The accidental result of compound $\text{TaCl}(\text{NMe}_2)_3 \{ [(\text{CH}_3)_2\text{CHN}]_2\text{CN}(\text{H})\text{CH}(\text{CH}_3)_2 \}$ pointed out the importance of purification for $\text{M}(\text{NMe}_2)_5$ starting materials.

Table 3.12. Summary of crystal data collection and structure refinement for
 $\text{TaCl}(\text{NMe}_2)_3 \{[(\text{CH}_3)_2\text{CHN}]_2\text{CN}(\text{H})\text{CH}(\text{CH}_3)_2\}$

Empirical formula	$\text{C}_{16}\text{H}_{40}\text{ClN}_6\text{Ta}$	
Formula weight	532.94	
Temperature	203(2) K	
Wavelength	0.71073 Å	
Crystal system	Monoclinic	
Space group	P2(1)/n	
Unit cell dimensions	$a = 10.5747(6)$ Å	$\alpha = 90$ deg.
	$b = 13.4281(8)$ Å	$\beta = 107.5830(1)$ deg.
	$c = 16.8615(9)$ Å	$\gamma = 90$ deg.
Volume, Z	$2282.4(2)$ Å ³ , 4	
Density (calculated)	1.551 Mg/m ³	
Absorption coefficient	4.943 mm ⁻¹	
F(000)	1072	
Crystal size	0.40 x 0.30 x 0.30 mm	
Theta range for data collection	1.98 to 25.00 deg.	
Limiting indices	-14 ≤ h ≤ 14, -16 ≤ k ≤ 18, -22 ≤ l ≤ 11	
Reflections collected	11506	
Independent reflections	4007 [R(int) = 0.0590]	
Absorption correction	SADABS empirical	
Max. and min. transmission	1.000000 and 0.546315	
Refinement method	Full-matrix least-squares on F ²	
Data / restraints / parameters	4007 / 0 / 217	
Goodness-of-fit on F ²	1.021	
Final R indices [I > 2σ(I)]	R1 = 0.0336, wR2 = 0.0796	
R indices (all data)	R1 = 0.0386, wR2 = 0.0815	
Largest diff. peak and hole	1.669 and -1.891 e Å ⁻³	

Table 3.13. Bond lengths [Å] for TaCl(NMe₂)₃{[(CH₃)₂CHN]₂CN(H)CH(CH₃)₂}

Ta-N(4)	1.976(4)
Ta-N(5)	1.984(3)
Ta-N(6)	1.997(4)
Ta-N(2)	2.160(3)
Ta-N(1)	2.246(3)
Ta-Cl	2.5729(10)
Ta-C(10)	2.652(4)
N(1)-C(10)	1.326(5)
N(1)-C(3)	1.458(6)
N(2)-C(10)	1.347(5)
N(2)-C(6)	1.468(5)
N(3)-C(10)	1.379(5)
N(3)-C(9)	1.478(5)
N(4)-C(12)	1.449(7)
N(4)-C(11)	1.467(7)
N(5)-C(13)	1.456(5)
N(5)-C(14)	1.462(6)
N(6)-C(15)	1.462(6)
N(6)-C(16)	1.470(8)
C(1)-C(3)	1.514(8)
C(2)-C(3)	1.531(7)
C(4)-C(6)	1.502(7)
C(5)-C(6)	1.516(7)
C(7)-C(9)	1.508(7)
C(8)-C(9)	1.523(6)

Table 3.14. Bond angles [deg] for TaCl(NMe₂)₃{[(CH₃)₂CHN]₂CN(H)CH(CH₃)₂}

N(4)-Ta-N(5)	95.7(2)	C(13)-N(5)-C(14)	109.2(4)
N(4)-Ta-N(6)	93.3(2)	C(13)-N(5)-Ta	126.1(3)
N(5)-Ta-N(6)	99.5(2)	C(14)-N(5)-Ta	123.7(3)
N(4)-Ta-N(2)	95.5(2)	C(15)-N(6)-C(16)	108.2(4)
N(5)-Ta-N(2)	158.17(13)	C(15)-N(6)-Ta	125.1(4)
N(6)-Ta-N(2)	98.5(2)	C(16)-N(6)-Ta	126.7(3)
N(4)-Ta-N(1)	91.9(2)	N(1)-C(3)-C(1)	110.2(4)
N(5)-Ta-N(1)	100.66(13)	N(1)-C(3)-C(2)	112.0(4)
N(6)-Ta-N(1)	158.5(2)	C(1)-C(3)-C(2)	111.0(5)
N(2)-Ta-N(1)	60.26(13)	N(2)-C(6)-C(4)	113.2(4)
N(4)-Ta-Cl	174.65(11)	N(2)-C(6)-C(5)	109.3(4)
N(5)-Ta-Cl	83.82(11)	C(4)-C(6)-C(5)	110.3(5)
N(6)-Ta-Cl	92.01(12)	N(3)-C(9)-C(7)	111.2(4)
N(2)-Ta-Cl	83.32(10)	N(3)-C(9)-C(8)	108.3(4)
N(1)-Ta-Cl	82.93(10)	C(7)-C(9)-C(8)	111.3(4)
N(4)-Ta-C(10)	96.00(14)	N(1)-C(10)-N(2)	111.7(4)
N(5)-Ta-C(10)	129.42(13)	N(1)-C(10)-N(3)	124.9(4)
N(6)-Ta-C(10)	128.6(2)	N(2)-C(10)-N(3)	123.3(4)
N(2)-Ta-C(10)	30.37(12)	N(1)-C(10)-Ta	57.8(2)
N(1)-Ta-C(10)	29.97(13)	N(2)-C(10)-Ta	54.2(2)
Cl-Ta-C(10)	80.34(9)	N(3)-C(10)-Ta	176.5(3)
C(10)-N(1)-C(3)	122.6(4)		
C(10)-N(1)-Ta	92.2(2)		
C(3)-N(1)-Ta	140.1(3)		
C(10)-N(2)-C(6)	123.2(3)		
C(10)-N(2)-Ta	95.4(2)		
C(6)-N(2)-Ta	138.4(3)		
C(10)-N(3)-C(9)	121.9(3)		
C(12)-N(4)-C(11)	108.7(4)		
C(12)-N(4)-Ta	127.4(4)		
C(11)-N(4)-Ta	123.8(4)		

References for Chapter 3:

- ¹ da S. Maia, J. R.; Gazard, P. A.; Kilner, M. Batsanova, A. S.; Howard, J. A. K. *J. Chem. Soc., Dalton Trans.* **1997**, 4625. Bailey, P. J.; Mitchell, L. A.; Parsons, S. *J. Chem. Soc., Dalton Trans.* **1996**, 2839.
- ² Robinson, S. D.; Sahajpal, A. *J. Chem. Soc., Dalton Trans.* **1997**, 3349.
- ³ Snaith, R.; Wade, K.; Wyatt, B. K. *J. Chem. Soc. (A)* **1970**, 380.
- ⁴ Bailey, P. J.; Gould, R. O.; Harmer, C. N.; Pace, S.; Steiner, A.; Wright, D. S. *Chem. Commun.* **1997**, 1161.
- ⁵ Bradley, D. C.; Thomas, I. M. *Can. J. Chem.*, **1962**, *40*, 1355. Bradley, D. C.; Thomas, I. M. *Can. J. Chem.*, **1962**, *40*, 449.
- ⁶ Chisholm, M. H.; Tan, L.-S.; Huffman, J. C. *J. Am. Chem. Soc.* **1982**, *104*, 4879.
- ⁷ Drew, M. G. B.; Wilkins, J. D. *J. Chem. Soc., Dalton Trans.* **1974**, 1579. Drew, M. G. B.; Wilkins, J. D. *J. Chem. Soc., Dalton Trans.* **1975**, 2611.

Chapter 4.

Reaction Between Guanidines with Metal Alkyl Groups Protonation Pathways to Metal Guanidinate Complexes II

Introduction:

In Chapter 3, the results for the reaction of Nb and Ta amido complexes with trialkylguanidines were reported. The reaction between these species was a rapid protonation of amido ligand, elimination of amine, and formation of metal complex with dianionic guanidinate ligands. The structural features of these complexes were well illustrated through single crystal X-ray crystallography, which confirmed the bidentate nature of the guanidinate ligand.

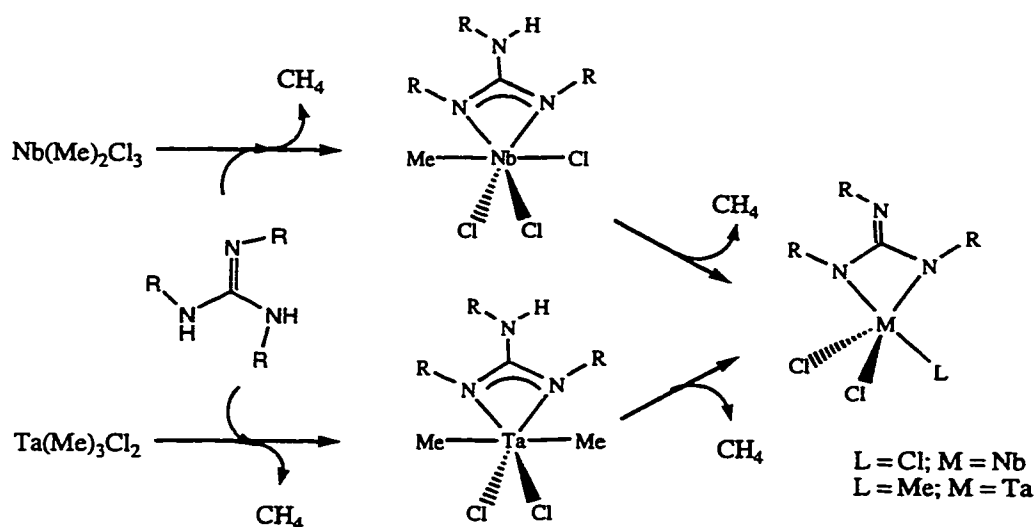
One of the issues raised by the investigations of Chapter 3 was the fact that the third nitrogen atom of the guanidinate did not become involved in bonding with metal. Perhaps the presence of strongly π donating amido ligands reduced the electron deficiency of the metal center. The steric congestion provided by the amido ligands may be an added reason for the lack of coordination of the third nitrogen atom.

The results described in this chapter began with an interest in addressing the role of π donors in guanidinate complexes by substituting the amido ligands with less π donating ligands. Would such a substitution result in coordination of the third guanidinate nitrogen? Keeping in mind the strategies outlined in Chapters 1 and 3 and the necessary features for protonation reactions outlined in Chapter 3, obvious choices for groups to consider for the elimination reaction are halo or alkyl moieties.

In the reported examples of elimination of HX, the addition of excess guanidine to trap HX as the guanidinium salt was required.¹ This could lead to problems with purification of products. In contrast, elimination of alkane seemed to offer a route with byproducts that are often volatile and in any case rather unreactive. Although only one

example of such a reaction was found in the literature search,² an alkyl group should be more basic than dimethylamido and, therefore, subject to similar reaction with guanidine.

The final avenue of investigation as outlined in Scheme 1.5 of Chapter 1 was the introduction of guanidinate ligands by a protonation of a metal alkyl and elimination of alkane. This is the subject of Chapter 4. These efforts began with the selection of Ta and Nb alkyl complexes and, based on several factors such as ease of synthesis and purification, the compounds of formula $M(\text{Me})_x\text{Cl}_y$ ($M = \text{Ta}$, $x = 3$, $y = 2$; $M = \text{Nb}$, $x = 2$, $y = 3$) were chosen as starting materials.³ These chloro alkyl complexes were then reacted directly with N,N',N'' -tricyclohexylguanidine and N,N',N'' -triisopropylguanidine in an effort to investigate the reactions outlined in Scheme 4.1. Somewhat surprisingly, the isolated products were the result of a single proton transfer and incorporation of the monoanionic guanidinate. Two of these compounds were characterized by single crystal X-ray diffraction analysis thus confirming their connectivity and the bonding features of the guanidinate ligands. The preliminary results of efforts to get a second alkyl elimination are also reported.



Scheme 4.1

Experimental

General Considerations: All manipulations were carried out in either a nitrogen filled drybox or under nitrogen using standard Schlenk-line techniques. Solvents were distilled under nitrogen from Na/K alloy. Deuterated benzene and pyridine were dried by vacuum transfer from potassium. Preparation of TaMe₃Cl₂ and NbMe₂Cl₃ was carried out according to literature procedures.³ ¹H NMR spectra were run on either a Gemini 200 MHz or Bruker 500 MHz spectrometer, as specified, with deuterated benzene or pyridine as a solvent and internal standard. Infrared spectra were measured on a Galaxy 3020 FTIR spectrometer. All elemental analyses were run on a Perkin Elmer PE CHN 4000 elemental analysis system.

NbMeCl₃(CyN)₂C(NHCy) (4.1)

A Schlenk flask was charged with 0.470 g NbMe₂Cl₃ (1.81 mmol) in toluene give a bright orange colored solution. N, N', N''-tricyclohexylguanidine (**3.1**) (0.552 g, 1.81 mmol) was dissolved in toluene and slowly added to the reaction flask while stirring. During the addition, the solution became cloudy and dark red in color. The reaction mixture was stirred at room temperature for 5 hours. The precipitate was separated by filtration and the resultant light reddish compound was dried under vacuum give 0.41 g of **4.1** (43% yield). Compound **4.1** was dissolved into THF and cooled to -30°C to give light yellowish crystals.

Spectroscopic data: IR (Nujol, cm⁻¹) 3350 (m) N-H, 1619 (s) C-N stretch

¹H NMR (pyridine-d₅, ppm) 4.41 (br mult., 1H, CNCH), 4.05 (br, 1H, NH), 3.85 (br mult., 2H, NCH), 2.31 (br s, 3H, Nb-CH₃), 2.05-0.90 (br, 30H, C₆H₁₁),

^{13}C NMR (pyridine- d_5 , ppm) 160.00 (CN₃), 52.68(NCH), 51.59 (NCH),

37.37(NbCH₃), 33.58, 32.91, 27.61,25.36,24.94,24.09(4s, C₆H₁₁).

Anal. Calcd for C₂₀H₃₇N₃Cl₃Nb C 45.39; H6.57; N 8.36 Found: C 47.95; H 7.50; N 7.20

MS (FAB): [(CyNH)₂C(NCy)H]⁺ 306.3, [NbMeCl₃]⁺ 215.2

TaMe₂Cl₂(CyN)₂C(NCy) (4.2)

A Schlenk flask was charged with 0.50 g TaMe₃Cl₂ (1.77mmol) in 30 mL of toluene to give a light yellow solution. N, N',N''-tricyclohexylguanidine (**3.1**) (0.54 g, 1.77mmol) was dissolved in toluene and slowly added to the reaction flask while stirring. Fifteen minutes after the addition, the color of the solution was bright yellow and a yellow precipitate had formed. The reaction mixture was stirred at room temperature for 5 hours. The precipitate was separated by filtered and dried under vacuum to yield 0.59 gm of **4.2** (56 % yield). Compound **4.2** was dissolved in THF and cooled to -30°C to give yellowish crystals.

Spectroscopic data: IR (Nujol, cm⁻¹) 3395(m) N-H, 1612 (s) C-N stretch

^1H NMR (C₆D₆, 500 MHz, ppm) 4.04(mult, 1H, CNCH), 3.81(mult, 2H,TaNCH),

3.16(mult, 1H, NH), 1.62(s, 6H, Ta-CH₃), 2.05-0.72(b, 30 H, C₆H₁₁).

^{13}C NMR(C₆D₆, ppm) 175.77 (CN₃), 81.52(Ta-CH₃), 58.86 (NCH), 54.80(CNCH),

34.91,33.72,27.01,26.59,25.67,24.90(C₆H₁₁)

Anal. Calcd for C₂₁H₄₀N₃Cl₂Ta C 43.01; H6.88; N 7.17 Found:C 43.27; H 6.90; N 7.40

MS (FAB): [(CyNH)₂C(NCy)H]⁺ 306.3

NbMeCl₃{[(CH₃)₂CHN]₂C[NHCH(CH₃)₂]} (4.3)

A procedure similar to the synthesis of **4.1** was followed using 0.300g NbMe₂Cl₃ (1.30 mmol) dissolved in 30 mL toluene and adding N, N', N''-triisopropylguanidine (**3.2**)

(0.242 g, 1.30mmol) that had been dissolved in hexane. Similar observations were made during the addition and reaction which was stirred at room temperature for 5 hours. Removal of the resultant reddish brown solid by filtration and drying under vacuum gave 0.24 g of **4.3** (48 % yield).

Spectroscopic data: IR (Nujol, cm^{-1}) 3353 (m)N-H, 1617 (s) C-N stretch

^1H NMR (pyridine- d_5 , 500 MHz, ppm) 4.45(br mult, 1H,CNCH), 4.02(br mult ,2H, NCH), 3.90 (br, 1H, NH), 2.10(br s, 3H, NbCH₃), 1.32(d, 12H, $J_{\text{CH}}=6.6\text{Hz}$, CHCH₃), 0.74 (d, 6H, $J_{\text{CH}}=6.6\text{Hz}$, CHCH₃).

^{13}C NMR (pyridine- d_5 , ppm) 154.02 (CN₃), 46.62(NCH), 45.76(NCH), 41.20(Nb-Me) 22.77, 23.13 (CH₃,Cy).

Anal. Calcd for C₁₁H₂₅N₃Cl₃Nb C 33.14; H6.27; N 10.54 Found: C 33.17; H 6.51; N10.77

MS (FAB) {[(CH₃)₂CHN(H)]₃C}⁺ 186.2, (M+2)⁺ 400.4

TaMe₂Cl₂{[(CH₃)₂CHN]₂C[NHCH(CH₃)₂]} (4.4)

A procedure similar to the synthesis of **4.2** was followed using 0.890 g TaMe₃Cl₂ (2.98 mmol) dissolved in 30 mL of toluene and adding N, N', N''-triisopropylguanidine (**3.2**) (0.550g, 1.23 mmol) that had been dissolved in toluene. Similar observations were made during the addition and reaction, which was stirred at room temperature for 4 hours. The resultant light yellowish solid was separated by filtration and dried under vacuum to yield 0.512g of **4.4** (36 % yield). Yellowish crystals of compound **4.4** could be obtained from toluene.

Spectroscopic data: IR (Nujol, cm^{-1}) 3362 (m)N-H, 1615 (s) C-N stretch

^1H NMR (C₆D₆, ppm) 4.10 (sept, 2H, 2CH), 3.35 (mult,1H, CH), 3.58(br, 1H, NH), 1.63 (s, 6H, TaCH₃), 1.21(d, 12H, $J_{\text{CH}} = 6.6 \text{ Hz}$, CH₃), 0.66(d, 6H, $J_{\text{CH}}=6.6\text{Hz}$, CH₃).

^{13}C NMR(C_6D_6 , ppm) 169.57 (NC(Nipr)N), 81.87 (2Ta- CH_3), 48.89 (2TaNCH),
47.51 (CNCH), 23.55, 22.97 (CHCH_3)

Anal. Calcd for $\text{C}_{12}\text{H}_{28}\text{Cl}_2\text{N}_3\text{Ta}$: C 30.91; H 6.01; N 9.01 Found: C 31.04; H 6.09; N 9.39

MS (FAB): $\{[(\text{CH}_3)_2\text{CHN}(\text{H})]_3\text{C}\}^+$ 186.2,

Results and Discussion:

The reaction of $\text{Nb}(\text{CH}_3)_2\text{Cl}_3$ or $\text{Ta}(\text{CH}_3)_3\text{Cl}_2$ with one equivalent of trisubstituted guanidine proceeded rapidly at room temperature to produce an insoluble product. In addition to a color change and precipitate formation, a small amount of bubbling was noted in all of the reactions. The insolubility of the products, especially in the case of the Nb complexes, **4.1** and **4.3**, required that some of the NMR spectra be carried out in pyridine- d_5 .

Both ^1H and ^{13}C NMR spectra for these new compounds confirmed the incorporation of guanidine ligands into the products and gave guanidine alkyl (Cy or ^iPr) resonances with a 2:1 ratio. Furthermore, these spectra indicated that some metal-methyl functions remained in all of the products. The integrated methyl:guanidinate ratio of 1:1 for **4.1** and **4.3** and 2:1 for **4.2** and **4.4** indicated that only one of the methyl groups of the starting materials have reacted and been eliminated. This was a surprising contrast to the results obtained in Chapter 3 in which two dimethylamido ligands were rapidly protonated and eliminated from the starting metal complex. Infrared spectra were consistent and clearly showed the presence of a residual N-H function ($3350\text{-}3400\text{ cm}^{-1}$). Mass spectral data were not too informative giving only signals arising from the guanidinate ligands.

In order to confirm the identity and to investigate the detailed structural features of these products, two crystal structural analyses were undertaken. A single crystal of compound **4.1** was subjected to X-ray analysis. The results of this analysis are provided in Figure 4.1 and Tables 4.1, 4.2 and 4.3.

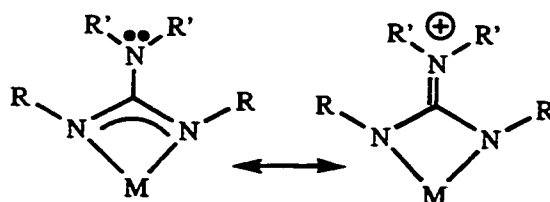
Consistent with the spectroscopic observations, **4.1** consisted of one monoanionic guanidinate ligand with one Nb-Me group remaining from the starting material.

This complex is the product of protonation of a single Nb-Me group and coordination of a bidentate guanidinate ligand.

The geometry of the metal center is based on a distorted octahedral ligand array with pseudo-axial chloro ligands, Cl(3) and Cl(1), and an equatorial plane (sum of angles around Nb = 360°) consisting of the two coordinated guanidinate nitrogens (N(1) and N(2)), one chloro ligand (Cl(2)), and the remaining methyl group (C(20)). The pseudo-axial chloro ligands are distorted away from the guanidinate ligand plane with an Cl(1)-Nb-Cl(3) angle of 163.2° .

The guanidinate ligand exhibits the typical acute bite angle ($63.0(4)^\circ$) and through coordination to the Nb center yields the planar four-membered cycle consisting of the metal center and the three sp^2 hybridized atoms (N(1), N(2), and C(19)) as observed for all other complexes reported in this thesis.

The third guanidinate nitrogen atom, N(3), lies outside of the metal coordination sphere but nearly co-planar with the M-N-C-N plane (N(3)-C(19)-Nb angle of $174.8(11)^\circ$). The one measurable angle around N(3), C(18)-N(3)-C(19), of $131.0(13)^\circ$ is indicative of an sp^2 N. The potential for conjugation of the p orbital localized lone pair on N(3) with the π system of the coordinated atoms is shown by the small angle (24.6°) between the mean planes defined by atoms bonded to N(3) and the N(1)-C(19)-N(2) group. Further evidence for the contribution of the zwitterionic structure **V** (Scheme 1.4)



V

is provided by relatively short C(19)-N(3) distance of $1.320(16)\text{\AA}$ compared to the three N-C(cyclohexyl) bonds (N(1)-C(6), N(2)-C(12), N(3)-C(18)) which average 1.48\AA .

However, free rotation of the C(19)-N(3) bond, the reason for the observation of only two different Cy groups in the ^1H and ^{13}C NMR spectra of **4.1**, is contradictory to a strong π interaction between these two atoms.

Nb-CH₃ the remaining from the starting material, Nb-C(20) has distance of 2.17°A which is slightly shorter to literature value 2.22°A.⁴

A single crystal of **4.4** that was satisfactory for X-ray analysis was also obtained during these investigations. A single crystal X-ray study was carried out in order to compare this complex with **4.1**. The similarities between these two species are obvious upon inspection of Figure 4.2 and comparison with Figure 4.1. A summary of the crystallographic study and the bond distances and angle for **4.4** is provided in Table 4.4 to 4.6.

Complex **4.4** is also the product of a single protonation of a metal-methyl bond of the starting material by the guanidine, release of methane and coordination of the guanidate anion. Like **4.1**, this compound exhibited the metal center in a distorted pseudo-octahedral coordination environment. However, in this case the pseudo-axial ligands, which are distorted away from the guanidate ligand forming an angle of 150.8(3)°, are one chloro (Cl(2)) and one methyl (C(11)) originating from the starting material.

The Ta atom lies in the pseudo-equatorial plane defined by the remaining chloro (Cl(1)) and methyl groups (C(12)) and the bidentate guanidate ligand. The bite angle (62.5(2)°) and planarity of the Ta-N(1)-C(10)-N(2) cycle are reminiscent of **4.1**.

Figure 4.1. ORTEP diagram of $\text{NbMeCl}_3(\text{CyN})_2\text{C}(\text{NHCy})$ (4.1)

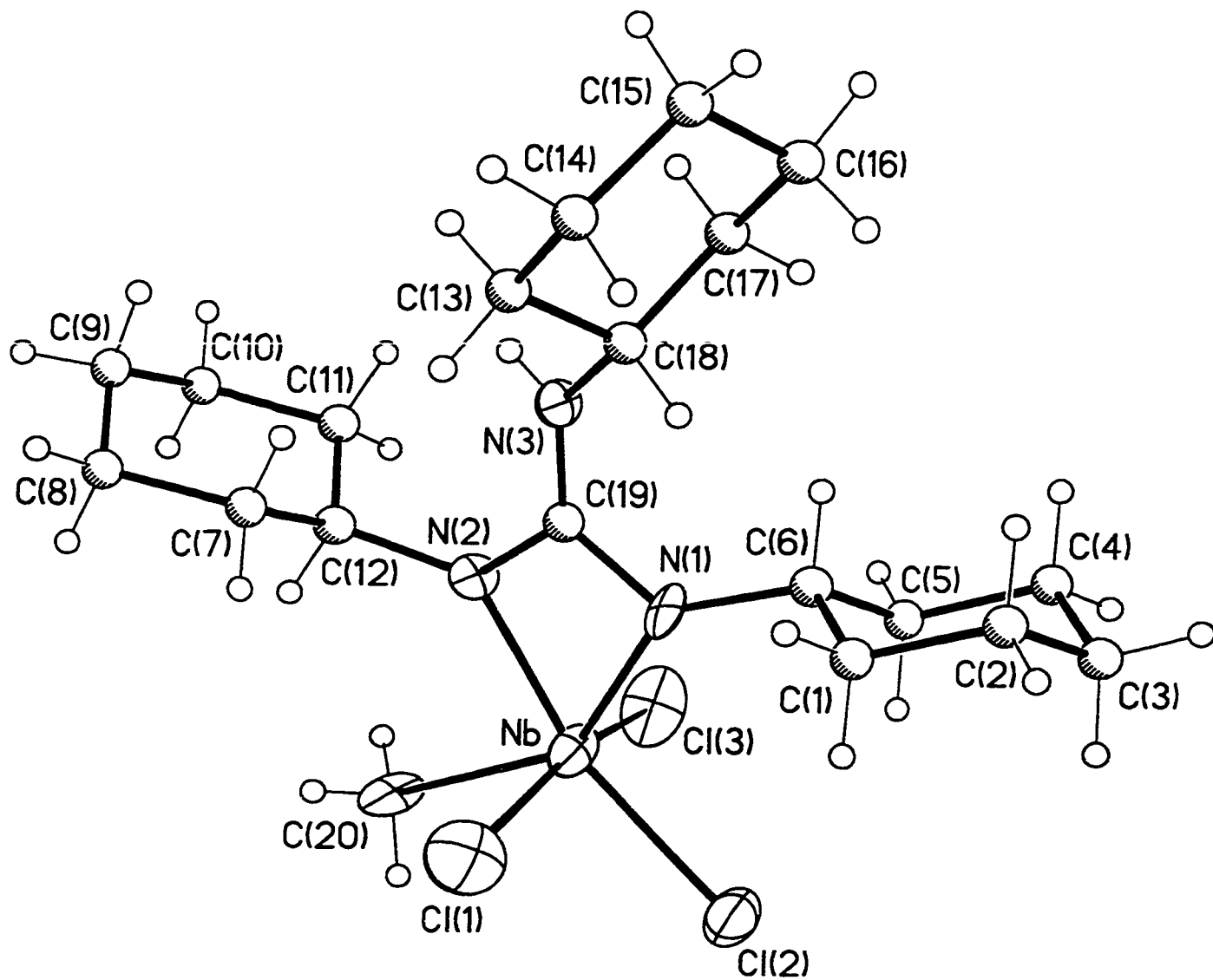


Table 4.1. Crystal data and structure refinement for NbMeCl₃(CyN)₂C(NHCy) 4.1

Empirical formula	C ₂₀ H ₃₇ Cl ₃ N ₃ Nb	
Formula weight	518.79	
Temperature	293(2) K	
Wavelength	0.71073 Å	
Crystal system, space group	Triclinic, P-1	
Unit cell dimensions	a = 8.907(9) Å	α = 67.899(9) deg.
	b = 11.522(9) Å	β = 80.38(3) deg.
	c = 12.610(9) Å	γ = 82.71(5) deg.
Volume	1179(4) Å ³	
Z, Calculated density	2, 1.461 Mg/m ³	
Absorption coefficient	0.861 mm ⁻¹	
F(000)	540	
Crystal size	0.05 x 0.1 x 0.1 mm	
Θ range for data collection	1.91 to 20.00 deg.	
Limiting indices	-8 ≤ h ≤ 8, -9 ≤ k ≤ 11, 0 ≤ l ≤ 12	
Reflections collected / unique	2192 / 2192 [R(int) = 0.0000]	
Completeness to theta	20.00 99.9 %	
Absorption correction	None	
Refinement method	Full-matrix least-squares on F ²	
Data / restraints / parameters	2192 / 0 / 149	
Goodness-of-fit on F ²	1.059	
Final R indices [I > 2σ(I)]	R1 = 0.0840, wR2 = 0.1901	
R indices (all data)	R1 = 0.1551, wR2 = 0.2141	
Largest diff. peak and hole	0.570 and -0.694 e Å ⁻³	

Table 4.2. Bond lengths [Å] for 4.1.

Nb-N(1)	2.005(11)
Nb-N(2)	2.102(12)
Nb-C(20)	2.178(14)
Nb-Cl(1)	2.300(7)
Nb-Cl(3)	2.347(7)
Nb-Cl(2)	2.377(6)
Nb-C(19)	2.553(17)
N(1)-C(19)	1.379(16)
N(1)-C(6)	1.482(17)
N(2)-C(19)	1.303(16)
N(2)-C(12)	1.482(17)
N(3)-C(19)	1.320(16)
N(3)-C(18)	1.472(16)
C(1)-C(6)	1.468(18)
C(1)-C(2)	1.507(19)
C(2)-C(3)	1.47(2)
C(3)-C(4)	1.543(19)
C(4)-C(5)	1.533(18)
C(5)-C(6)	1.529(19)
C(7)-C(12)	1.480(19)
C(7)-C(8)	1.57(2)
C(8)-C(9)	1.37(2)
C(9)-C(10)	1.47(2)
C(10)-C(11)	1.55(2)
C(11)-C(12)	1.438(19)
C(13)-C(18)	1.502(18)
C(13)-C(14)	1.535(19)
C(14)-C(15)	1.50(2)
C(15)-C(16)	1.46(2)
C(16)-C(17)	1.514(18)
C(17)-C(18)	1.491(18)

Table 4.3. Bond angles [deg] for 4.1.

N(1)-Nb-N(2)	63.0(4)	C(3)-C(2)-C(1)	110.4(13)
N(1)-Nb-C(20)	142.7(5)	C(2)-C(3)-C(4)	111.7(14)
N(2)-Nb-C(20)	79.8(5)	C(5)-C(4)-C(3)	109.2(13)
N(1)-Nb-Cl(1)	97.2(4)	C(6)-C(5)-C(4)	108.8(12)
N(2)-Nb-Cl(1)	96.3(4)	C(1)-C(6)-N(1)	112.8(13)
C(20)-Nb-Cl(1)	83.3(5)	C(1)-C(6)-C(5)	111.6(13)
N(1)-Nb-Cl(3)	99.0(4)	N(1)-C(6)-C(5)	110.2(12)
N(2)-Nb-Cl(3)	94.9(4)	C(12)-C(7)-C(8)	106.1(13)
C(20)-Nb-Cl(3)	86.5(5)	C(9)-C(8)-C(7)	113.2(16)
Cl(1)-Nb-Cl(3)	163.23(19)	C(8)-C(9)-C(10)	115.2(18)
N(1)-Nb-Cl(2)	100.3(4)	C(9)-C(10)-C(11)	109.8(15)
N(2)-Nb-Cl(2)	163.3(3)	C(12)-C(11)-C(10)	111.3(14)
C(20)-Nb-Cl(2)	116.9(4)	C(11)-C(12)-C(7)	116.2(14)
Cl(1)-Nb-Cl(2)	85.4(2)	C(11)-C(12)-N(2)	113.3(13)
Cl(3)-Nb-Cl(2)	87.4(2)	C(7)-C(12)-N(2)	113.1(12)
N(1)-Nb-C(19)	32.5(4)	C(18)-C(13)-C(14)	110.6(13)
N(2)-Nb-C(19)	30.6(4)	C(15)-C(14)-C(13)	111.4(15)
C(20)-Nb-C(19)	110.2(5)	C(16)-C(15)-C(14)	113.2(14)
Cl(1)-Nb-C(19)	96.3(4)	C(15)-C(16)-C(17)	113.2(13)
Cl(3)-Nb-C(19)	99.7(4)	C(18)-C(17)-C(16)	110.3(13)
Cl(2)-Nb-C(19)	132.7(4)	N(3)-C(18)-C(17)	112.7(12)
C(19)-N(1)-C(6)	127.4(12)	N(3)-C(18)-C(13)	108.0(11)
C(19)-N(1)-Nb	96.2(9)	C(17)-C(18)-C(13)	112.3(12)
C(6)-N(1)-Nb	135.5(9)	N(2)-C(19)-N(3)	127.1(14)
C(19)-N(2)-C(12)	124.1(12)	N(2)-C(19)-N(1)	106.4(13)
C(19)-N(2)-Nb	94.2(9)	N(3)-C(19)-N(1)	126.5(14)
C(12)-N(2)-Nb	139.3(9)	N(2)-C(19)-Nb	55.2(8)
C(19)-N(3)-C(18)	131.0(13)	N(3)-C(19)-Nb	174.8(11)
C(6)-C(1)-C(2)	111.8(13)	N(1)-C(19)-Nb	51.3(7)

The third guanidinate nitrogen atom, N(3), lies outside of the metal coordination sphere. As in complex 4.1 the evidence for resonance contribution from of the zwitterionic structure V (Scheme 1.4) is provided by the C(7)-N(3)-C(10) angle (130.3(6)°), relatively short C(10)-N(3) distance of 1.336(9)Å, and by the small angle (19.1°) between the mean planes defined by atoms bonded to N(3) and the N(1)-C(10)-N(2) group.

However, like **4.1**, the free rotation of the C(10)-N(3) bond as observed in the ^1H and ^{13}C NMR spectra is contradictory to a strong C=N bond. Average Ta-C(11) and Ta-C(12) bond distance are 2.209 Å, which is longer than literature value 2.17 Å.⁵

Efforts to get the elimination of a second methyl group and generation of the coordinated guanidinate dianion are currently underway. To this end, samples of **4.1-4.4** were left to stir in toluene solutions for several days. In the case of **4.3** the preliminary results for this reaction are quite compelling. After 3 days at room temperature under N_2 , the color of a solution of **4.3** became darker and evaporation of the solvent resulted in isolation of a dark material with ^1H NMR indicating a single broad multiplet at 4.19 ppm and a single doublet at 1.78 ppm. The ^{13}C NMR gave corresponding signals at 45.49 and 23.23 ppm and the central sp^2 C appeared at 170.02 ppm. Neither spectrum gave an indication of a Nb-Me signal. Microanalysis gave results consistent with a formula $\text{NbCl}_3 \{[(\text{CH}_3)_2\text{CHN}]_2\text{C}[\text{NCH}(\text{CH}_3)_2]\}$.⁶ Together these results suggest that simply extending the reaction time will allow the preparation of the desired dianionic guanidinate-containing species. It is particularly interesting to note that the presence of a single isopropyl signal seems to be consistent with either structure X in Scheme 1.4 or with a highly fluxional species.

In conclusion, this chapter presents the fact that compounds (**4.1-4.4**) can be formed perfectly in reasonable yield. Continued reaction of compound **4.3** gave some hope to receive η^3 coordinated compound are possible. Further studies are required.

Fig.4.2 ORTEP diagram of $\text{TaMe}_2\text{Cl}_2\{[(\text{CH}_3)_2\text{CHN}]_2\text{C}[\text{NHCH}(\text{CH}_3)_2]\}$ (4.4)

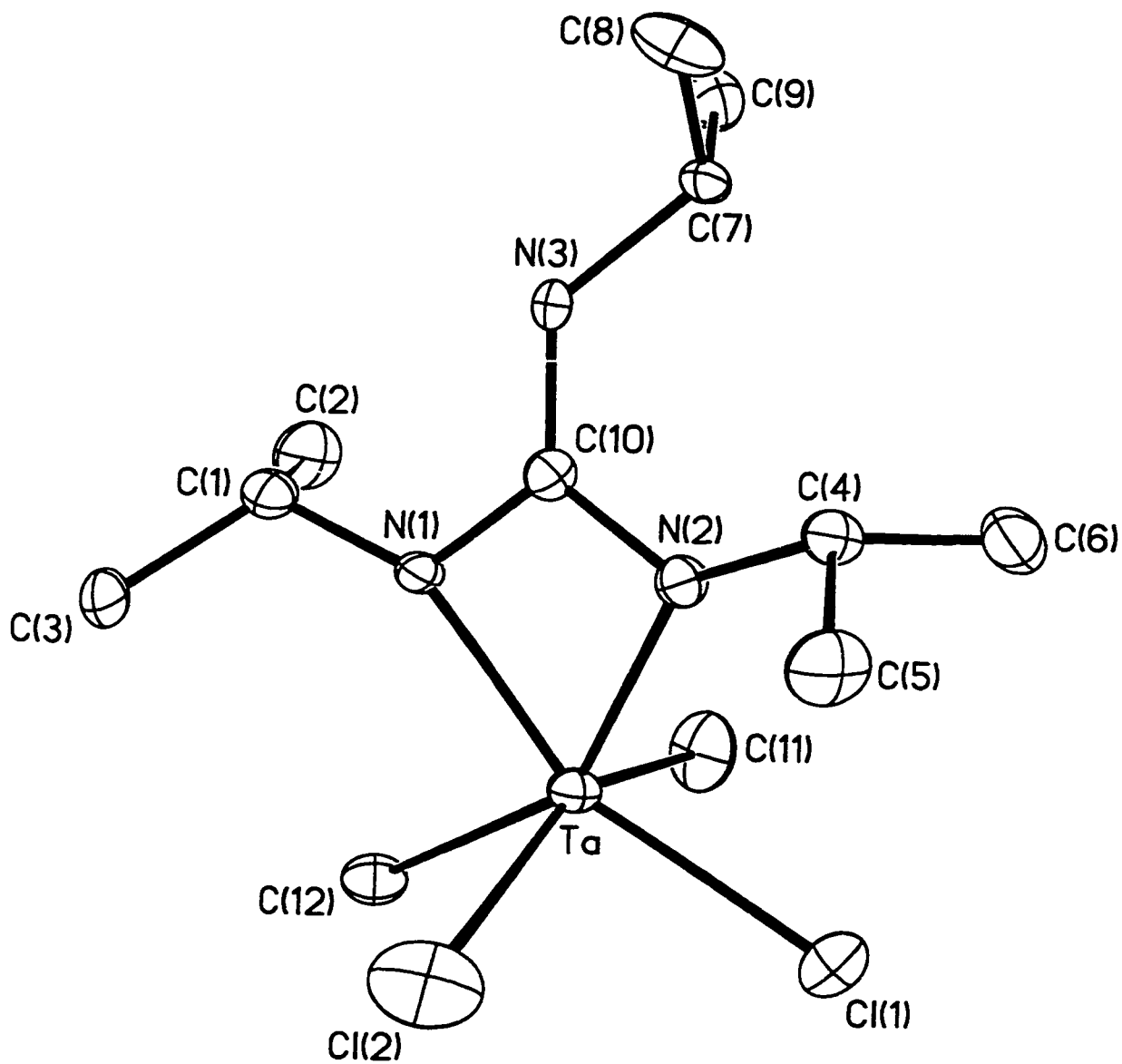


Table 4.4. Crystal data and structure refinement for
 $\text{TaMe}_2\text{Cl}_2\{[(\text{CH}_3)_2\text{CHN}]_2\text{C}[\text{NHCH}(\text{CH}_3)_2]\}$ 4.4

Empirical formula	$\text{C}_{12}\text{H}_{28}\text{Cl}_2\text{N}_3\text{Ta}$	
Formula weight	466.22	
Temperature	203(2) K	
Wavelength	0.71073 Å	
Crystal system, space group	Monoclinic, P2(1)/c	
Unit cell dimensions	$a = 9.278(3)$ Å	$\alpha = 90$ deg.
	$b = 16.036(6)$ Å	$\beta = 106.355(6)$ deg.
	$c = 12.588(4)$ Å	$\gamma = 90$ deg.
Volume	$1797.0(11)$ Å ³	
Z, Calculated density	4, 1.723 Mg/m ³	
Absorption coefficient	6.404 mm ⁻¹	
F(000)	912	
Crystal size	0.05 x 0.2 x 0.2 mm	
Theta range for data collection	2.11 to 28.66 deg.	
Limiting indices	$-12 \leq h \leq 11, 0 \leq k \leq 21, 0 \leq l \leq 16$	
Reflections collected / unique	4365 / 4209 [R(int) = 0.0922]	
Completeness to theta	28.66 91.2 %	
Absorption correction	None	
Refinement method	Full-matrix least-squares on F ²	
Data / restraints / parameters	4209 / 0 / 163	
Goodness-of-fit on F ²	1.010	
Final R indices [I > 2σ(I)]	R1 = 0.0403, wR2 = 0.0788	
R indices (all data)	R1 = 0.0872, wR2 = 0.0834	
Largest diff. peak and hole	1.944 and -1.167 e Å ⁻³	

Table 4.5. Bond lengths [\AA] for 4.4.

Ta-N(2)	2.079(6)
Ta-N(1)	2.104(6)
Ta-C(11)	2.187(8)
Ta-C(12)	2.232(7)
Ta-Cl(2)	2.396(4)
Ta-Cl(1)	2.403(2)
Ta-C(10)	2.583(8)
N(1)-C(10)	1.361(8)
N(1)-C(1)	1.467(9)
N(2)-C(10)	1.350(9)
N(2)-C(4)	1.481(8)
N(3)-C(10)	1.336(9)
N(3)-C(7)	1.470(8)
C(1)-C(3)	1.529(10)
C(1)-C(2)	1.530(11)
C(4)-C(6)	1.497(10)
C(4)-C(5)	1.533(10)
C(7)-C(8)	1.504(10)
C(7)-C(9)	1.514(10)

Table 4.6. Bond angles [deg] for 4.4.

N(2)-Ta-N(1)	62.5(2)	C(10)-N(1)-Ta	93.9(4)
N(2)-Ta-C(11)	99.5(3)	C(1)-N(1)-Ta	144.8(5)
N(1)-Ta-C(11)	101.2(3)	C(10)-N(2)-C(4)	125.0(6)
N(2)-Ta-C(12)	147.2(3)	C(10)-N(2)-Ta	95.4(5)
N(1)-Ta-C(12)	85.2(3)	C(4)-N(2)-Ta	139.1(5)
C(11)-Ta-C(12)	80.8(3)	C(10)-N(3)-C(7)	130.3(6)
N(2)-Ta-Cl(2)	106.49(19)	N(1)-C(1)-C(3)	111.4(6)
N(1)-Ta-Cl(2)	102.46(18)	N(1)-C(1)-C(2)	112.0(6)
C(11)-Ta-Cl(2)	150.8(3)	C(3)-C(1)-C(2)	111.8(7)
C(12)-Ta-Cl(2)	84.4(2)	N(2)-C(4)-C(6)	111.0(6)
N(2)-Ta-Cl(1)	92.76(18)	N(2)-C(4)-C(5)	109.9(6)
N(1)-Ta-Cl(1)	155.22(17)	C(6)-C(4)-C(5)	112.7(7)
C(11)-Ta-Cl(1)	82.2(2)	N(3)-C(7)-C(8)	109.8(6)
C(12)-Ta-Cl(1)	119.5(2)	N(3)-C(7)-C(9)	108.7(6)
Cl(2)-Ta-Cl(1)	83.44(11)	C(8)-C(7)-C(9)	111.5(7)
N(2)-Ta-C(10)	+ 31.4(2)	N(3)-C(10)-N(2)	128.5(7)
N(1)-Ta-C(10)	31.7(2)	N(3)-C(10)-N(1)	125.1(7)
C(11)-Ta-C(10)	97.4(3)	N(2)-C(10)-N(1)	106.3(7)
C(12)-Ta-C(10)	115.9(3)	N(3)-C(10)-Ta	167.5(5)
Cl(2)-Ta-C(10)	111.65(19)	N(2)-C(10)-Ta	53.3(4)
Cl(1)-Ta-C(10)	123.71(18)	N(1)-C(10)-Ta	54.4(4)
C(10)-N(1)-C(1)	119.2(6)		

References for Chapter 4:

- ¹ da S. Maia, J. R.; Gazard, P. A.; Kilner, M. Batsanova, A. S.; Howard, J. A. K. *J. Chem. Soc., Dalton Trans.* **1997**, 4625. Bailey, P. J.; Mitchell, L. A.; Parsons, S. *J. Chem. Soc., Dalton Trans.* **1996**, 2839.
- ² Snaith, R.; Wade, K.; Wyatt, B. K. *J. Chem. Soc. (A)* **1970**, 380.
- ³ Fowles, G. W. A. ; Rice, D. A.; Wilkins, J. D. *J. Chem. Soc. Dalton Trans.* **1974**, 1080.
Fowles, G. W. A. ; Rice, D. A.; Wilkins, J. D. *J. Chem. Soc. Dalton Trans.* **1973**, 961. Fowles, G. W. A. ; Rice, D. A.; Wilkins, J. D. *J. Chem. Soc. Dalton Trans.* **1972**, 2313. Juvinal, G. L. *J. Am. Chem. Soc.*, **1964** , 86, 4202.
- ⁴ Kenneth E. Stockman, Kart L. Houseknecht, Eric A. Boring, Michal Sabat, M.G. Finn and Russell N. Grimes *Organometallics* **1995**, 14, 3014
- ⁵ Linda R. Chamberlain, Ian P. Rothwell, and John C. Huffman *J. Am. Chem. Soc.* **1986**. 108, 1502
- ⁶ Anal. Calcd for C₁₀H₂₁N₃Cl₃Nb C 31.40; H 5.53; N 10.98; Found C 31.76; H 5.65; N 10.87;